ORNL/SPR-2022/2421
Task Order 313110021N0002

The Use of Powder Metallurgy and Hot Isostatic Pressing for Fabricating Components of Nuclear Power Plants

David T. Hoelzer

May 2022

OAK RIDGE National Laboratory

ORNL IS MANAGED BY UT-BATTELLE LLC FOR THE US DEPARTMENT OF ENERGY

ORNL/SPR-2022/2421
Task Order 31310021N0002

Materials Science and Technology Division

THE USE OF POWDER METALLURGY AND HOT ISOSTATIC PRESSING FOR FABRICATING COMPONENTS OF NUCLEAR POWER PLANTS

David T. Hoelzer

May 2022

Prepared by
OAK RIDGE NATIONAL LABORATORY
Oak Ridge, TN 37831
managed by
UT-BATTELLE LLC
for the
US DEPARTMENT OF ENERGY
under contract DE-AC05-00OR22725

ACKNOWLEDGEMENTS

Financial support for this report was provided by the Nuclear Regulatory Commission (NRC).

CONTENTS

LIST OF FIGURES

LIST OF TABLES

ABBREVIATIONS

2D	two-dimensional
3D	three-dimensional
AIM	air induction melting
AISI	American Iron and Steel Institute
ALWR	advanced light-water reactor
AM	additive manufacturing
AMM	additive manufacturing method
AMRC	Advanced Manufacturing Research Centre
AMT	advanced manufacturing technology
ANL	Argonne National Laboratory
ANSI	American National Standards Institute
ASME	American Society of Mechanical Engineers
ASTM	ASTM International (formerly American Society for Testing and Materials)
ATLAS	Advanced Technology Large-Scale
bcc	body-centered cubic
BSE	backscattered electron
BWR	boiling water reactor
CE	carbon equivalency
CGR	crack growth rate
COD	crack-opening displacement
CPP	Carpenter Powder Products
CRD	control rod drives
CT	compact tension
C_v	Charpy V-notch
DOE	US Department of Energy
EBW	electron beam welding
ECP	electrochemical potentials
EDS	energy dispersive spectroscopy
EIGA	electrode induction melting gas atomization
EPRI	Electric Power Research Institute
EUROATOM	European Atomic Energy Community
FAC	flow-accelerated corrosion
fcc	face-centered cubic
FEM	finite element method
GB	grain boundaries
HHF	high heat flux
HIP	hot isostatic press
HSLA	high-strength low-alloy
HT	heat-treated
HV	Vickers hardness scale
IASCC	irradiation-assisted stress corrosion cracking
IGSCC	intergranular stress corrosion cracking
ID	identification
IGA	inert gas atomization
INCO	International Nickel Company
ISO	International Organization for Standardization
ITER	International Thermonuclear Experimental Reactor
LCF	low cycle fatigue

LMP	Larson Miller Parameter
LWR	light-water reactor
MA	mechanical alloying
MCC	material chemistry certification
MIM	metal injection molding
MLE	mils lateral expansion
RT_{NDT}	reference temperature of nil ductility transition
NIST	National Institute of Standards and Technology
NPP	nuclear power plant
NRC	US Nuclear Regulatory Commission
ODS	oxide dispersion strengthened
ORNL	Oak Ridge National Laboratory
PM	powder metallurgy
PSD	powder size distribution
PWR	pressurized water reactor
QA	quality assurance
QC	quality control
QM	Quality Management
RA	reduction in area
RCP	reactor circulating pump
RPV	reactor pressure vessel
SCC	stress corrosion cracking
SEM	scanning electron microscopy
SMR	small modular reactor
UEL	uniform elongation
URC	Uniform Rapid Cooling
UTS	ultimate tensile strength
TEL	total elongation
VIM	vacuum induction melting
YS	yield strength

EXECUTIVE SUMMARY

Powder metallurgy (PM) combined with hot isostatic pressing (HIP), or PM-HIP, is an advanced manufacturing technology (AMT) being developed for manufacturing nuclear power plant (NPP) components, including large components used in the manufacture of the reactor pressure vessel (RPV) of light-water reactors (LWRs) and advanced small modular reactors (SMRs). The purpose for using PM-HIP instead of traditional manufacturing methods involving casting, forging, rolling, and welding is to reduce the cost and time for producing reactor components while maintaining the safety and component integrity required for nuclear reactor operation. Manufacturing by PM-HIP consists of (1) producing metal powders by inert gas atomization, (2) filling an empty capsule fabricated from stainless or mild steel with the metal powder, (3) degassing and sealing the capsule, and (4) compacting the capsule to densify the metal powder by HIP at high temperatures and pressures into the shape of the component.

R&D efforts using PM-HIP have demonstrated that large valve bodies and tee sections up to several tons in weight can be produced from 316 stainless steel (SS) powder with mechanical properties such as tensile strength and toughness similar to or better than those of similar, conventionally fabricated SS components. For nuclear applications, the American Society of Mechanical Engineers Boiler and Pressure Vessel Code (ASME Code) currently permits Grade 316 SS components manufactured using the PM-HIP process via a nuclear code case which has been endorsed by the US Nuclear Regulatory commission (NRC). R&D efforts using PM-HIP have demonstrated that Grade 91, creep strength-enhanced ferritic steel (used primarily for fossil generation applications) components can be successfully manufactured with acceptable properties. Although Grade 91 materials such as forgings, seamless tube/pipe, and plate are permitted for use in high-temperature reactors, Grade 91 components fabricated using PM-HIP are not currently permitted. Grade 91 PM-HIP components are permitted by ASME Code for fossil fuel power plants via a non-nuclear code case. PM-HIP low-alloy steel material grades (e.g., A508) which are used to fabricate RPVs, are not permitted for nuclear components and are not governed by any ASTM specification.

A project is underway to demonstrate and test several new manufacturing/fabrication technologies to produce the vital assemblies for a ⅔-scale SMR pressure vessel. Participants in the project are the Electric Power Research Institute (EPRI), The US Department of Energy (DOE), Nuclear Advanced Manufacturing Research Centre (Nuclear-AMRC), and NuScale Power. The new technologies being investigated are PM-HIP, electron beam welding, diode laser cladding, bulk additive manufacturing (weld buildup), and advanced machining. The PM-HIP components to be fabricated as part of the project include an A508 low alloy steel lower reactor head, an upper reactor head, a steam plenum, steam plenum accesses ports, and the upper transition shell. The project will explore the relevance of the advanced technologies to the production of SMRs, advanced light-water reactors (ALWRs), GEN IV plants, ultra-supercritical fossil plants, and supercritical CO_2 plants. One intended outcome of this project is to assemble the data needed to support a nuclear code case to use PM-HIP low alloy steel (A508) to fabricate heavy-section RPV components.

This report covers the development and use of PM-HIP for fabricating NPP components. It includes the technical review of PM-HIP, covering the production and characteristics of SS and low alloy steel powders by inert gas atomization, the components comprising a HIP unit, the important steps involved with producing components via HIP, and the microstructure and properties of SS and low-alloy steel nuclear components produced by PM-HIP. This review is followed by a technical review of the R&D of PM-HIP for producing heavy-section large components of nuclear reactors.

A gap analysis addresses issues and concerns with using PM-HIP to produce heavy-section large components and to assure the quality and performance of the final component. The technical gap analysis addresses aspects of the powder production, HIP processing, and final component properties and

performance, with ranking and discussion for each identified gap. The report also provides an analysis of nuclear codes and standards that already exist for 316 SS, along with those that must be established for low alloy steels such as A508 and Grade 91 creep strength-enhanced ferritic steel. Currently, the primary PM-HIP materials of interest to the nuclear industry are type 316 SS and type A508 low alloy steel. Given the potential future use of Grade 91 PM-HIP components for high-temperature reactors, some limited discussion is provided in this report. Because nickel-based alloys are not of primary interest at this time, they are not covered in any detail in this report, but they may be included in a future update of this report.

The NRC has developed a companion document to this report (Agencywide Documents and Access Management System Accession No. ML22164A439) that provides context to the gaps identified in this report from a regulatory perspective and highlights key technical information related to PM-HIP-fabricated components in NPPs.

1. INTRODUCTION

There is growing interest in the nuclear power industry for manufacturing the structural components of nuclear reactors using powder metallurgy (PM) and hot isostatic pressing (HIP). This interest is mainly driven by the capabilities to produce fully dense, near-net shape components using PM-HIP. A new focus is to use PM-HIP to produce large components of advanced nuclear reactors, including the reactor pressure vessel (RPV).

1.1 COMMERCIAL NUCLEAR REACTOR TECHNOLOGY

All operating US commercial power reactors are light-water reactors (LWRs) which include pressurized water reactors (PWRs) and boiling water reactors (BWRs). These nuclear power plants (NPPs) were licensed for an initial operating period of 40 years [1, 2], and their licenses can be renewed for a period up to an additional 20 years of operation [3], one or more times. These nuclear reactors are constructed of pressure boundary components such as valves, piping, and pump casings, as well as the RPV [4]. The RPV is the most safety-significant component in an LWR, containing the reactor core that is cooled and moderated by water at an elevated pressure during NPP operation. The materials historically used for construction of an LWR RPV must withstand exposure to neutron radiation that can degrade the RPV's mechanical properties. Figure 1 shows the materials typically used to construct the RPV, including 300-grade stainless steels (SSs) for internal reactor components, and SA533 and SA508 low alloy steels for the RPV [2]. The response of the RPV steels to neutron irradiation at operating temperatures and pressures is an important factor in determining the operating parameters and service life of an NPP.

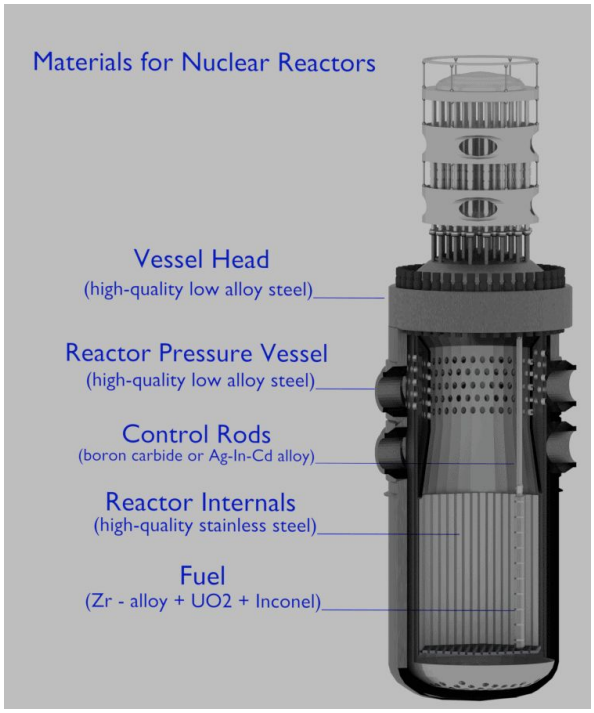

Figure 1. Materials typically used for construction of RPVs, internals, and fuel [2].

RPVs in currently operating NPPs are fabricated from low alloy steel SA508 forgings and SA533 plate. Although some reactor designs currently approved by the US Nuclear Regulatory commission (NRC) permit SA508 as well as SA533, the current trend in RPV manufacturing is to use forgings to minimize the number of RPV full-penetration welds. Forged RPV components are constructed by casting steel

ingots and forging the ingot into the shape of the vessel component. For large pressure vessels, the forging press must produce very high forces with maximum loads measured as tons. As nuclear reactor technologies progress, Generation III+ nuclear reactors require very large pressure vessels, starting with steel ingots that weigh over 600 tons [5]. These large ingots require forging presses with capacities in the range of 12,000 to 17,000 tons. RPVs are produced in sections by welding large forgings together to form the single vessel. RPVs for use in the United States, whether produced in the US or internationally, must be designed and fabricated in accordance with the American Society of Mechanical Engineers (ASME) Boiler and Pressure Vessel Nuclear Code and any additional requirements imposed by NRC regulations. Internationally based companies that produce nuclear components for use outside of the United States use similar standards.

1.2 POWDER METALLURGY-HOT ISOSTATIC PRESSING

PM is a significant industry in the United States and in many foreign countries for manufacturing parts and structural components with metal and metal alloyed powders [6-11]. The PM industry consists of several technologies, ranging from producing metal powders to manufacturing them into solid structural components for a variety of commercial and technical markets. Metal powders are first produced by processes such as atomization, deposition, and comminution, and they can either be blended together or used separately with or without alloying additions. The metal powder is compacted into a dense solid by either (1) cold compaction to form the porous green compact, followed by sintering at elevated temperatures for densification, or (2) hot compaction at high temperatures and pressure, such as HIP, for direct densification of the metal powder. A series of secondary and finishing operations are used to produce the final part or structural component. Metal powders produced by the PM industry are also used in other manufacturing technologies such as mechanical alloying (MA), metal injection molding (MIM), and additive manufacturing (AM) for producing materials with tailored properties for structural applications that may experience high temperatures, high stresses, and corrosive environments [12-17].

HIP of metal powders is a mature processing method used in the PM industries for manufacturing products of different dimensions with simple and complex shapes with near or full density on a multitude of advanced alloy systems. HIP is used for commercial applications in the automotive, tool, power generating gas and steam turbine, and aerospace industries [18, 19]. The HIP process combines high pressures and temperatures for consolidating the metal powders [20, 21]. The early development of HIP occurred in the United States in the mid-1950s at the Battelle Memorial Institute for bonding Zircaloy cladding to uranium-oxide fuel rods for corrosion resistance [22, 23]. The emergence of inert gas atomization (IGA) in the 1960s for producing high-quality metal powders attracted significant interest, leading to extensive commercial growth of HIP and equipment manufacturing primarily in the automotive, aerospace, and aircraft industries [11]. A summary of research activities in HIP applications and an extensive list of metals and alloy powders has been compiled [24]. This list includes aluminum, beryllium, cobalt, iron, nickel, titanium, intermetallic compounds, and refractory metals of molybdenum, niobium, tantalum, and tungsten.

1.3 PM-HIP OF NUCLEAR REACTOR COMPONENTS

The combination of PM and HIP has recently been explored in the nuclear industry as an advanced manufacturing technology (AMT) to produce near-net shaped components in different sizes and dimensions for nuclear reactors [25-27]. Extensive R&D efforts demonstrated that large valve bodies and tee sections up to several tons in weight can be produced from 316L and 304L SS powders by PM-HIP with mechanical properties such as tensile strength and toughness similar to or better than those of similar SSs produced in standard product forms [10, 25, 28-33]. Valve body components have also been produced by PM-HIP using Grade 91 metal powders which exhibited creep properties comparable to the average range of data obtained for wrought Grade 91 [25]. ASTM International published three standards

for use of PM-HIP to produce components such as valves, flanges, and other parts for high-temperature service applications with SS (ASTM A988/A988M), ferritic steel (ASTM A989/989M), and nickel-based alloys (ASTM B834) [34, 35]. ASME Code Case N-834, *ASTM A988/A988M-11 UNS S31603, Subsection NB, Class 1 Components Section III, Division 1,* permits the use of ASTM A988/988M, with additional requirements listed in the code case, for the fabrication of ASME Code Class 1 Type 316 SS components. Code Case N-834 was published by ASME in March 2013 and is approved for use by the NRC; it is listed in NRC Regulatory Guide 1.84 *Design, Fabrication, and Materials Code Case Acceptability,* ASME Section III, Revision 39, December 2021*,* as acceptable for use without conditions. No information is available to suggest that this code case has ever been used to fabricate a pressure-retaining component that has been installed in a US nuclear plant.

There is growing interest in the nuclear industry to use PM-HIP to produce larger components for advanced nuclear reactors. This interest includes but is not limited to the upper and lower head of the RPV for small modular reactors (SMRs) and the shield blanket for the fusion energy International Thermonuclear Experimental Reactor (ITER) [19, 36, 37]. The advantage of producing large components using PM-HIP instead of forgings is that the latter produces internal defects and nonuniform grain structures, whereas the former can produce components with uniform fine grain structure throughout the microstructure and isotropic mechanical properties. Nevertheless, the trend for using PM-HIP to manufacture large components for nuclear reactors is associated with many challenges, such as developing the procedures for powder production and handling and establishing the operating setup for producing large components, such as fabrication of the large steel can that holds the metal powder.

The NRC has developed a companion document to this report (Agencywide Documents and Access Management System Accession No. ML22164A439) that provides context to the gaps identified in this report from a regulatory perspective and highlights key technical information related to PM-HIP-fabricated components in NPPs.

2. POWDER METALLURGY AND HOT ISOSTATIC PRESSING TECHNICAL REVIEW

2.1 MANUFACTURING METHODS

This section addresses the production of powder for nuclear-grade low alloy steels and SSs, as well as HIP for producing the components for LWRs.

2.1.1 Powder Production

The HIP process requires production of high-quality powders to be used to manufacture a variety of nuclear components for current LWRs and advanced nuclear reactors. Gas atomization using primarily argon (Ar) and nitrogen (N) has emerged as the most popular method for producing high-quality powders with spherical morphology and accurate, reproducible compositions of a wide range of SSs, low alloy steels and nickel-based alloys. Guidelines for using gas-atomized powders and HIP to produce components are contained in the three ASTM standard specifications listed above in Section 1.3: A988/A988M, A989/A989M, and B834. The ASTM A988/988M (SS) and ASTM A989/989M (CrMo steels) Standard Specifications permit melting with any method capable of producing the specified chemical composition, to include, but not limited to, air or vacuum induction melting, followed by gas atomization. ASTM B834 (nickel alloys) requires that powder be produced by vacuum melting, followed by gas atomization.

ASME Code Case N-834 was approved in 2013 for use of ASTM A988/A988M, with additional requirements for Section III, Division 1, Subsection NB, Class I components constructed using type 316L SS. This code case specifies using gas atomization to produce powders with an allowable size smaller than 0.5 mm, the storage of powder in N or Ar atmosphere, and the use of protrusions on the steel can that contains the powder for consolidation by HIP. The protrusions are used to verify the density, microstructure, mechanical properties, and other factors of the component.

The development of components for nuclear reactors using gas-atomized powders and HIP have been led mainly by Rolls Royce in the United Kingdom and the Electric Power Research Institute (EPRI) in the United States [16, 21]. In both programs, large components such as the recirculating pump bowl and the valve bodies of 304L and 316L SSs have been manufactured by PM and HIP process with extensive testing and characterization studies. More recently, EPRI teamed with NuScale and Carpenter Powder Products (CPP) to demonstrate the use of PM-HIP for producing heavy-section large components of the small modular reactor vessel. The ⅔-scale mockups, produced so far as part of the project, included the lower RPV head and the transition shell sections which were fabricated as part of the project. The results obtained from EPRI's testing and characterization studies on the PM-HIP low alloy A508 steel components support establishing this manufacturing method as an ASTM standard specification and eventually implementing it into ASME through a separate code case.

2.1.1.1 Atomization Processes

The atomization process is widely used for commercial production of metal and alloy powders [3, 17, 27, 28]. Figure 2 shows the structural components of a gas atomizer [38]. The atomization process involves melting the metal and alloying elements with the desired composition, followed by pouring through a tundish into a nozzle or by forcing through a nozzle where the melt stream interacts with a high velocity stream of liquid or gas. The molten stream disintegrates into droplets and solidifies during cooling, passing through the spray chamber into the collection chamber.

Powder quality and characteristics are influenced by the steps of the powder production process, including the melt method and environment, as well as the atomization method and environment. In general, reducing exposure to air during the melt and atomization processes, such as through use of vacuum or inert gas environments, greatly reduces the levels of oxygen and other contamination and increases powder quality.

The most commonly used atomization processes methods are gas atomization with argon (Ar) and nitrogen (N), as well as limited use of helium (He) gases and water [29]. When the molten stream of metal impinges on the stream of gas, the droplets have a greater chance of forming a spherical shaped particle with a wide range of sizes and size distribution. Small quantities of each gas species can be absorbed in the metal powder during solidification. The use of Ar and N gases is more popular than He because of lower costs for ultra-high purities [39]. However, the heat transfer characteristics in terms of thermal conductivity of He gas are much higher than those of Ar and N gases, which may influence the solidification rate of the molten metal droplet during gas atomization [40].

Water atomization produces irregularly shaped particles with higher oxygen levels than those obtained using gas atomization. Irregularly shaped particles reduce the packing density and increase the likelihood of voids and incomplete densification, whereas higher oxygen levels tend to degrade properties and performance in the final component. Therefore, water atomization is not a suitable powder manufacturing method for PM-HIP components for nuclear reactors.

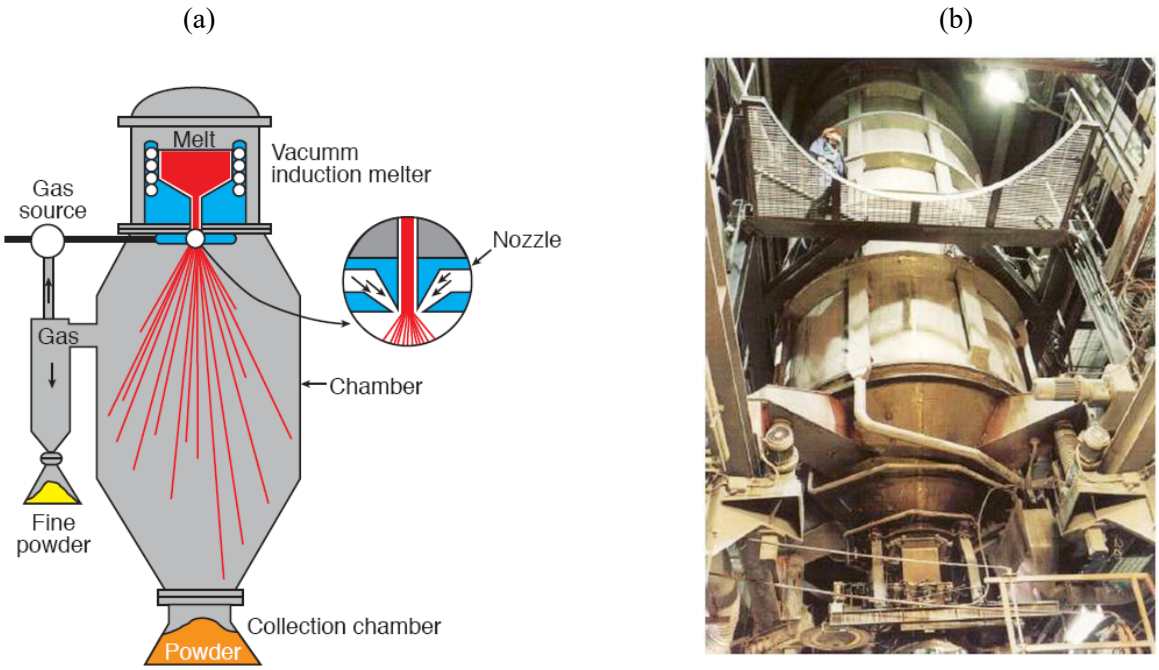

Figure 2. The structural components of a gas atomizer: (a) sketch and (b) image [38].

2.1.1.1 Preparation of Melt

The atomization process begins with melting the metal and alloying elements [41]. The melting methods are based on using a crucible or crucible-less, as shown in Figure 3. Induction heating is the most common melting method. Both induction heating and plasma torch methods use a crucible. The melted metal or alloy flows through a nozzle and into the atomization chamber. The major drawback for using a crucible is the potential contamination from the ceramic material of the crucible and from remnant material remaining on the crucible surface from prior melting batches.

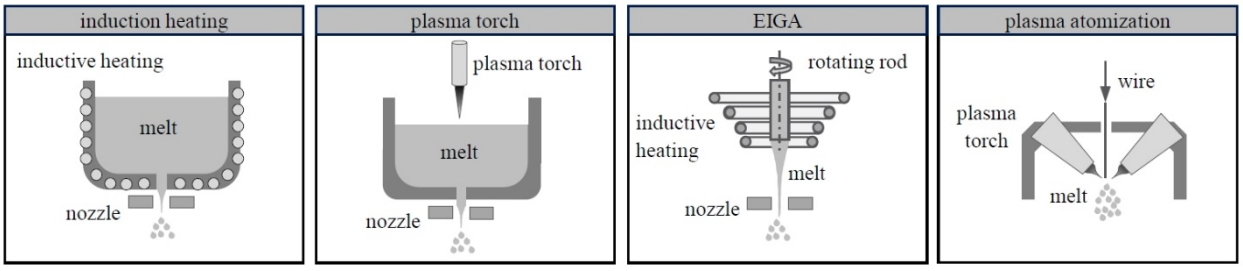

Figure 3. Melt heating methods for atomization and powder production [41].

To minimize contamination of the metal or alloy during the melting process, the electrode induction melting gas atomization (EIGA) and plasma atomization methods do not use a crucible. Both EIGA and plasma atomization melting methods were developed primarily for producing powder from reactive metals such as titanium, zirconium, and several refractory alloys of niobium and tantalum. For the EIGA process, a vertically oriented electrode of the metal or alloy in the shape of a rod is rotated in a specially designed induction coil, which heats the electrode that causes it to melt at one end that then drops into the center of the nozzle. The plasma atomization method is a direct combination of melting and producing powder [41].

In this process, metal or alloy wire is fed into three focused plasma torches, where it is melted and then atomized into fine powder in one step. After the melting process, the metal or alloy then flows by gravity or is forced through a nozzle, where it then interacts with a high-velocity liquid or gas stream.

Primarily three gas atomization powder production methods involve induction heating [35]: air atomization, inert gas atomization (IGA), and vacuum induction melting (VIM) with IGA. *Air atomization* involves air induction melting (AIM) and the use of compressed air jets for atomization. This method results in metal powders with high oxygen contents. The combination of AIM and IGA using Ar and N gases results in spherical metal with lower oxygen levels compared to that obtained using air atomization. Induction melting in air with IGA using nitrogen has been the primary method to produce powders used by EPRI in its work on 316 and A508 PM-HIP components. The use of vacuum induction melting (VIM) with IGA results in spherical metal powders with significantly lower oxygen contents, which favors the production of alloys based on Fe, Ni, and Al that are sensitive to oxidation. Although the VIM-IGA method using N gas is considerably more expensive, it is being explored by EPRI to produce lower oxygen A508 powder to improve impact toughness [16, 42]. Table 1 summarizes the heating and atomization methods, the melt and atomization environments, and the powder characteristics of the different atomization methods for producing metal powders.

Table 1. Methods for heating and atomization and environments for melting and atomization used in different powder production methods [3, 43]

<table>
<tr><th>Powder production method</th><th>Heating method</th><th>Melt environment</th><th>Atomization method</th><th>Atomization environment</th><th>Use / powder characteristics</th></tr>
<tr><td>Water atomization</td><td rowspan="2">Induction or plasma torch</td><td rowspan="3">Air</td><td>Water</td><td>Water / air</td><td>Irregular powder shape with high oxygen levels</td></tr>
<tr><td>Air atomization</td><td rowspan="4">Gas</td><td>Air</td><td>Spherical powder shape with high oxygen levels</td></tr>
<tr><td>AIM-IGA</td><td rowspan="3">Induction</td><td rowspan="3">Inert gas (Ar, N, or He)</td><td>Spherical powder shape with lower oxygen levels</td></tr>
<tr><td>VIM-IGA</td><td>Vacuum</td><td>Spherical powder shape with lowest oxygen levels</td></tr>
<tr><td>EIGA</td><td>Inert gas (Ar or He)</td><td rowspan="2">Used for reactive metals (e.g. Ti and Zr)</td></tr>
<tr><td>Plasma atomization</td><td>Plasma torch</td><td>Inert gas (Ar or He)</td><td>Plasma torch</td><td>Inert gas (Ar or He)</td></tr>
</table>

2.1.1.2 Gas Atomization

The gas atomization process directs a high velocity stream of gas, such as argon, into the flowing metal or alloy stream as it exits the nozzle to form small droplets that then to rapidly solidify to form the powder. The kinetic energy associated with the gas stream is transferred to break the molten stream into small droplets during impact in the spray chamber. The velocity of the gas stream depends on pressure and reaches sonic velocity with pressure of ~0.1 MPa, but higher pressures cause only small increases in gas velocity. Therefore, the kinetic energy transfer by the gas stream to the molten metal stream does not increase above 0.1 MPa [4, 29]. Other factors that also affect the powder size and powder size distribution (PSD) include the melt superheat and gas recirculation. An increase in melt superheat reduces the powder size and minimizes solidification of the melt prior to the dissolution into spherical particles by impingement with the gas stream. After the melt stream is broken up by the gas stream, the particles will spiral around in the spray chamber while solidifying before reaching the collector. As the droplets are spiraling around, they may collide with other particles in the liquid or semi-solid state, forming larger particles and surface agglomerates, or satellites. A gas recirculation system filters most of the gas from

the particles for recycling, which improves the flow pattern in the spray chamber and reduces the migration of particles into the atomization zone. Gas recirculation leads to a decrease in particle size and improvement in the spheroidization of the particles.

In general, the nozzle designs commonly used in gas atomization consist of free fall, close-coupled, and De Laval ultrasonic nozzles [41]. Figure 4 [3] illustrates the three nozzle designs. The free fall nozzle system consists of a large gap that the molten metal fills before it enters the gas stream. When the molten stream impinges with the gas stream, molten metal droplets are formed that then solidify as they fall into the atomizer chamber. The velocity of the gas exiting the free fall nozzle is decreased by the time it impinges on the molten metal stream, which lowers the kinetic energy transfer, resulting in a lower yield of powder with fine size. Close-coupled nozzles use a ceramic metal delivery tube to feed the molten metal to the inner diameter of the gas nozzle exit. This causes the molten metal to form a recirculation zone that wets the bottom of the melt delivery tube where it meets the gas at higher velocities, which shears the melt to form the droplets. The higher gas velocity in the close-coupled nozzle increases the efficiency of producing fine powder sizes compared to the free fall nozzle. However, a problem with the close-coupled nozzle is that the molten metal stream can solidify at the end of the tundish, thus blocking the flow of metal through the nozzle. In the De Laval ultrasonic nozzle, a high-frequency pulsation is applied to the gas stream, accelerating it to supersonic speeds [41]. This nozzle design uses less gas and produces fine spherical-shaped powders with a narrow size distribution of 15 to 45 microns.

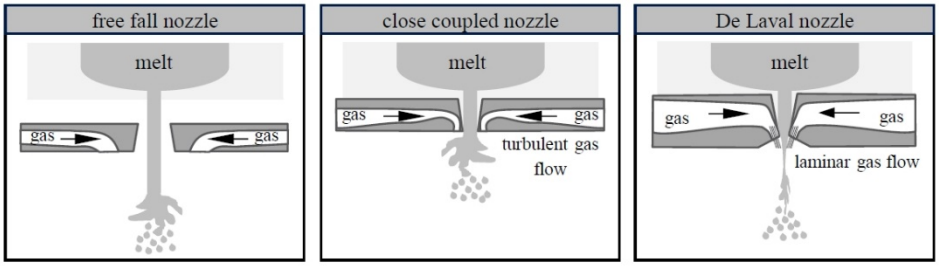

Figure 4. Illustration of nozzles [41].

The pressure-swirl-gas-atomization process is an improved method for decreasing the size and size distribution of metal powders [44-46]. This approach uses a pre-filming step that consists of a pressure nozzle for creating pressure differences of up to 1 MPa on the molten metal to push it into the swirl chamber. The pressure induces rotational and centrifugal forces on the melt stream, causing it to swirl around the inside of the pressure-swirl chamber. Figure 5 [44] illustrates the pressure-swirl-gas atomizer. The molten metal exits through the pressure-swirl nozzle as a conical hollow cone comprised of a thick liquid lamella that decreases in thickness and fragments into large liquid droplets with increasing distance from the pressure swirl nozzle. The atomization process occurs when the high-velocity gas stream from the ring nozzle impacts the liquid droplet stream, causing further fragmentation into smaller liquid droplets that solidify into metal particles. Modeling and simulations of the initial droplet fragmentation process show that it depends on the aerodynamic force that deforms the droplet, as well as the surface tension and viscosity of the molten metal that resist the deformation. The balance between these factors is influenced by the atomization process conditions, resulting in the three types of breakup illustrated in Figure 6 [45]. When surface tension is high relative to the aerodynamic force, the *bag breakup mechanism* occurs, forming a thin disk from the droplet that deforms to a hollow shell, with the center blown downstream forming a large number of small droplets and subsequent breakup of the shell into several larger droplets. A low surface tension relative to the aerodynamic forces results in the *sheet stripping mechanism*. In this case, thin sheets form at the periphery of the thin disk that evolve into thin ligaments and are consumed by disintegrating into small droplets, leaving a core droplet. The *multimode*

breakup lies between the bag breakup and sheet stripping and is characterized by formation of small droplets from the center of the thin disk, along with the formation of a long ligament in the center of the hollow shell that fragments, as the shell forms droplets in many sizes. Overall, the pressure-swirl-gas-atomization method produces metal powders with a very small size and narrow size distribution.

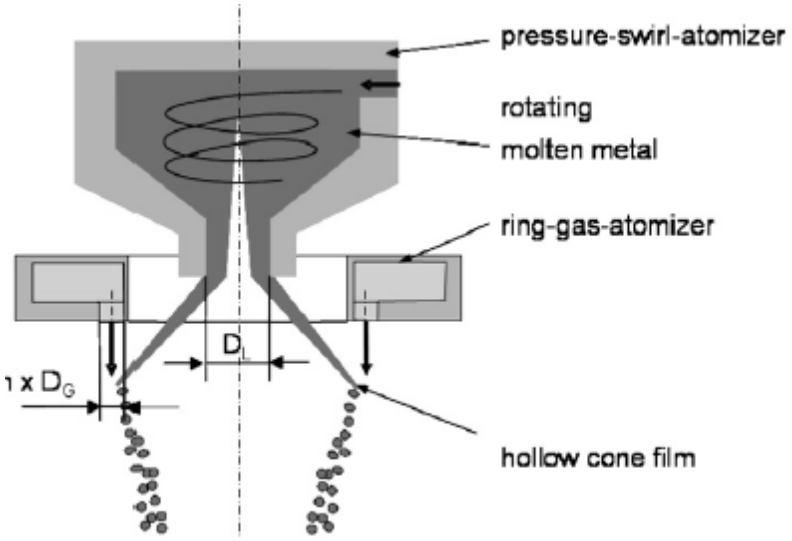

Figure 5. Illustration of pressure-swirl-gas-atomizer [44].

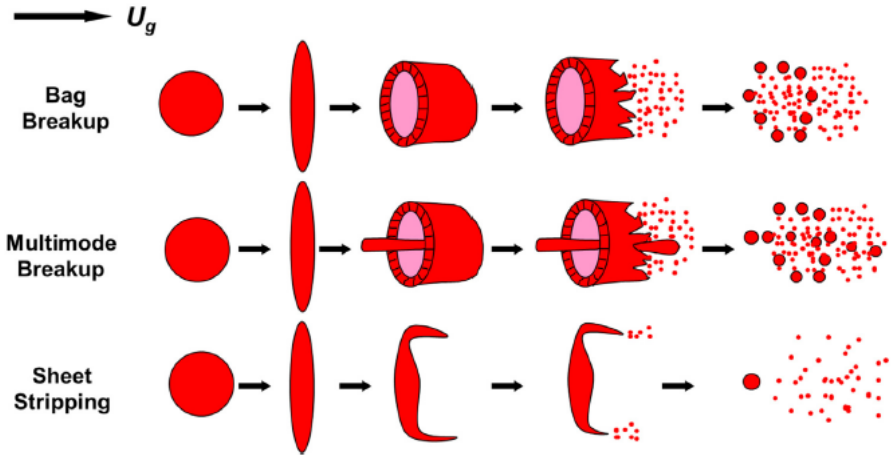

Figure 6. Modes of droplet breakup [45].

2.1.1.3 Economics

The most important economic factor to consider in the choice of atomization method to be used for producing metal powders is the yield within a selected range based on size and mass. In general, the manufacturing costs to produce metal powders by gas atomization are higher than costs for other metal powder atomization methods based on limited data in the literature [47]. This cost advantage is because there is a greater production yield of powder by other atomization methods, such as water atomization

compared to gas atomization. However, the cost effectiveness of water atomization over gas atomization must be evaluated for the product application, because the former produces irregularly shaped powders with greater potential of surface contamination, whereas the latter produces spherically shaped particles with much cleaner surfaces as a result of the protective inert gas. The use of high water pressure to improve the spheroidicity of the metal powder will increase the manufacturing cost [48].

2.1.1.2 Composition

Producing metal powders by atomization is the preferred method, because any composition can be produced accurately to specifications. This is because any combination of metal and alloy raw materials can be melted together to match the desired composition before flowing through the nozzle and into the atomization chamber [17, 41]. To produce high-quality metal powders with low contamination levels, metal stocks of high purity are used to make the melt pool with the desired composition.

As described above, inert gas atomization methods are superior to air and water atomization methods, because the surfaces of the molten metal droplets are protected by the inert gas atmosphere during solidification to form powder with varying sizes that have low oxygen content. Inert gas atomizers based on EIGA or plasma atomization prevent the molten metal from contacting the crucible or liner to further decrease the chances for contamination of components. Therefore, this method is appealing for use with reactive metals or refractory materials.

IGA produces metal powders with compositions that are accurate to specifications and reproducible. This was demonstrated recently in two projects led by EPRI [49, 50]. In one project, CPP produced three ~500 lb heats of A508 steel with Grade 3 Class 1 specification by gas atomization [18]. The particle size of the powder was ≤500 μm. Table 2 shows the chemical compositions of the three A508 heats produced by CPP using a material test report from an actual RPV steel material as guidance. The RPV steel had a C_{eq} of 0.60. The intent was to meet a chemistry close to the actual RPV chemistry as possible, resulting in a hardenability of approximately C_{eq}=0.60. The chemistries of the three heats of powder produced represent low, medium and high hardenability ranges for A508 Class 3 material. The concentration levels of the remaining solute additions were similar, showing the good reproducibility of gas atomization.

Table 2. Comparison of the compositions between the three heats and the ASTM specification for A508 steel

	C	Mn	P	S	Si	Ni	Cr	Mo	V	Cu	Al	O_{63}	C_{eq}
A 508 Cl 3 Min	--	1.20	--	--	--	0.40	--	0.45	--	--	--		--
A 508 Cl 3 Max	0.25	1.50	0.025	0.025	0.40	1.00	0.25	0.60	0.05	0.20	0.025		--
Carpenter Heat 160114	0.20	1.46	0.011	0.003	0.16	0.84	0.13	0.50	0.01	0.02	0.02	0.024	0.62
Carpenter Heat 160115	0.24	1.48	0.012	0.008	0.18	0.85	0.19	0.55	0.01	0.03	0.02	0.022	0.69
Carpenter Heat 160116	0.17	1.26	0.014	0.006	0.18	0.84	0.09	0.48	0.01	0.03	0.02	0.018	0.55

Note: O_{63} and O_{250} denote the oxygen level measured when the powders have been sieved way under 63 and 250 microns, respectively[51] .

The second project led by EPRI assessed three powder manufacturers for producing powder of 316L steels, with guidance on composition specifications to follow [50]. The project goal was for the three powder manufacturers, which were anonymous as A, B and C in the report, to produce enough powder to fill 9 steel cans by each of three HIP providers, X, Y and Z. The dimensions of the steel cans were 15.0 × 15.0 × 40.6 cm, for holding ~50 kg of powder. Each powder manufacturer (A, B, C) supplied about 450 kg of atomized powder to three HIP companies (X,Y,Z). Each of the 27 (9 each from X, Y, Z) steel cans were filled with 50 kg of powder, degassed, and sealed, and they were identified as AX, AY, AZ, BX, BY, BZ, CX, CY, and CZ. Each HIP company applied HIP hold times of 2, 4, and 8 h to each of the 9 steel cans: AX2, AX4, AX8, and so on, for a total of 27 billets following HIP consolidation. This approach allowed a direct comparison of the results from each holding time for the powders supplied by manufacturers A, B, and C.

Table 3 shows the results of chemical analysis—obtained using inductively coupled plasma mass spectrometry and high-temperature combustion—of the 316L powders produced by the A, B and C powder manufacturers. For comparison, the composition specifications from ASTM A988 and the EPRI led project for 316L are included. With the exception of Powder B, which had a nitrogen (N) level of 1,070 parts per million (ppm), which was higher than the 1,000 ppm N specification, the compositions of the three powders were within range or below the set levels of the powder specification. The most significant achievement of the three powder manufacturers was maintaining oxygen (O) levels below the 130 ppm specification.

Table 3. Comparison of the compositions (wt%) of three powders of 316L SS produced by N gas atomization by anonymous vendors A, B and C with the ASTM A988 specification and the powder specification set by EPRI [50]

Element	ASTM A988	Powder Specification	Powder A	Powder B	Powder C
Cr	16.0–18.0	16.0–18.0	17.31	17.14	17.21
Ni	10.0–14.0	10.0–13.0	10.93	10.73	11.26
Mo	2.0–3.0	2.0–3.0	2.20	2.13	2.45
Mn	<2.00	<2.00	0.59	1.30	1.71
Si	<1.00	0.2–0.75	0.55	0.58	0.70
P	<0.045	<0.02	0.001	0.007	0.007
Al	-	<0.01	0.047	0.043	0.047
B	-	<0.01	0.023	0.021	0.023
Cu	-	<0.1	0.033	0.034	0.035
C	<0.030	<0.02	0.012	0.015	0.017
S	<0.030	0.008–0.015	0.009	0.003	0.008
O (O_{63})	-	<130 ppm	110	70	117
N	<0.1	<0.1	0.057	0.107	0.064
H	-	-	5 ppm	3 ppm	8 ppm

2.1.1.3 Morphology

The type of gas atomization used influences the morphology of metal powders. Figure 7 shows the typical shapes of particles of low alloy 4130 steel that were produced by inert gas atomization and water atomization [47]. In general, the steel particles produced by inert gas atomization have spherical morphology (Figure 7a), whereas water atomization produces steel particles with irregular morphology (Figure 7b). For inert gas atomization, the surface tension of the metal or alloy and the heat capacity of the inert gas, which is often Ar, are important factors for producing the spherical particle morphology [17, 41]. The particle shape can vary some with inert gas atomization, depending on the solidification rate of the molten metal droplets. The solidification rate and surface tension of the molten droplets affect the transition from an irregular shape to a spherical shape before solidification. The use of high water pressure can improve the yield of particles with smoother surfaces and spherical shape [52, 53].

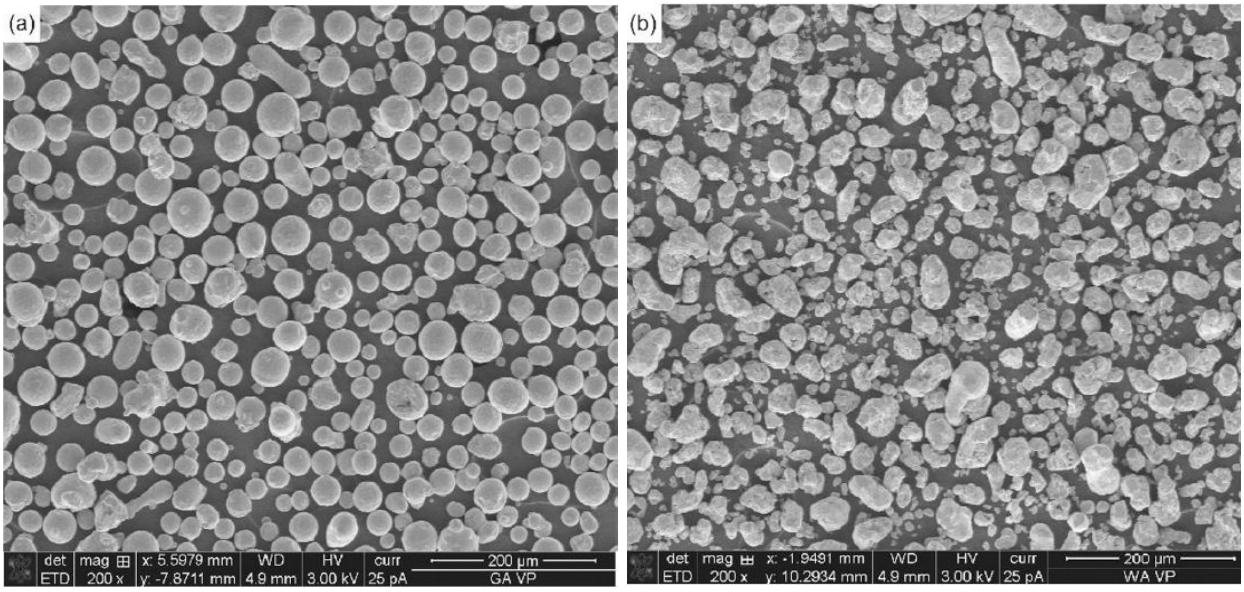

Figure 7. Morphology of 4130 steel particles produced by (a) inert gas atomization and (b) water atomization [47].

The more typical spherical shape of metal powders produced by inert gas atomization may still vary, depending on the processing equipment and parameters used by the powder manufacturer. In the EPRI-led project to assess the production of 316L SS powders, three anonymous powder manufacturers were selected based on their development of improved melting and atomization processes to reduce the oxygen content of the 316L powder to less than 130 wppm. This approach was intended to ensure that good impact properties of the HIP-consolidated product were achieved [50]. The specifications EPRI supplied to the three powder suppliers was for using a nitrogen atmosphere for gas atomization and controlling the particle size distribution with a 500 mesh sieve. Even though these specifications were used by each powder supplier for producing the 316L powder, some differences were observed in terms of spheroidicity and surface defects [50]. Figure 8 shows the 316L powders that were produced by the anonymous powder suppliers identified as company A (Figure 8A), B (Figure 8B) and C (Figure 8C). The results obtained by scanning electron microscopy (SEM) showed particles varying in shape, from spherical to ellipsoidal, with some particles having small protrusions on their surfaces. A more quantitative assessment of the powder morphology was obtained using the Malvern Morphologi G3 system, which samples several thousand particles for good statistics. Based on the assessments using the Morphologi G3 and the SEM, the shapes of the analyzed particles were categorized as (1) highly spherical, (2) slightly spherical, (3) elongated, (4) satellited, (5) agglomerated, (6) deformed, and (7)

fractured. Examples of the powders with these shapes are shown with insets in Figure 8. As seen in the assessment results, the 316L powders produced by manufacturer A showed the highest population of spherical particles and the lowest amount of fraction particles with satellites, whereas the 316L powders produced by manufacturer C contained the highest population of particles with ellipsoidal shapes and the most particles with satellites and agglomerates. The EPRI report did not provide a reason for the differences between the three powder manufacturers [50]. As noted in Table 3, the compositions of the 316L powders showed good agreement with most alloying elements and some variations with O and N levels. Variations in process parameters - such as temperature of the melt prior to entering the tundish of the atomization unit and temperature of the melt stream passing through the tundish - may affect the solidification rate and influence collisions between solidifying particles as they are impacted by the high-pressure gas streams.

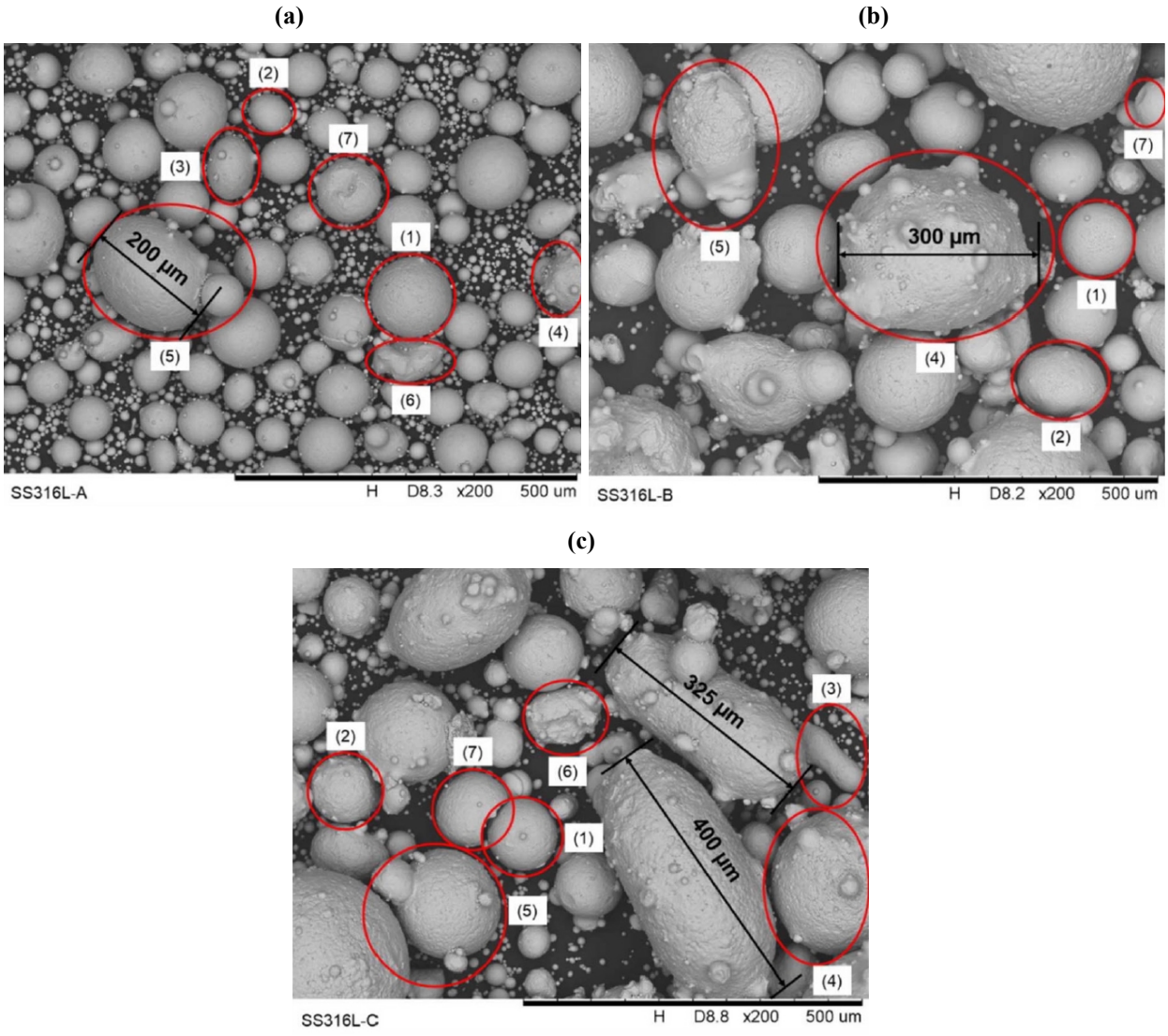

Figure 8. Morphology of 316L SS powders produced by three anonymous powder manufacturers using N gas atomization [50].

2.1.1.4 Size and size distribution

The particle size and size distribution characteristics of metal powders are influenced by the atomization method. Plasma atomization produces metal particles with an average size of 40 μm and with narrow size distribution compared to the average size of 80 μm produced by gas atomization [54]. EPRI reported that the PSD of the 316L SS powders produced by the three anonymous powder suppliers was between 10 μm and 500 μm: the latter powder size resulted from using a 35 mesh sieve to filter out larger powder sizes [50]. For A508 powder that CPP produced by N gas atomization, the unsieved PSD was listed as ≤500 μm after the 35 mesh sieving [49].

When establish a contract with a metal powder manufacturer specializing in gas atomization, it is typical to specify the range of particle sizes required. After producing the metal powders, the manufacturer will sieve the powders through an upper and lower mesh size as established in the contract. For example, a typical upper size powder range would be 500 μm to 150 μm, and the lower size range could be 45 μm. For powders of 316L SS and A508 low alloy steel that were produced by N gas atomization in the EPRI-led projects, the technical specifications were for a powder size of 500 μm or less after sieving [49, 50]. The EPRI project involving N gas-atomized A508 low alloy powder investigated the differences in oxygen content by removing the smallest size powder by sieving into two size ranges of 53–500 μm and 0–500 μm [49]. Typically, powders that are larger and smaller than the sieve ranges are waste, so there is a cost incentive for the metal powder manufacturer to develop the technology for gas atomization that reduces waste by producing powder sizes closer to the desired range.

2.1.1.5 Microstructure

The microstructure of gas-atomized metal powders typically consists of fine grain sizes caused by the rapid solidification of the molten droplets as they pass into the collection chamber. To illustrate this, Figure 9 shows the microstructure of Ar gas-atomized powders with a composition of Fe-14Cr-3W-0.4Ti (wt%), which is the pre-alloyed powder that is mechanically alloyed with $0.3Y_2O_3$ powder to produce the advanced oxide dispersion-strengthened 14YWT ferritic alloy [55]. The pre-alloyed powders were mounted in an epoxy mount and polished using metallographic procedures. A light etch was applied after polishing to enhance microstructure features. The cross-section view of multiple particles in Figure 9a and Figure 9b show the presence of grain boundaries (GBs) delineating grains that have an average size of ~21 μm. Some of the particles contain pores (arrows in Figure 9a) that show dark contrast. At higher magnification, Figure 9b shows the presence of dendrites (D) that formed during solidification by some degree of composition segregation. Protrusions or satellites are also revealed on the surfaces of some particles that result from particle-particle collisions following solidification of the molten droplets.

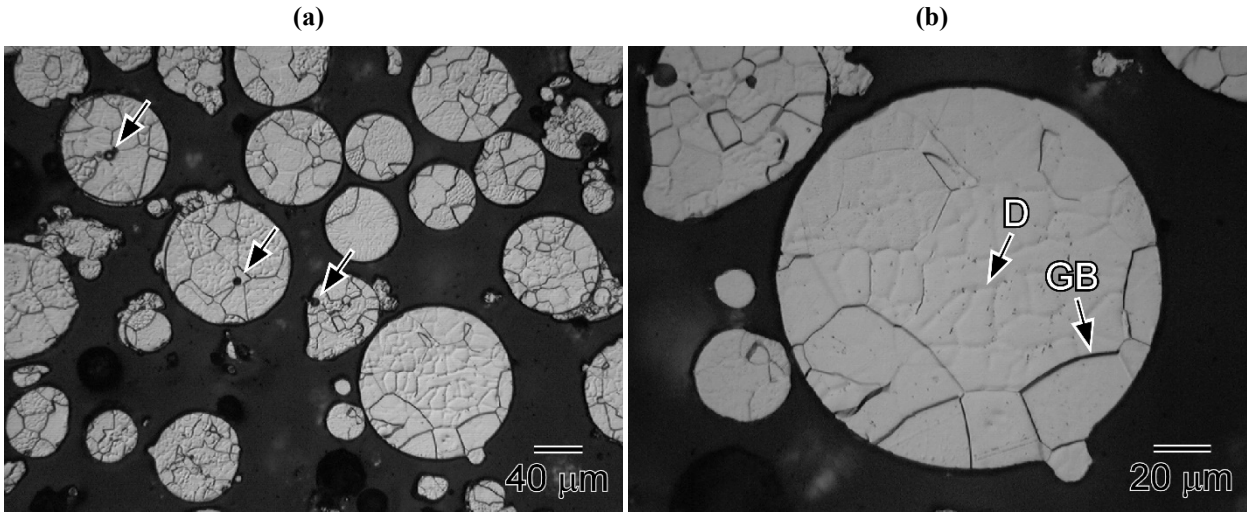

Figure 9. Cross-section view of Ar gas-atomized powders of composition Fe-3W-0.4Ti (wt%).

2.1.1.6 Properties

The physical properties of metal powders that can affect the sintering rate and densification processes during HIP include average size, size distribution, and morphology [51]. The sintering rate of powders is described by a mean particle size and a width parameter related to the breadth of the particle size distribution [56, 57]. Mono-size particles have a higher contact surface area causes particles with a small mean size to sinter and densify faster than particles with a large mean size [57]. Particle size distribution affects sintering rate because the particles with a broad width or large size distribution will sinter at a faster rate than particles with a narrow width [56]. However, it was determined that for mono-size particle distributions, the pores that existed between particles become isolated after the initial sintering stage, causing further densification by bulk and GB vacancy diffusion [57]. In this case, the sintering rate of a broad particle size distribution can decrease vs. that of a narrow size distribution if enhanced grain growth occurs in the microstructure of the particles [57]. The morphology of the particles will influence the packing density of the metal powder, or tap density, which also affects the densification processes during HIP. The tap density of the metal powder is measured by mechanically tapping a container containing the powder, which is lower than the bulk density of the solid product [58]. High tap densities are achieved by using particles with a spherical morphology, a narrow particle size distribution, and a small average size [17, 43]. High tap densities will increase the densification rate of the metal powder and minimize the dimensional shrinkage that occurs with the product during HIP [59].

2.1.2 Hot Isostatic Pressing (HIP)

Metal powders are consolidated into finished products by using compaction and sintering processes to achieve high theoretical densities of ~95–100%, thus ensuring good mechanical, electrical, and magnetic properties of PM products. Metal powders can be consolidated through cold and hot compaction processes. The majority of products produced in the PM industries involve consolidating the metal powders by cold compaction, which involves pressing the powder into to a shape with a green density between ~50–75% of the theoretical density, followed by heating at elevated temperatures to increase the density of the PM product through sintering processes [60, 61]. However, this method would be unacceptable for nuclear system pressure-retaining applications because cold compaction and sintering produce components with insufficient density. Hot compaction avoids many of the problems encountered with cold compaction by applying pressure to the metal powders at high temperatures so that sintering processes result in high theoretical densities [62]. Extrusion and pressing are common methods for hot

compaction of metal powders, but the components produced by these methods have simple geometric dimensions.

HIP emerged in the 1960s in the PM industries as a popular method for consolidating metal powders into solid products by simultaneous application of high gas pressure and high temperature [11, 63-66]. Early development of HIP occurred in the United States at the Battelle Memorial Institute in the mid-1950s to bond Zircaloy cladding to uranium-oxide fuel rods to improve corrosion resistance [22, 59]. The success of this research and the development of inert gas atomization in the 1960s led to extensive commercial growth of the PM-HIP industries [11, 65]. HIP is used for consolidation of powders, diffusion bonding of dissimilar metals and alloys, and elimination of pores from cast, and additively manufactured metals and alloys. HIP is also used to produce ceramic and composite products. HIP products are typically net shape or near net shape. The material properties of HIP products are often fully isotropic, with improvements in strength, fatigue, creep, ductility, and impact properties compared to products manufactured by conventional practices involving casting, thermo-mechanical processing, welding, and machining [59, 63]. Most of the products produced in the PM-HIP industries are relatively small in scale mainly because of limitations of the HIP equipment, capabilities, and the requirements for estimating volumetric shrinkage during consolidation of the metal powders. Challenges for PM-HIP exist primarily when manufacturing large products such as those required in fission and fusion nuclear reactor designs, which will be addressed in Section 2.4.

Consolidation by HIP is one of the few manufacturing methods that can produce fully dense products from metal powder. Figure 10 compares HIP with other pressing and sintering methods based on the final density of American Iron and Steel Institute (AISI) 4640 high-strength, low-alloy (HSLA) steel [59]. Compaction of metal powder by cold pressing followed by standard or high-temperature sintering resulted in densities that are ~88–89% that of the ~7.86 g/cm^3 full density. Warm pressing, including double-pressing and double-sintering, increased the density to ~94% that of full density. Powder forging uses a forging press to compact the powders, as well as a specially designed sintering furnace to consolidate powder close to the full density of the HSLA steel, whereas HIP combines hydrostatic pressure at high temperatures in a furnace that can produce the full density of 7.86 g/cm^3.

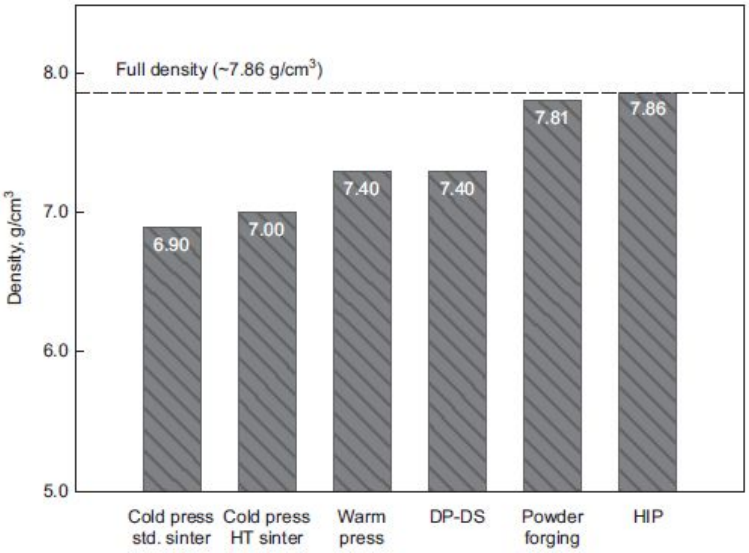

Figure 10. Comparing the density of AISI 4640 HSLA steel achieved using several pressing and sintering methods, powder forging, and HIP [59].

Both spherical and irregularly shaped powders can be consolidated by HIP. High energy ball milling, referred to as *mechanical alloying* (MA), produces irregularly shaped particles that are significantly smaller in size and can cause solid-state reactions between phases [11-13, 67, 68]. MA was developed in mid-1960 by the International Nickel Company (INCO) for dispersing oxide particles in nickel- and iron-based alloys known as oxide dispersion strengthened (ODS) alloys [69]. Because of the greater thermal stability of oxide particles dispersed in the microstructure of ODS alloys compared to carbides and nitrides dispersed in low alloy steels and SSs, ODS alloys are attractive for several applications in advanced nuclear reactors such a fuel cladding in fast reactors that requiring high temperature strength and creep performance and improved resistance to degradation of mechanical properties due to significantly higher neutron doses compared to LWRs.

2.1.2.1 Concept

Products produced by PM-HIP involve the production of metal powder, canning and degassing the metal powder, and consolidating the metal powder to the finished product shape under high pressures and temperatures [11, 21, 63-66]. The most popular method for producing metal powders for HIP is gas atomization due to the flexibility in combining alloying elements to the base metal and producing the alloyed powders with precise composition, high purity levels, spherical shape, and small average size. The metal (alloy) powder is canned in a container, or can, typically fabricated from low carbon steel or SS. In addition, the can material must form an impenetrable seal between the metal powder and the pressurized gas during HIP and must not react with the metal powder at elevated temperatures. The metal powder is added to the can and enclosed by welding a mating lid with a feed-through tube to the base can. The enclosed metal powder is degassed under vacuum at a temperature that promotes desorption of adsorbed molecules on the surface of the metal powder. After this procedure is complete, the feed-through tube is crimped or welded shut to hermetically seal the metal powder in the can. The metal powder inside the can is consolidated with pressure at high temperatures during HIP. In the HIP process, the rate at which the pressure and temperature should be increased, as well as their peak values and holding times vary according to the metal powder properties and the capability of the HIP equipment.

2.1.2.2 Hot Isostatic Pressing Process

In the HIP process, the pressure vessel containing the metal powder enclosed in the steel can is evacuated and filled with an inert gas. Hydrostatic pressure in the form of isostatic compressive forces is applied to the steel can using a hydraulic pump to cause volumetric shrinkage during densification of the metal powder. Heat is applied to the steel can with constant pressure and is held constant at a high temperature that increases the densification rate of the metal powder [21, 59, 70, 71]. Several HIP parameters influence the densification process and the microstructural evolution of metal powder [56], including the ramp rates and holding times of temperature and pressure, as well as powder size, PSD, and chemical composition. The HIP temperature is typically 70-80% of the melting point of the metal or alloy powder to ensure that the applied pressure is significantly higher than the yield strength (YS) of the metal or alloy powder. As a result, consolidation of the powder occurs more rapidly to near or full theoretical density because of the sintering mechanisms and the deformation processes (e.g., plastic flow and thermal creep involving Naborro-Herring and Coble diffusion mechanisms). Higher temperatures also lead to recrystallization and grain growth, which also influence the component's mechanical properties.

Sintering is the main process for consolidating the metal powder by HIP. Initially, the metal powder is composed of individual particles in contact with each other, forming a 3D network of pores. The particles become bonded together during sintering at elevated temperatures, resulting in the formation of necks at the contact points. As the neck diameter between particles increases, the volume of the pores decreases, resulting in the increased density of the PM product. The thermodynamic driving force for sintering is the reduction in total surface area of the pores caused by capillary forces. This process involves the transport

of atoms by surface diffusion between contacting particles [51, 72, 73]. In general, densification occurs with the growth of the bond between particles, with elimination of pores during the early stage of sintering. Significant grain growth and decreasing rate of densification occurs during the later stage of sintering [72]. Figure 11 illustrates the densification process that occurs in the microstructure of 316L SS at different sintering times with no applied pressure. *Note that no micron scale bar is provided for the optical micrographs* in Figure 11. The densification rate gradually decreases as the interconnected pores become isolated, reducing the surface diffusion processes and relying on lower bulk diffusion mechanisms [9, 51, 72, 74]. The reduction of pores continues at a lower rate until the pores are completely isolated and densification is effectively stopped. By applying pressure during HIP at high temperatures, the metal powder consolidates more rapidly to near or full theoretical density because of the sintering mechanisms and deformation processes (e.g., plastic flow and thermal creep involving Naborro-Herring and Coble diffusion mechanisms). Figure 13 shows the typical microstructure of 316L powder after consolidation by HIP [75].

As a result of the reduction of porosity during the sintering processes, products experience volumetric shrinkage. Figure 13 shows the volumetric shrinkage of a 316L SS latch after pressureless sintering. The range of PSD affects the magnitude of shrinkage and the dynamic recrystallization of 316L SS powder [56]. Figure 14 demonstrates the volumetric shrinkage of a large 316L SS valve body powder filled can before and after HIP [75].

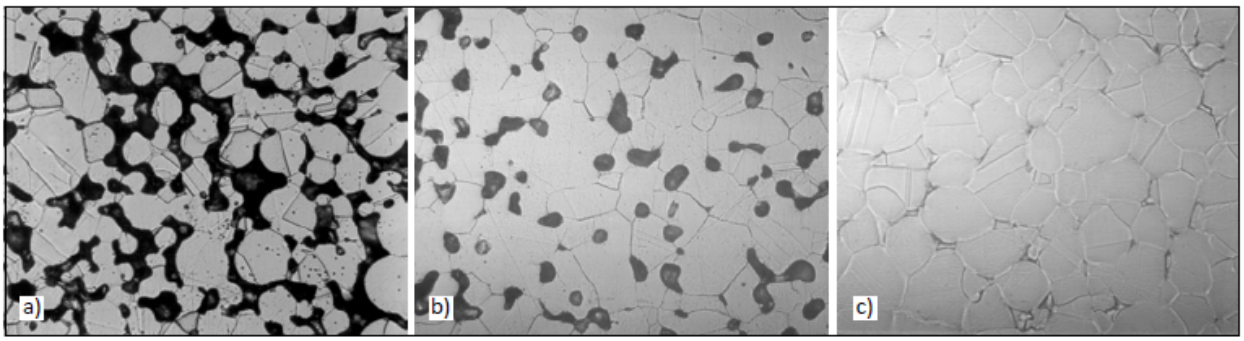

Figure 11. Densification of 316L powder by reduction of porosity during pressureless sintering, with time increasing from (a) to (c) [72].

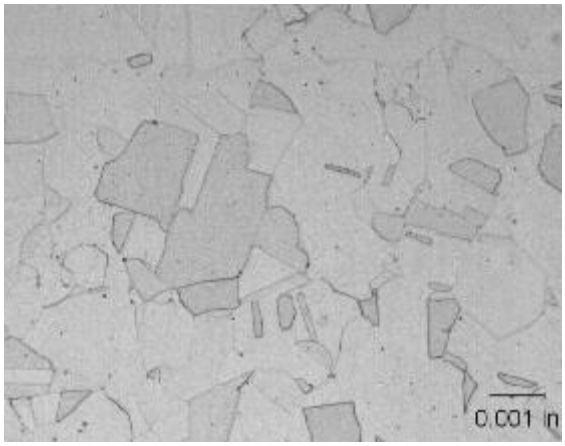

Figure 12. Typical microstructure of 316L produced by PM-HIP [75].

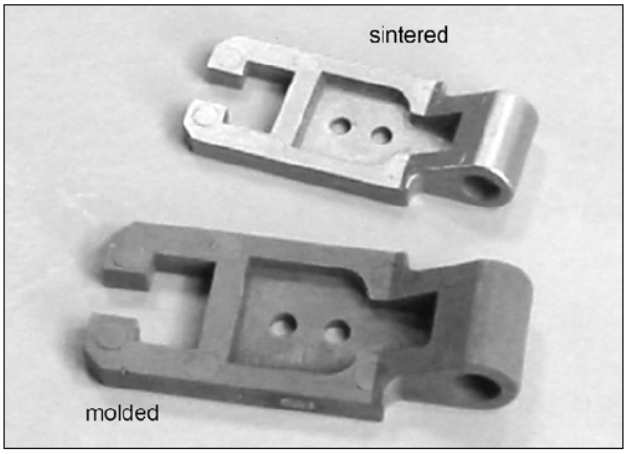

Figure 13. Volumetric shrinkage of SS latch during pressureless sintering [72].

Figure 14. Volumetric shrinkage of large 316L SS valve body powder-filled can before (left) and after HIP (right) [75].

2.1.2.3 Densification

The morphology of the metal powders can affect the amount of volume shrinkage and subsequently whether full density can be obtained [17, 43, 59]. Powders with spherically shaped morphologies fill the volume of the can efficiently. Spherically shaped powders are commonly produced by inert gas atomization processes. Powder processing methods that produce metal particles with irregularly shaped morphologies do not fill the volume of the can efficiently and have a lower tap density, which is measured by mechanically tapping a container containing the powder [58]. Irregularly shaped powders can have tap densities of 50% or less, whereas spherically shaped powders have a tap density of up to 70%. A can filled with metal powder that has a tap density of 50% will shrink in volume by 50% vs. 30% shrinkage for metal powder with a tap density of 70%. To reach full density, the HIP parameters for the powder with high tap density favor shorter times than powder with low tap density using the same temperature and pressure. The temperature and pressure will influence grain structure and the subsequent mechanical properties of the final product.

The characteristics of the PSDs can also influence the densification rate of HIP components [56]. In this study, two 316L SS powders with different PSDs were produced by two powder manufacturers, as shown

in Figure 15. Powder A had a narrow PSD, and powder B had a broader PSD. These powders were consolidated by HIP at 700°C and 75.6 MPa and at 850°C and 92.2 MPa to study the early stages of metal powder consolidation. After HIP, the cans containing the 316L powder were sectioned and characterized. Figure 16 shows the microstructures of the 316L powder after HIP at 700°C and 850°C. These results indicate that very little bonding occurred between the 316L particles by surface diffusion at the 700°C HIP temperature, whereas more extensive bonding occurred between the 316L particles at the 850°C HIP temperature. The backscattered electron (BSE) micrographs show the broader PSD of powder B (Figure 16d) compared to that of powder A (Figure 16c) at the 700°C HIP temperature, which agrees with the PSD plots of Figure 15. Based on 3D x-ray tomography measurements of porosity associated with the 316L powder at the 850°C HIP temperature, the isolated pores are much finer for powder B compared to powder A, indicating that the densification rate occurs more rapidly with the broad PSD for powder B. The mechanism proposed for this observation was that more rapid recrystallization occurred for smaller particles located near the larger particles, resulting in localized plastic deformation that favored diffusion bonding between the particles. The plot in Figure 17 shows the evolution of pores, or void volume fraction, that occurred in powders A and B as a function of HIP temperatures from the start of densification at 850°C to the fully dense condition at 1,050°C. These results show that for any value of void volume fraction, the broad PSD of powder B occurs at a HIP temperature that is nearly 50°C lower than that of powder A, even near full densification at the high HIP temperatures.

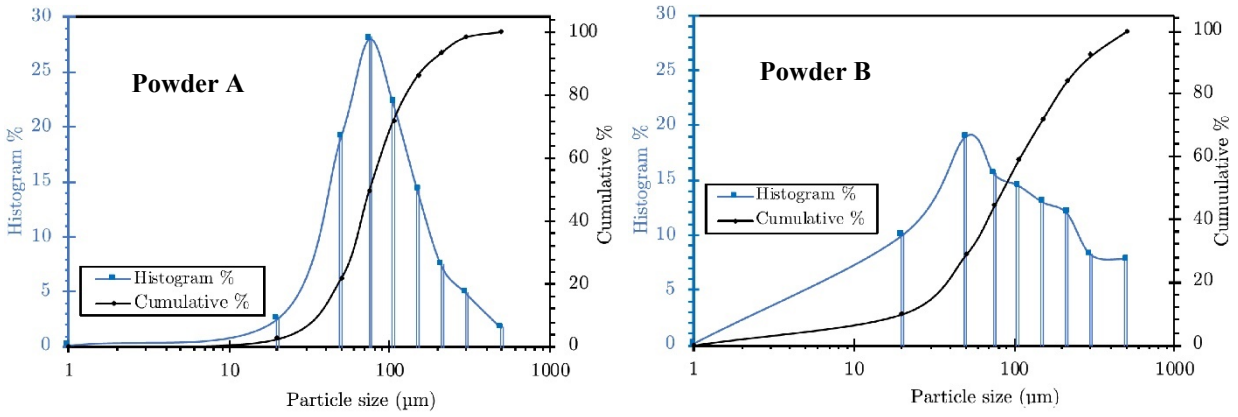

Figure 15. PSD and accumulative percentage for powders A and B [56].

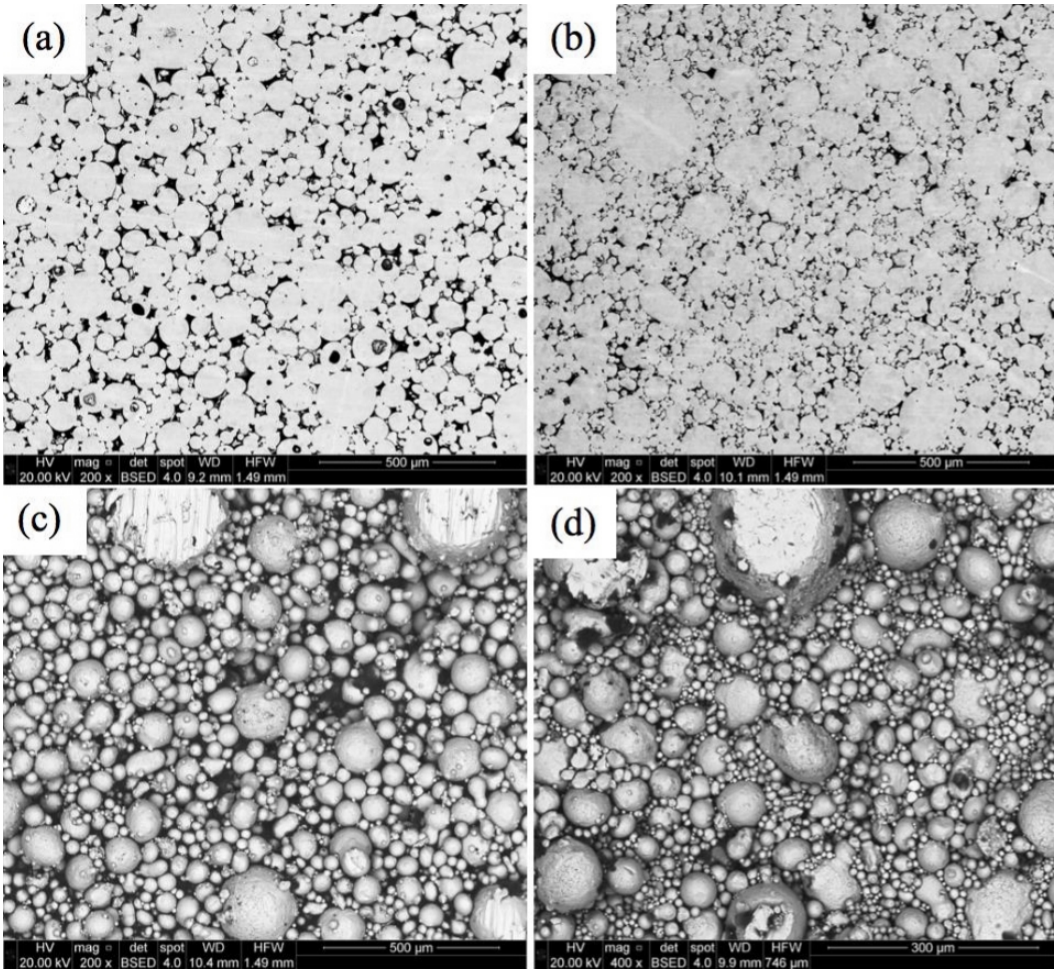

Figure 16. BSE micrographs showing powder A (a) and powder B (b) after HIP at 850°C, and powder A (c) and powder B (d) after HIP at 700°C [56].

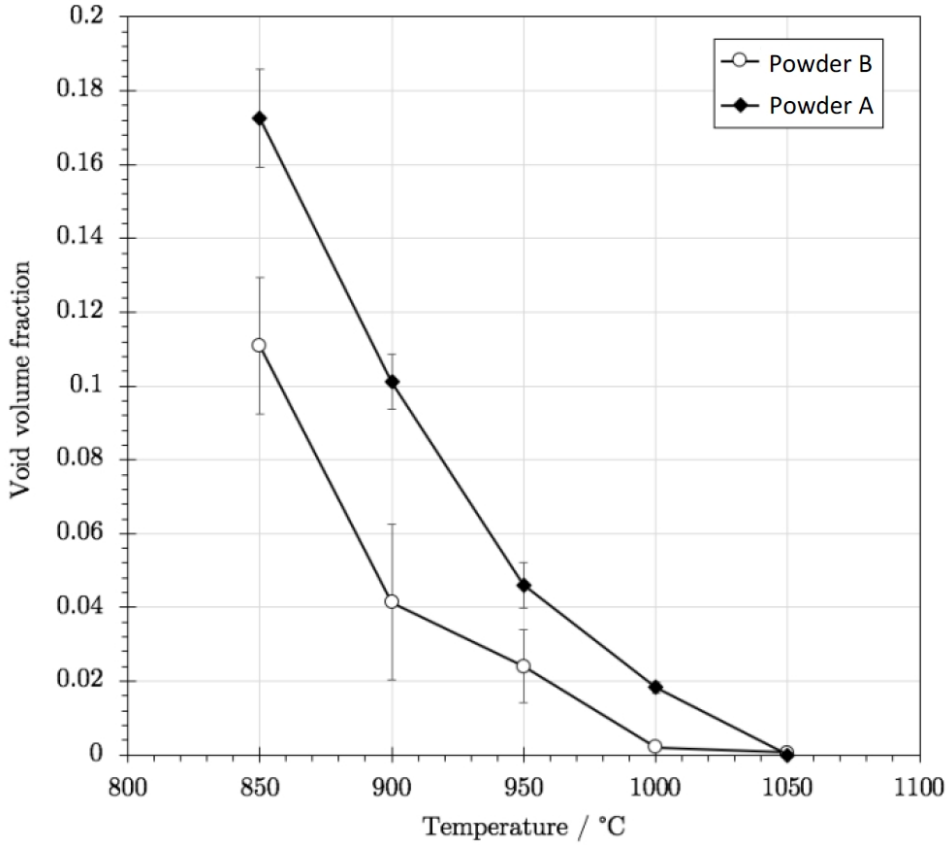

Figure 17. Void volume fraction as a function of HIP temperatures for 316L SS powders A and B [56].

Densification of the PM-HIP component can be measured by two methods, depending on the size and mass of the component. For small components, the density is determined by measuring the weight and volume based on Archimedes' principle, such as hydrometer or hydrostatic balance.

Ultrasonic testing [11], the method used to estimate the density of large components, uses ultrasonic waves that travel through the microstructure of the component to detect internal defects such as porosity.

2.1.2.4 Modeling

Modeling the PM-HIP process has been attractive since the early 1960s for mainly predicting the densification of the metal powder under pressureless sintering and HIP conditions [71, 76-79]. Early simulations of the models attempted to predict density as a function of pressure, time, and temperature of sintering; heating and pressuring rates; as well as aspects of the metal powders such as packing density (green state) and particle size. Most developed models are based on a continuum of mechanics, such as micromechanical simulations and constitutive relations using the finite element method (FEM) to calculate the distributions of stress and density of the metal powder enclosed can [71, 76, 77, 79, 80]. These approaches include plasticity models used to analyze mechanical properties such as yielding and hardening of the metal powder during compaction, and continuum models used to predict the effects of sintering on changes in grain size, densification, and plastic deformation of the metal powders. An early attempt using micromechanics to simulate the densification of a nickel-based superalloy powder is shown in Figure 18 [81]. This study revealed density changes that occurred with a particle size of 100 μm diameter as a function of pressure at 1,175°C (Figure 18a) and a particle size of 50 μm diameter as a function of temperature at 100 MPa (Figure 18b). Both simulations show different regions of

densification based on diffusion processes, power-law creep, and yielding during plastic deformation. The data in both plots showed more rapid attainment of full density with higher stresses at constant temperature and higher temperatures at constant stress. Despite the continuing efforts to develop relevant, accurate models to simulate the densification process during HIP, simulations are still unrepresentative of actual densification because HIP process data related to dimensional changes are not measured and must be either extrapolated or estimated. Other factors include variations in particle size, size distribution, morphology and composition between production lots and effects of temperature and pressure on the HIP components during compaction of the metal powder. Input from the experiences of HIP design engineers remains important for development and use of models for predicting the powder densification and shrinkage behavior and obtaining optimum can geometries and dimensions. These types of computer models provide a general understanding of the effects of pressure, temperature, and time on densification of the metal powder, but they do not predict near-net-shape forming of powder enclosed in steel cans that may have sharp corners and different thicknesses in different sections of the can [77].

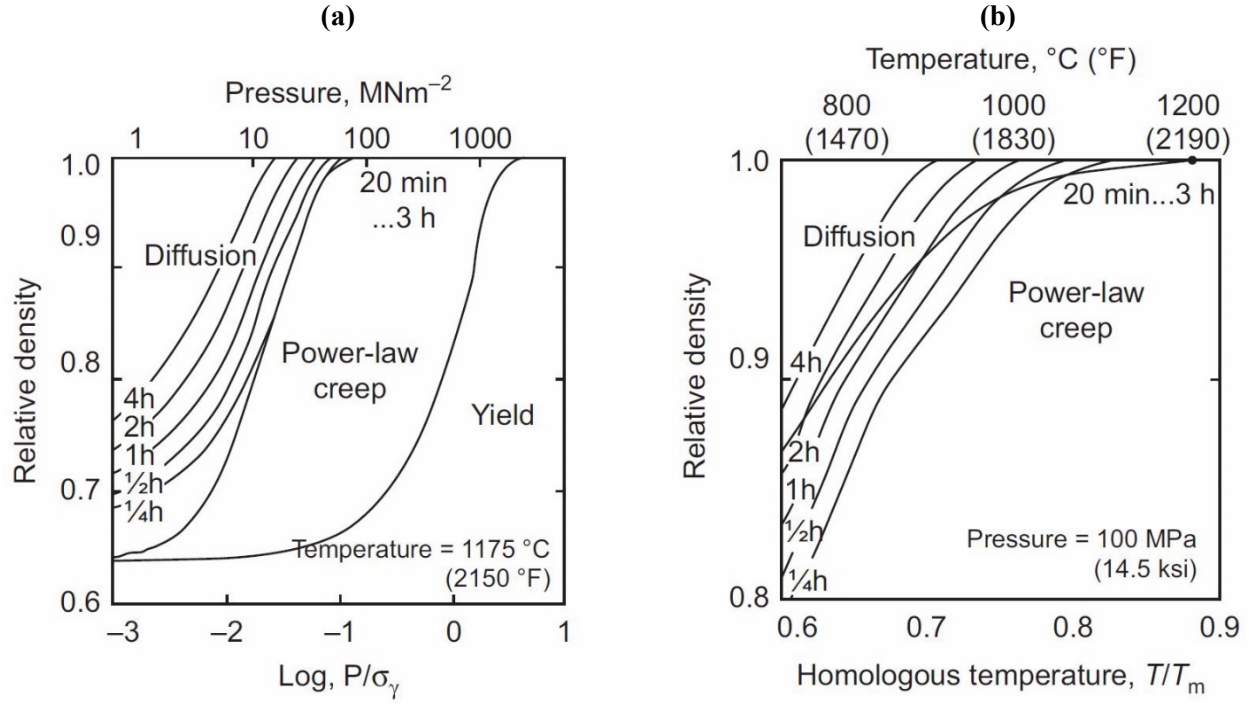

Figure 18. Density maps of a nickel-based superalloy as a function of:(a) pressure at constant temperature of 1,175°C and particle size of 100 µm diameter, and (b) temperature at constant pressure of 100 MPa and particle size of 50 µm diameter. [81] reproduced from [59].

Another focus area arose in relation to near-net-shape forming of metal powders by HIP. Predicting the changes in volume and dimensions that occur with the can during HIP is challenging, especially for cans with complex shapes [77, 80, 82-84]. However, several EPRI-led projects with CPP demonstrated that volume shrinkage of complex can designs during HIP can be predicted within acceptable tolerances for large, near-net-shape components such as a 316L SS valve body and A508 low-alloy steel RPV components for the NuScale SMR design [25, 49, 85, 86]. The work performed by EPRI and others on 316L SS was used to support the development of ASME Code Case N-834, which is based on ASTM A988/A988M Standard Specification, for construction of nuclear components of 316L SS by PM-HIP. The work being performed on the A508 material will be used as a basis for a corresponding ASTM standard specification and will eventually be used to support an associated ASME code case. More details on this topic are covered in Section 2.2.2 on canning**.**

2.2 PROCESSING

2.2.1 Components

The consolidation of metal powders to full density requires high temperatures and pressures that the HIP components must withstand. The main components of the HIP system are the pressure vessel, furnace, gas pressure system and systems for controls, cooling, vacuum and monitoring of temperature, pressure, and atmosphere [63]. Figure 19 shows an image of the EPSI pilot HIP unit and an illustration of the HIP components. The pressure vessel is one of the most important components because it contains the furnace separated by the cooling system and the pressurized gas. The pressure vessel is typically constructed of pressure vessel–quality steels having the required high strength and toughness to ensure safe operation of the HIP through the cycle. The cycle includes heating to elevated temperatures, pressurization of the inert gas, dwell time, and a subsequent cooling period. The size of the work zone contained inside the pressure vessel limits the physical size of the product that can be produced by HIP. The furnace applies heat to the metal powder enclosed in the can by radiation, natural convection, or forced convection [21, 87]. Convection furnaces transfer heat indirectly to the can, whereas radiation furnaces use heat elements to expose the can to direct heat sources. The furnace must precisely transfer heat to the can surface at a specific rate up to the peak temperature, and it must maintain that temperature for the specified dwell time. The furnace also heats the inert gas for transmitting hydrostatic pressure to the can. The properties of the inert gas control the heat transfer mechanisms consisting of conduction, convection, and radiation, and the pressure applied to the container [63]. Argon is widely used as the inert gas in HIP. The cooling system provides thermal insulation between the furnace and the internal wall of the pressure vessel. The properties of the thermal insulation can affect the heating and cooling rates of the HIP cycle. The thermal insulation must protect the vessel wall by keeping it at low temperatures, withstand the high temperatures induced by the furnace, and provide sufficient thermal conductivity for heat dissipation during the cooling cycle.

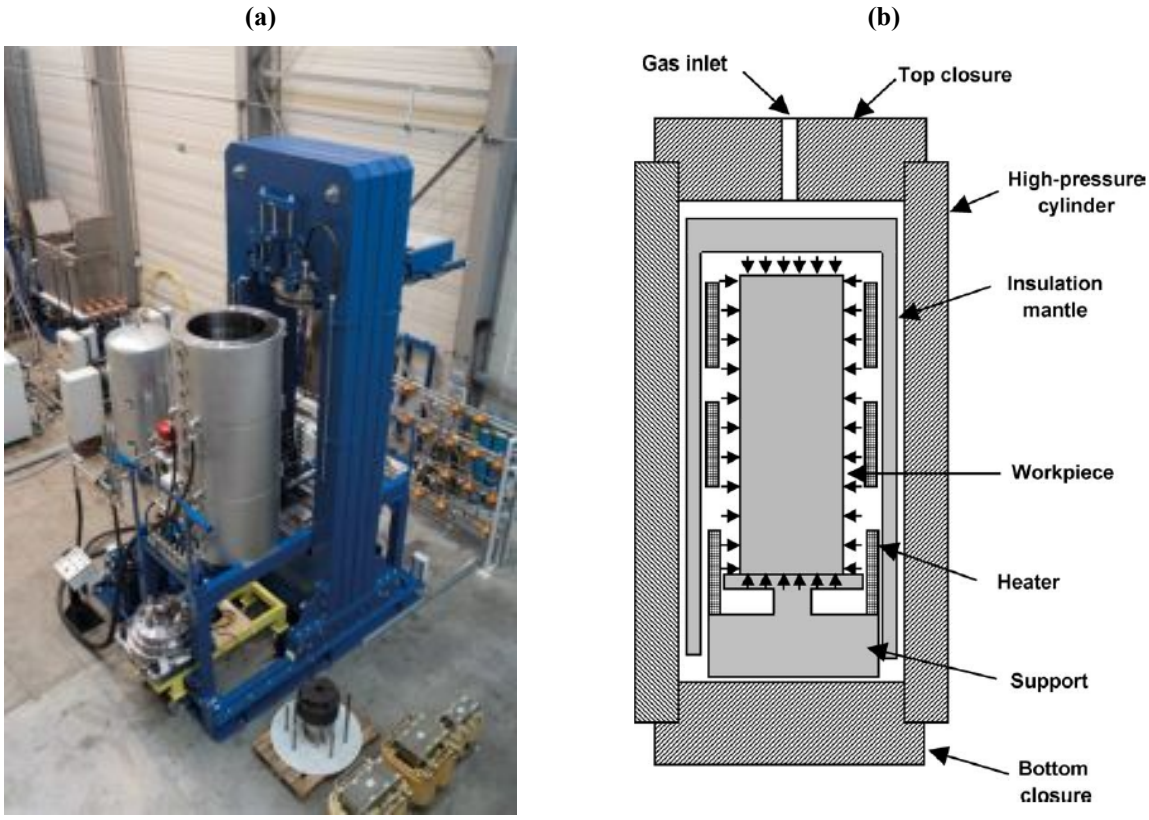

Figure 19. EPSI pilot production HIP unit with up to 16-inch diameter hot zone (a) [88] and illustrated the components of a HIP system (b) [63].

The gas handling system uses a compressor to pressurize the gas-which is usually Ar but can also be He and N-which induces the hydrostatic compressive force on the surface of the can containing the metal powder. The Ar gas produces convective thermal heat as a result of its large coefficient of thermal expansion [21, 63]. The heat generated by the furnace and the convective thermal heat cause an increase in pressure. An increase in Ar gas density will promote better heat transfer to the can, resulting in rapid heating [21]. The compressor must maintain the Ar gas pressure as the furnace heats the can to the HIP temperature, and it must also increase the gas pressure to the desired HIP pressure. Several preferred compressor designs are available for different HIP conditions based on peak pressures, the ability to reuse Ar gas, and the purity of the Ar gas [21]. Multiple thermocouples in the HIP unit measure the temperature in different zones of the pressure vessel and provide feedback to the control system to help maintain the desired heating rate to peak temperature, dwell time, and subsequent cooling rate to room temperature [21, 63].

2.2.2 Canning

The canning stage is important for producing products by HIP from metal powder. The can used to enclose the metal powder will undergo extensive volumetric shrinkage to the final shape of the product during HIP. The materials used for fabricating the can must have high strength for dimensional stability and ductility for plastic deformation during the dimensional reduction of the can to the fully dense product. The materials typically used for fabricating the can are SS and low carbon steels based on their combined strength and ductility properties. High isotropic stresses at high temperatures are applied to the can, which must completely enclose the metal powder from the surrounding atmosphere during volumetric shrinkage during HIP. The wall thickness of the can is important to consider. The can must be

thick enough to not crack or fail during the HIP process, but not thick enough to resist plastic deformation compared to thinner wall. ASTM PM-HIP specifications require that the can material be selected to ensure that it has no deleterious effect on the final product. For the work performed by EPRI to date, low carbon steel has been used to manufacture the cans. Low carbon steel would not be expected to have a negative impact on SS or low alloy steel components, and there is no indication from the work performed so far that would indicate otherwise.

The design and geometric dimensions of the can are important factors that must be optimized for predicting the volume shrinkage and to minimize post-HIP machining of the can from the product. For small products and can designs with simple geometric dimensions, such as a rectangular shaped billet, the volumetric shrinkage is more easily predicted by trial and error. More complex can geometries are required to produce products with near-net-shape and full theoretical density. Models are required to predict volumetric shrinkage for complex can designs. This also applies to very large can designs, because the number of large products typically produced by PM-HIP is limited. An investigation to optimize the can design for producing a near-net-shape thick wall tube with 316L SS powder combined constitutive models with finite element analysis to predict the densification and deformation of the powder during HIP [80]. The densification process was modeled using power-law creep. The initial can design was based on 304 SS with an inner (30 mm diameter) and outer (76 mm diameter) tube and 2 mm thick plugs for the top and bottom of the can, with a ventilation tube of 8 mm in diameter and 1 mm thickness on the top plug for degassing [80]. The desired shape of the tube after HIP was 50 mm in height with a 70 mm outer diameter and a 40 mm inner diameter. No optimization of the can was conducted on the initial can design. Figure 20 shows the initial can design prior to HIP and after HIP at 1,125°C, with 100 MPa pressure for two h. The final product was fully dense, but there were cusps at the top corners and a concave shape near the center that differed from the desired shape of the product. The finite element calculations based on the constitutive model using power-law creep agreed favorably with the experimental data.

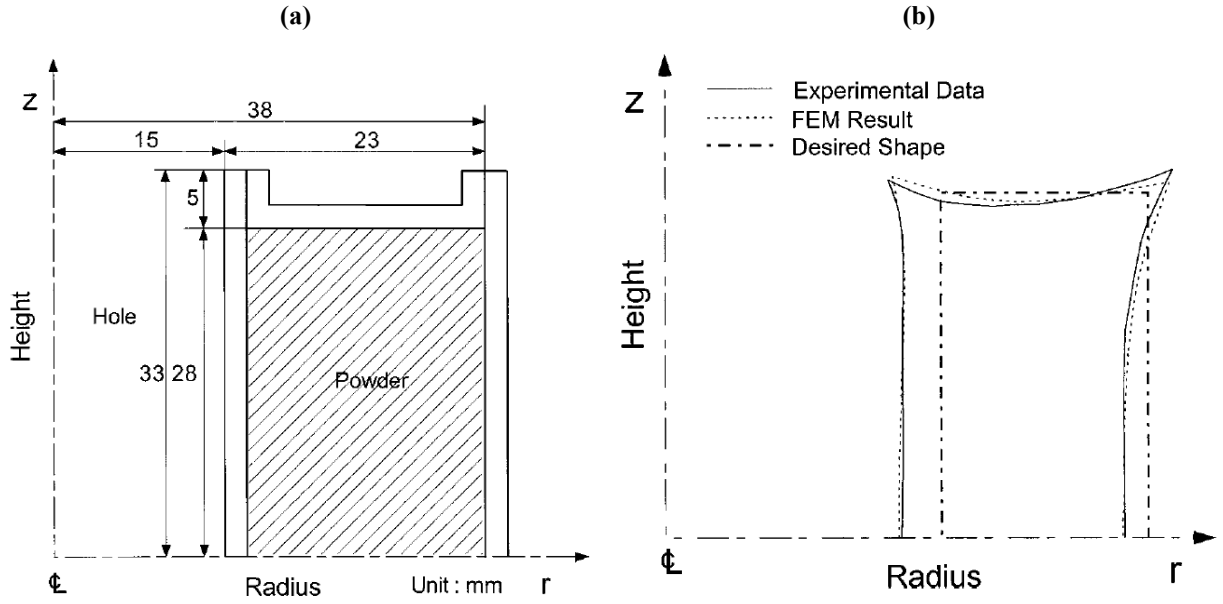

Figure 20. Initial can design for HIP of 316 SS powder: initial can design prior to HIP (a), and desired shape (b) (experimental data recorded during HIP and finite element calculations) [80].

For producing the thick wall tube from 316L SS powder in the desired shape, an optimization technique using finite element meshes was applied to the can design. Figure 21 shows the can shape from the

optimization technique prior to HIP, along with the desired shape and the shape based on the experimental data from the can after HIP. In the optimized shape, the can has convex shaped sides because those surfaces experienced more shrinkage during HIP. Following HIP, the final shape of the product has very small cusps of 0.4 mm at the upper right corner. The agreement between the experimental data and finite element calculation was +/-0.2 mm, indicating that the model for optimizing the can design and predicting volumetric shrinkage developed in this study is very useful for items produced with near-net-shape by PM-HIP. Figure 22 shows cross sections of the modified can design shape based on the design shown in Figure 21 before (a) and after HIP (b). The modified can design used a convex shape on the external surface, with the maximum diameter of the can at the midpoint of the tube length axis, which resulted in the desired shape of the thick wall tube of 316L SS.

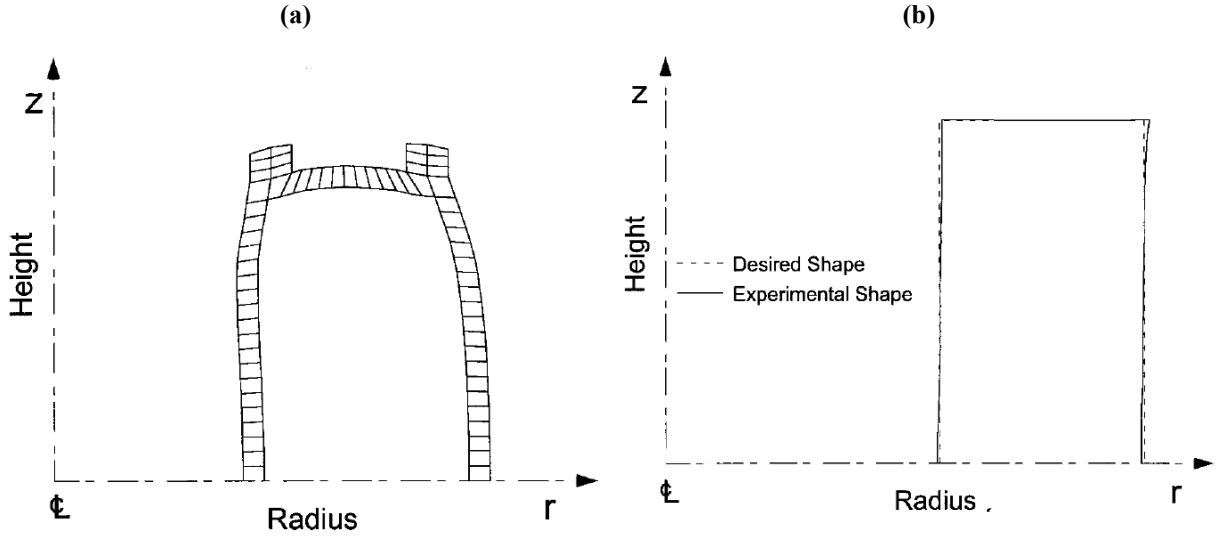

Figure 21. The optimized can design for HIP of 316 SS powder: can design after optimization based on finite element calculations prior to HIP, (a), and desired shape and experimental shape of the can after HIP (b) [80].

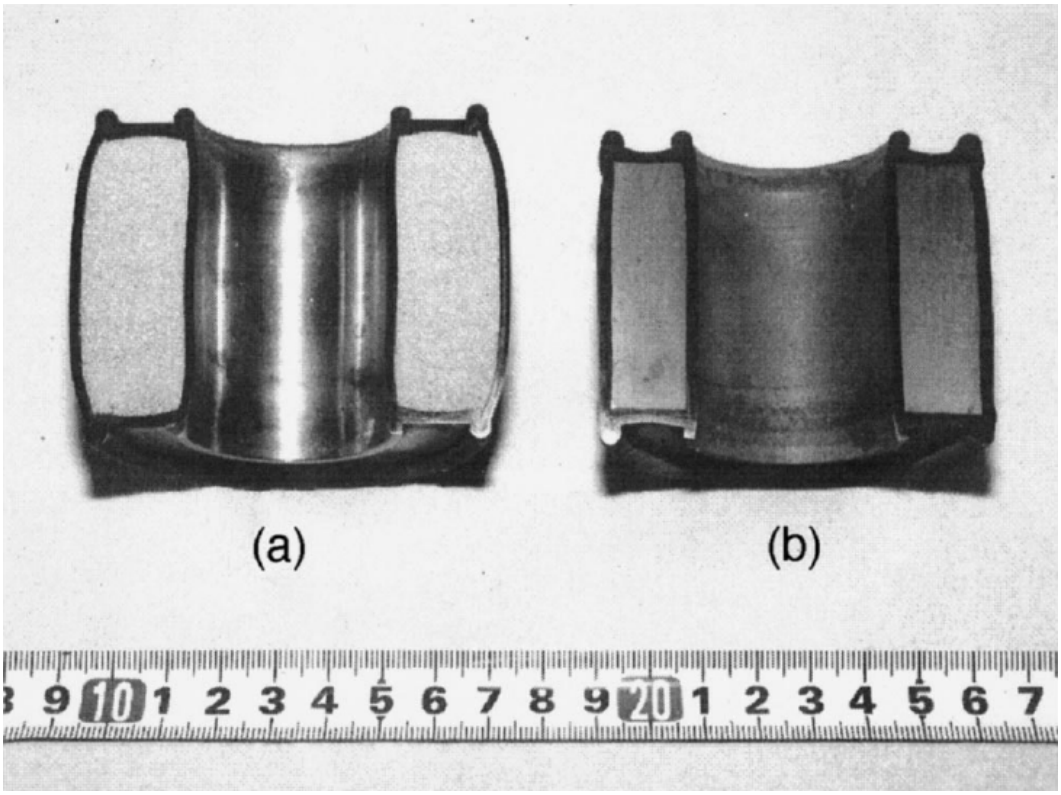

Figure 22. Cross-section views of consolidated 316L SS powder after optimizing the model to predict volumetric shrinkage during HIP: initial can design, (a) and consolidated thick wall tube with desired shape after HIP (b) [80].

2.2.3 Degassing

The degassing of metal powders enclosed in the steel can prior to HIP is a very important processing step. After gas atomization of the metal powders, care must be taken to control the atmosphere surrounding the metal powders during storage and transportation from the powder manufacturer to the customer. Because of the large surface area of metal powders, adsorption of air molecules will occur if they are not protected. Air is the most common contributor to contamination of metal powder. The most common components of molecules in dry atmospheric air are N_2 (~78%), O_2 (~21%), Ar (~0.93%), and CO_2 (~0.033%) in volume percent. The partial pressure of water vapor varies considerably: for example, for a relative humidity of 50% at 20°C, water vapor is equal to the third largest component of air [89, 90].

The adsorbed gas molecules can interact with the metal atoms at the surfaces of the particles by physisorption and chemisorption processes, which depend on the type of bonding that occurs [89, 90]. The bonding energy of physisorbed molecules is low (~ <8 kcal/mole) and is time-dependent, whereas the bonding energy of chemisorbed molecules is higher (~ >15 kcal/mole). An example of physisorption bonding is Van der Waals, and for chemisorption bonding, examples are hydrogen, ionic, or covalent. It should be noted that the chemisorbed state of bonding is not related to the bonding in an oxide or nitride state because a different potential energy condition exists for the oxide or nitride. The amount of contamination that occurs on the surfaces of the metal particles will depend on the adsorption gas coverage, which is a function of the sticking probability of the molecules and the mobility of the molecules on the particle's surface. The sticking probability is the probability that an impinging gas species will adsorb onto the particle's surface as a function of the gas pressure and temperature either in air or in a closed storage container. The mobility of molecules on the particle's surface depends on the

heat of desorption and the bonding characteristics of the molecules with the solute atoms associated with the metal powder. The primary role of degassing is to remove the molecules from the surface of the metal particles by desorption.

Once the metal powder is loaded in the steel can, the degassing operation involves the simultaneous evacuation of the can using a vacuum pump while increasing the temperature of the steel can for a specific length of time [90, 91]. Proper degassing conditions must be used for successful desorption of all adsorb molecules associated with contamination. However, several factors should be carefully considered to ensure an effective degassing operation. Degassing effectiveness is influenced by the combination of the vacuum pump properties (e.g., pressure, flow rate) and the design and placement of the degassing ports and lines connecting to the pump.

The design and placement of ports on the steel can are important for the process of filling the can with the metal powder and for the degassing operation when connected to the vacuum pump. The diameter of the port(s) used for degassing and the diameter and length of the vacuum line (pipe or hose) connected to the vacuum pump are critical factors for the degassing operation, because they affect the conductance and flow properties of the gas molecules. In general, it is important to ensure that the vacuum lines and ports have sufficient conduction for gas flow by having large enough diameters and short enough lines connecting to the pump.

In addition to the vacuum lines and ports, the type of vacuum pump and the level of vacuum pressure that can be achieved will influence how effectively the desorbed molecules from the metal powder surfaces are removed by the vacuum. The pressure and temperature of molecules in the gas phase will influence the interactions that occur between a molecule and another molecule and with surfaces of the metal powder and internal surface of the can, depending on the molecular impingement rate per unit area and the molecular mean free path.

There are three gas flow regimes (viscous, transition, and molecular) that depend on the vacuum pumping speed and the conductance of the port(s) and vacuum line. An effective degassing operation is designed to produce molecular gas flow in the system. For molecular gas flow, a vacuum pump rated for a very low pressure of less than ~10^{-6} Torr is used so that molecular collisions occur with the internal surfaces of the steel can, and gas removal is more effective. The molecular gas flow regime is obtained with high vacuum pumps, including diffusion, turbomolecular, ion, sputter ion, and cryogenic pumps. Viscous gas flow occurs by either laminar or turbulent flow when the vacuum pressure is relatively high, such as when a mechanical vacuum pump is used that can only reach pressures of ~10^{-2} Torr. In viscous flow, the probability is high for gas molecules to collide, resulting in slow-flow kinetics of the gas and a poor gas removal rate. A less ideal situation (but better than viscous flow) is the case in which the vacuum pressures reach the transition gas flow regime and include both molecular/molecular and molecular/wall surface interactions.

In addition to removing desorbed gas molecules, it is also important to consider the removal of adsorbed molecules from the surface of the metal powders. In general, the factors controlling the adsorption of molecules on the surface of the metal powders are similar to those that control the desorption of the molecules during degassing. However, the use of a high degassing temperature can promote the transition from physisorbed molecules to chemisorption, thus resulting in stronger chemical bonding of the molecules with the surface atoms on the metal powders. This will make it more difficult to desorb the molecules, especially for a compound such as an oxide phase forms. Therefore, the degassing temperature should be carefully controlled to avoid chemisorption from occurring.

2.2.4 Cycles

The PM-HIP process is implemented through temperature, pressure, and time cycles [21, 59]. Figure 23 shows a typical time cycle that involves an increase in temperature and pressure at a specified rate, or *ramp*, to the peak temperature, where it is held constant for a period of time, or *soak*, followed by the cooling state. During the cooling state, temperature and pressure are decreased to room temperature and atmospheric pressure. A typical PM-HIP cycle can last 12 h [18]. A HIP cycle can be modified in any way, depending somewhat on the capabilities of the HIP unit. For example, Figure 23 shows the temperature pressure profiles for conventional (broken line) and rapid cooling (solid line) HIP cycles. In this example, the pressure is increased first, and then the temperature is increased, reaching the peak HIP condition at the same time. In addition, the cycle may involve increasing the temperature before starting to increase pressure while reaching the peak at the same time, or simultaneous increases in temperature and pressure while reaching the peak at the same time. Rapid cooling rates can be used to avoid formation of detrimental phases, or it can allow solution heat treatment to be performed simultaneously with the HIP process [59]. The different cycle profiles also depend on the properties of the powder and considerations of processing time [21].

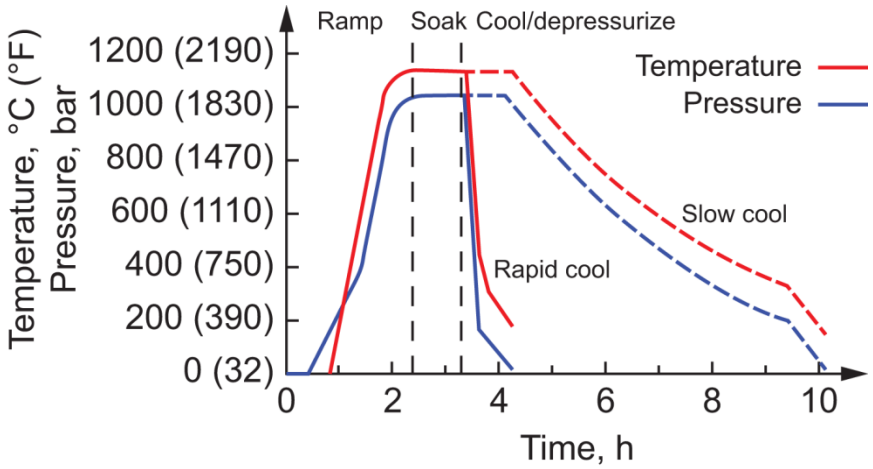

Figure 23. Typical HIP cycle with conventional cooling rate (broken line) and rapid cooling rate (solid line) [59].

2.2.5 Cooling Rate

An early objective in PM-HIP development was to reduce distortions caused by uneven temperatures in the enclosed metal powders, or workpiece, during cooling [21, 42]. In cans with complex geometries, differences in the thicknesses of sections enhance the distortions resulting from uneven cooling rates caused by gas flow disturbances on the component's surface. The cooling cycle requires a high heat transfer coefficient (α-W/m^2°C) for the pressurized Ar gas to reduce temperature differences between the sections of the can with different thicknesses. Reducing the cooling rate can reduce the temperature differences, but it adds time to the cooling cycle. Using a fan to increase the heat transfer coefficient of the pressurized gas minimizes the gas flow disturbances on the surface of the workpiece and produces less distortions [42]. Reducing distortions during cooling produces products with improved mechanical properties.

2.2.6 Heat Treatment Capabilities

Heat treatments are important for controlling the evolution of SS and low alloy steel microstructures to the final condition that results in the desired properties for the application. Heat treatments of PM-HIP

components can be conducted after HIP with the consolidated metal powder still enclosed in the steel can. In some cases, heat treatments can be integrated into the HIP cycle to obtain the final microstructure of the component. Depending on the composition of the stainless or low alloy steel, heat treatments typically consist of a high-temperature austenitizing or solution heat treatment, followed by rapid cooling to lower temperatures for tempering. To accomplish this, new developments in HIP technology have enabled very fast cooling rates to be achieved under isostatic pressure [70, 71]. These HIP units contain an ultra–high-pressure Ar gas system for forced convection cooling of the component following the cycle stage, during which pressure and high temperature lead to densification of the metal powder. This in-situ heat treatment can generate cooling rates that allow martensite to form in steels with the appropriate compositions. After the quench, heat will be applied during the cycle to reach the temperature for tempering.

2.2.7 Witness Specimens and Protrusions

To confirm the quality and performance of the PM-HIP component for the intended application, material for conducting tests to determine the microstructure, mechanical properties, and corrosion can be machined directly from a separately produced witness specimen or from a protrusion on the component(s) to be HIPed. For example, Code Case N-834 requires that a protrusion (extension or prolongation) of 8 in. (200 mm) or longer be added to one end of each item. The protrusion must equal or exceed the thickest section of that item. The protrusion is removed upon completion of the HIP process and heat treatment and is then used for microstructural characterization, density measurements, chemical testing, mechanical testing, and intergranular corrosion testing. Alternately, a witness specimen , which is a separate can (capsule) filled with the same powder and placed into the HIP unit with the component(s), can also be used for testing.

Witness specimens must be of a dimension and size that are relative to the component. Protrusions, which are designed and fabricated on the steel can that contains the metal powder during HIP, must be of suitable size, number, location, and orientation relative to the steel can. When producing heavy-section large components by PM-HIP, the dimensions of the witness specimens and protrusions should correlate with the largest thickness of the component. This ensures that microstructural inhomogeneities that may occur in the heavy-section large component are captured in the witness specimens and protrusions for correlation with mechanical property measurements. These inhomogeneities occur as a result of variations in the metal powder's tap density, variations in localized densification rates, and variations in surface and internal cooling rates. In the structural integrity requirements of ASTM Standard Specifications A989/A989M for HIP of alloy steels, A988/A988M for HIP of SSs, and B834 for nickel-based alloys, samples can be taken from the component stem, protrusion, or test part (witness specimen) that is made from the same powder consolidated in the same HIP unit using the same pressure, temperature, and time parameters and heat treated in the same final heat treatment charge after HIP.

It becomes impractical to confirm the density of heavy-section large PM-HIP components by traditional methods that are typically feasible for small PM-HIP components based on Archimedes' principle (e.g., hydrometer or hydrostatic balance). Therefore, the use of witness specimens and protrusions may be the only practical method for measuring the density of heavy-section large components. Options described above should be used to design the dimensions of the witness specimens and protrusions based on the steel can of the large component. Nondestructive methods such as ultrasonic testing are effective for estimating the density of large components produced from SSs and low alloy steels [81].

2.2.8 Can Removal, Surface Finish, and Post Processing

Once the product is produced by HIP, the can material must be removed. ASTM Specifications A988 (SS) and A989 (CrMo steel) require that, unless specified in the purchase order, the can material must be removed by chemical or mechanical methods such as pickling or machining. After pickling, Code Case

N-834 (SS) requires that all surfaces exposed to the process fluid be removed by machining or grinding to a depth of 0.008 in. (0.2 mm) or greater. ASTM Specification B834 (Nickel Alloys) simply requires that the can be removed from the final part, and no further specifics are given as to how this is to be accomplished. However, it is noted that either method could be used on nickel-based alloys. For A508 low alloy steel type material, the can removal would be limited to machining only, given that chemical removal could negatively impact the A508 material. Any future ASTM or ASME specification for A508 would be expected to include this limitation.

Despite the net or near-net manufacturing of PM-HIP, after can removal, many components will require a combination of surface finishing and post processing operations, because the resulting dimensions and tolerances are generally not within the requirements of the final component [59, 66]. Sometimes the dimensions of the steel can are intentionally oversized because of uncertainties in precisely predicting the volume shrinkage of the powder and deformation behavior of the steel can during HIP processing. Oversizing may be necessary for producing heavy-section large components for nuclear reactors by PM-HIP. A combination of machining, finish grinding, and other surface treatments may be used to obtain the component's final dimensions and tolerances. The PM-HIP component's machinability is not expected to differ significantly from conventionally manufactured components.

Post-HIP machining is important for ensuring an acceptable surface finish for the final component. Depending on the can removal method, a fairly rough surface may remain that could be more susceptible to corrosion and fatigue. Machining to the final dimensions addresses this issue by producing a uniform smooth surface that is similar to conventionally manufactured materials.

2.3 MICROSTRUCTURE AND MECHANICAL PROPERTIES OF PM-HIP COMPONENTS

2.3.1 Microstructure

The primary difference in microstructure of PM-HIP SSs and low alloy steels compared to the same steels produced by traditional manufacturing methods is smaller grain size [21, 65]. For 316L SS, the microstructure of the PM-HIP component will be fairly similar to that of the wrought 316L SS, but it will be much different than that of the cast 316L [85]. Figure 24 compares the microstructures of 316L SS in the PM-HIP condition (Figure 24a) and the wrought condition (Figure 24b). Both microstructures show equiaxed grains with some annealing twins, but the grains observed in the PM-HIP 316L SS are much smaller than those in the wrought 316L SS.

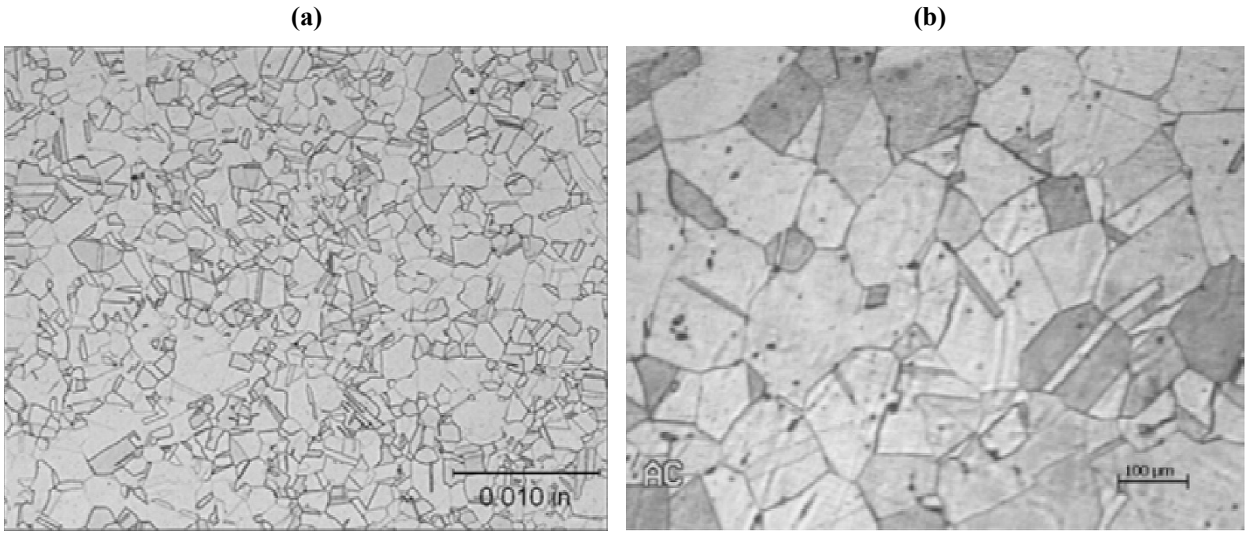

Figure 24. Optical micrographs of PM-HIP 316L SS produced by (a) PM-HIP and in the (b) wrought condition [85]. Note a small difference in magnification between the optical micrographs.

Another microstructural characteristic of PM-HIP is that the equiaxed grain structure does not change with location in the PM-HIP component. Figure 25 and Figure 26 demonstrate this characteristic by showing the microstructure of the 316L SS valve body that was produced by PM-HIP with a weight of 1,716 lbs., or 780 kg [26, 85]. The valve body shown in Figure 26 was sectioned, and metallography samples were prepared from three orientations pertaining to longitudinal, transverse and hoop directions. The optical micrographs shown in Figure 26 show the microstructure of the valve body viewed in the hoop, longitudinal, and transverse directions. These results indicate that there are effectively no differences in the size or the morphology of the grains in the microstructure. With PM-HIP, the hydrostatic stresses at elevated temperatures cause virtually no macroscopic strain deformations during densification by the sintering and creep mechanisms that would otherwise result in grain structure anisotropy. This densification mechanism is favorable for producing large structural components by PM-HIP.

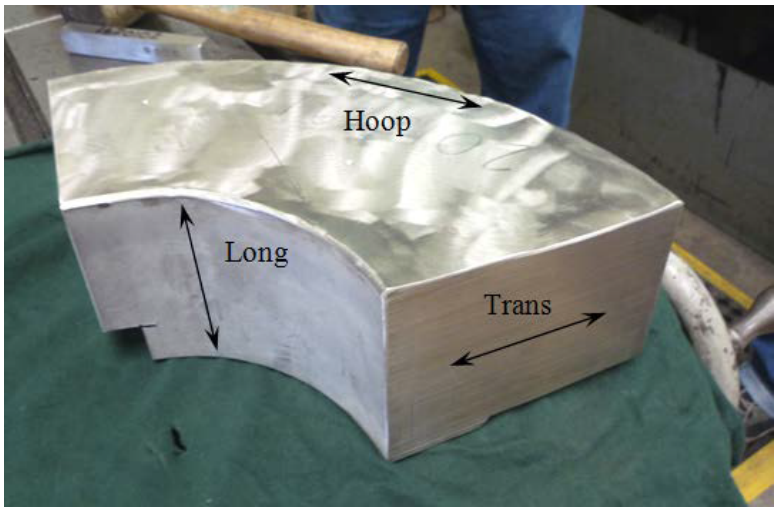

Figure 25. Section of the valve body of 316L SS produced by PM-HIP with marking to show three directions—hoop, longitudinal, and transverse - from which metallography samples were prepared [85].

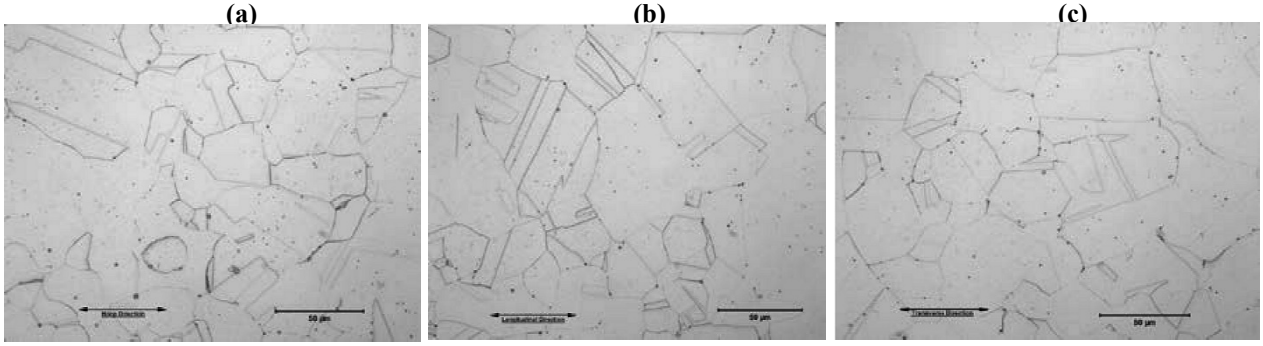

Figure 26. Optical micrographs of PM-HIP 316L SS showing the similar and isotropic grain size and morphology of the microstructure observed in (a) circumferential, (b) longitudinal and (c) transverse orientations [26]. Note: scale markers are 50 μm [85].

2.3.2 Tensile

The tensile properties of PM-HIP components are typically comparable to or better than those of components produced by traditional casting, forging, drawing, and rolling methods. During a collaboration between EPRI, Carpenter Technology, and Tyco Valves, the tensile properties were measured from ~25 to ~538°C for samples fabricated from each of three valve bodies of 316L SS produced by PM-HIP [85]. Figure 27 shows the tensile data obtained for the three 316L SS valve bodies (identification [ID] codes 815111, Y1620B and 814520) and the tensile requirements for a forged F316L SS flange for comparison. The results indicate that the values of YS (Figure 27a) and ultimate tensile strength (UTS) (Figure 27b) for all the PM-HIP 316L SS valve bodies were higher than those of the forged F316L SS flange requirements, which are the minimum tensile strength values from ASTM Specification A988/A988M.

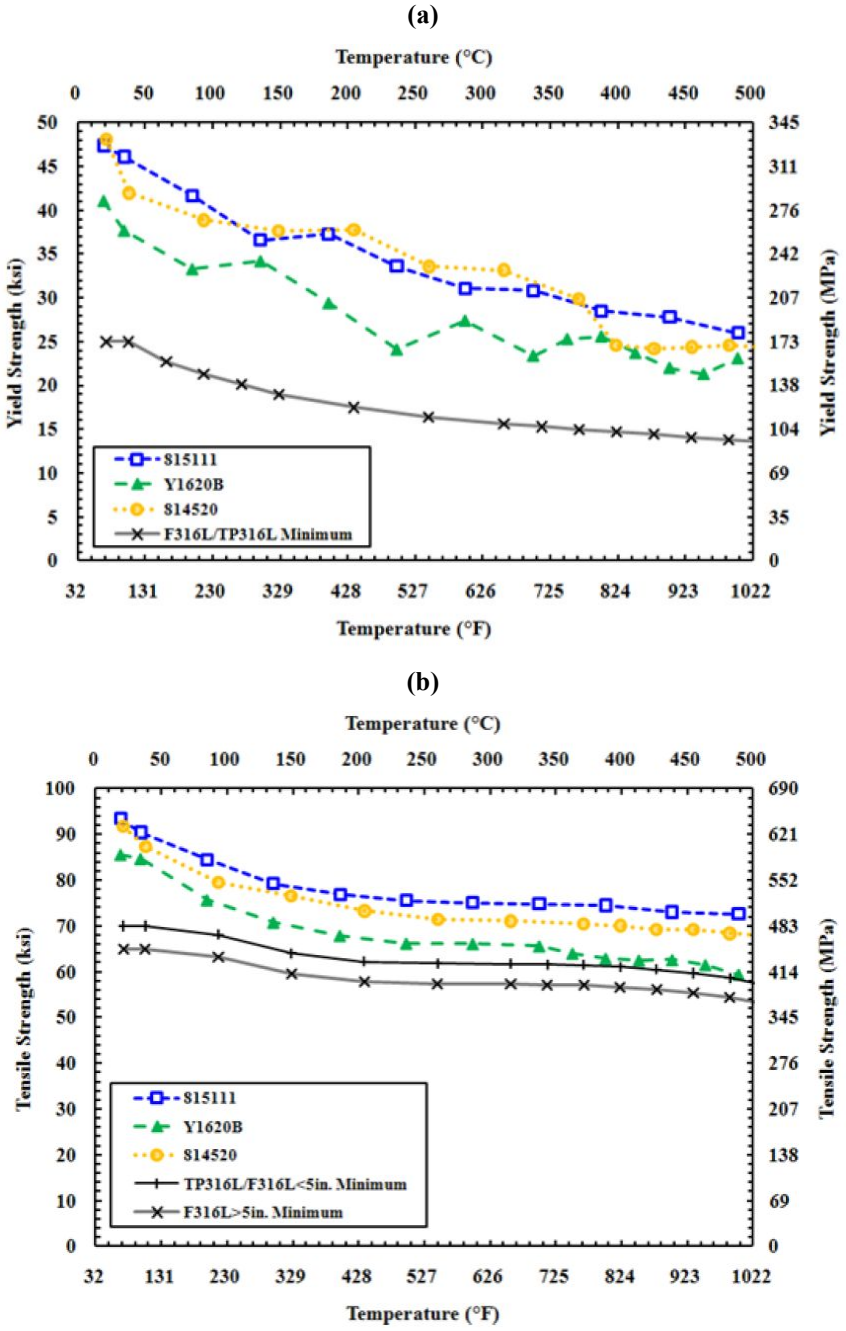

Figure 27. Comparison of the temperature dependence of (a) YS and (b) UTS between four PM-HIP produced heats of 316L SS and the minimum strengths of two forged flanges F316L SS [85].

In another project involving EPRI, Carpenter Technology, and GE-Dresser, three valve bodies of Grade 91 (9Cr-1Mo-0.25V) steel were manufactured by PM-HIP [10]. The mechanical properties of samples fabricated from each of the three valve bodies (ID Codes Y1549B, Y1550B, and Y1551B) were obtained by tensile tests from room temperature to 704°C. The main difference between the three ID codes for the Grade 91 steel valve bodies was the tempering treatment, which was 4 h at 777°C for Y1549B and Y1551B, and 4.5 h at 746°C for Y1550B. The measured values of UTS and YS as a function of temperature are shown in Figure 28, and the plot showing the measured values of elongation and reduction in area, as a function of temperature, are shown in Figure 29. The tensile data of wrought Grade

91 steel obtained from ORNL report 6303 [92] are included in Figure 28 and Figure 29 for comparison. Each plot shows a polynomial fit curve in yellow, representing minimum values for wrought Grade 91 material as established by ORNL as part of the modified 9Cr-1Mo (Grade 91) development program for advanced liquid metal reactors (LMRs). The figures show that the three Grade 91 PH-HIP valve bodies meet the minimum values established values for wrought Grade 91.

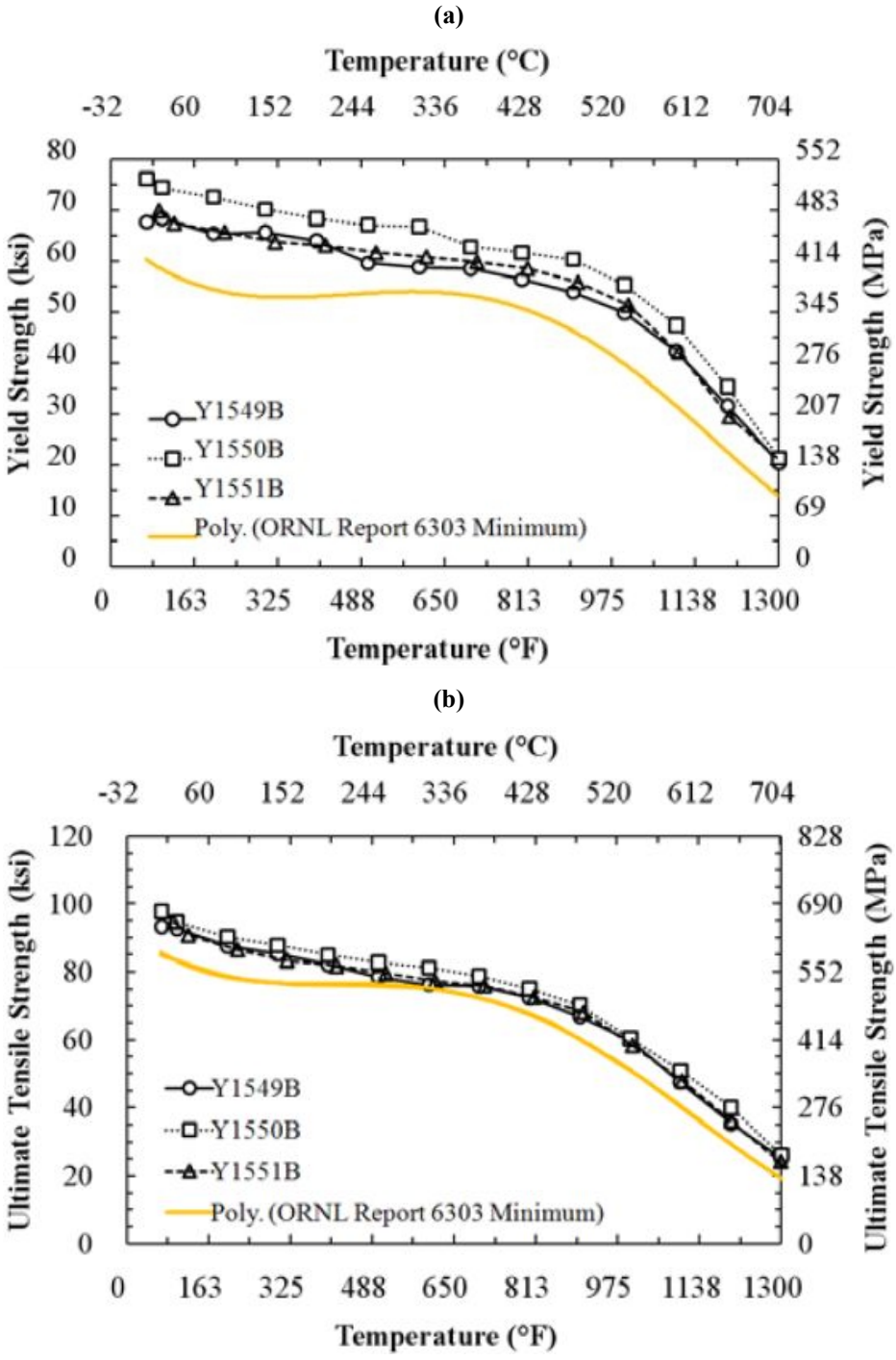

Figure 28. Comparison of the temperature dependence of (a) YS and (b) tensile strength for three Grade 91 PM-HIP valve bodies [10]. Polynomial fits in yellow show the minimum strength values for wrought Grade 91 developed by ORNL [92].

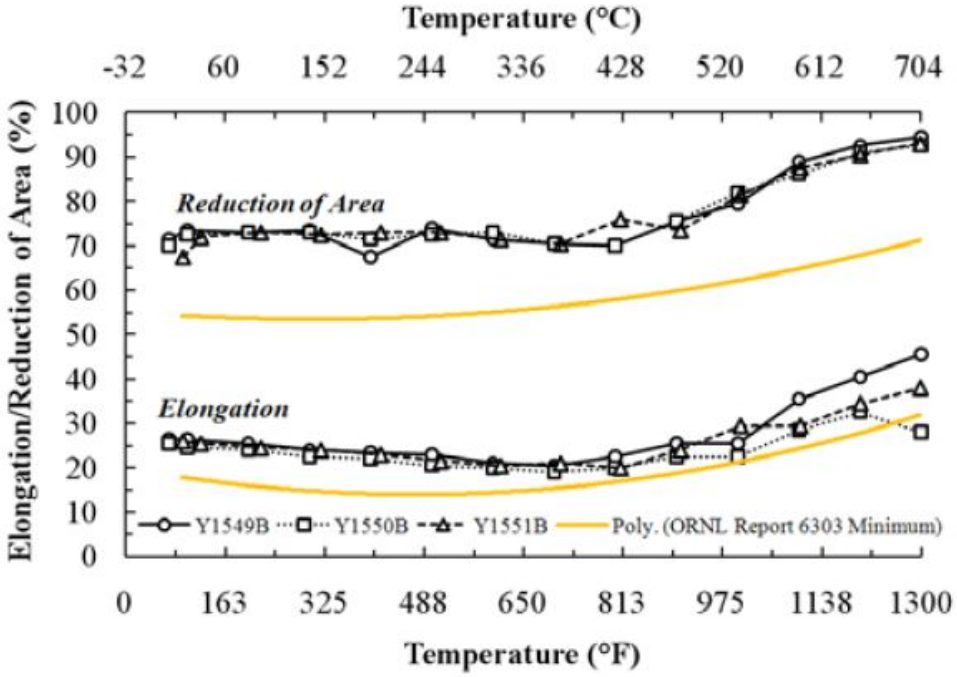

Figure 29. Comparison of the temperature dependence of elongation and reduction in the area between three PM-HIP–produced heats of Grade 91 [10]. The polynomial fit curve, shown in yellow, indicates the minimum elongation and reduction in area values for wrought Grade 91developed by ORNL [92].

2.3.3 Creep

Grade 91 (9Cr-1Mo-0.25V) steel was originally developed for use in LMRs because of the need for a material with improved high-temperature performance compared to type 304 and type 316 SSs [92]. In the project with EPRI, Carpenter Technology, and GE-Dresser, the thermal creep properties of the three PM-HIP Grade 91 valve bodies were obtained via time-to-rupture creep tests. Figure 30 shows the creep properties for numerous samples of the three Grade 91 valve bodies using the Larson Miller Parameter (LMP) method. The extensive collection of creep data for Grade 91 assembled by EPRI is provided in Figure 30. The results show that all creep data for the three PM-HIP produced valve bodies of Grade 91 generally lie within the range of creep data for wrought Grade 91. The data for the Y1550B heat that had the lower tempering treatment of 4.5 h at 746°C lie on the upper range of creep data for wrought Grade 91, which indicates better creep properties. Therefore, PM-HIP does not appear to negatively impact creep properties compared to those found in Grade 91 wrought material.

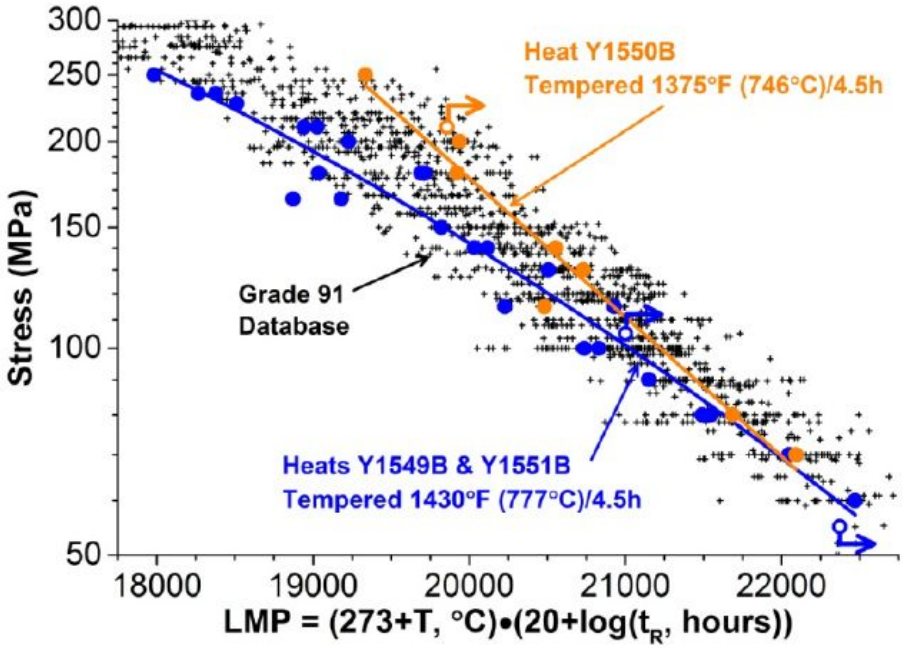

Figure 30. Comparison of the creep properties using the LMP for the three PM-HIP produced heats of Grade 91, with creep data compiled for conventionally manufactured Grade 91 by EPRI [10].

2.3.4 Impact Toughness

Low Alloy Steels for RPVs

The composition of low alloy steels and their microstructural characteristics, as affected by heat treatments, are major factors that influence toughness properties. In general, ferritic steels over ⅝-inch thick that are used in safety-related NPP components are required to be impact tested. For ASME Code Class 1 vessels such as the RPV, ASME Code Section III, NB-2331 specifies testing requirements to determine reference temperature of nil ductility transition (RT_{NDT}) using a combination of drop-weight testing to determine NDT and Charpy V-notch (C_v) testing to determine the temperature at which the material has a C_v energy of 50 ft-lb and 35 mils lateral expansion (MLE). Drop-weight tests are used to determine a temperature T_{NDT} that is at or above the NDT temperature. RT_{NDT} is higher than T_{NDT}, or it is the temperature at which three C_v specimens achieve a minimum of 50 ft-lb absorbed energy and 35 MLE - 60°F. Although the minimum C_v and MLE values in NB-2331 are required to define RT_{NDT}, there is no actual minimum RT_{NDT} requirement for vessels in NB-2331. Therefore, RT_{NDT} is used in conjunction with Figure G-2210-1 of Section XI, Appendix G, to determine the critical or reference stress-intensity factor K_{IC} as a function of temperature, which is a key input to determine pressure-temperature operating limits.

The origin of the C_v requirements is described in *Welding Research Council Bulletin, PVRC Recommendations on Toughness Requirements for Ferritic Materials, PVRC, Ad Hoc Group on Toughness Requirements*, August 1972 (WRC 175) [93], which shows a correlation between 35 MLE and 50 ft-lb of absorbed energy (at T_{NDT} +60 degrees) and a dynamic fracture toughness of 70 ksi-√in for A-533-B pressure vessel plate steel. Although A-508 low alloy steel was not included in this correlation, it was assumed at the time that A-508 material would exhibit a behavior similar to that of A-533. This is the origin of the requirements for the determination of RT_{NDT} in the ASME Code for ferritic vessel materials.

Given that A508 PM-HIP is a new product form that may behave differently from that of forgings, the correlation between Charpy impact properties and fracture toughness properties of PM-HIP A508 should be verified.

EPRI and several other organizations collaborated on a project to demonstrate the capability to produce large components with chemistry similar to SA-508 Grade 3, Class 1 material, using the PM-HIP process [49, 86, 94]. Three heats of A508 steel powder weighing ~500 lb (227 kg) were produced by CPP, with variations in composition for obtaining different hardenability levels based on carbon equivalency (CE). The three heats of materials produced -160114, 160115, and 160116 - had CE values of 0.62, 0.69, and 0.55, respectively. Additional information on these heats can be found in Section 2.1.1.2, Table 2 of this report. Each heat of powder was packed into a rectangular-shaped can to produce billets and was consolidated by HIP for 4 h at 2,050°F (1,121°C) and 15 ksi (103.4 MPa). Nine smaller plates were cut from each billet and solution annealed (4 h at 2,050°F [1,121°C] and gas quenched), followed by a normalizing treatment (10 h at 1,650°F [899°C] and gas quenched).

An extensive test matrix of tempering treatments for 4 h at 1,175°F (635°C), 1,200°F (659°C), and 1,225°F (663°C);10 h at 1,175°F, 1,200°F and 1,225°F (663°C); and 20 h at 1,175°F (635°C), 1,200°F (650°C), and 1,225°F (663°C) - for a total of nine conditions for each billet - was used to study the effects of tempering on the Charpy impact toughness properties on each heat of powder. These tests showed that all tempering treatments yielded toughness values exceeding the ASME SA-508 specification of 30 ft-lb at 40°F for Grade 3 Class 1 material. Heat 160116 tempered at 1,200°F for 10 and 20 h was identified as having the best balance of tensile and toughness properties. Although not reported in the references, it is believed that all three heats of powder were manufactured using vacuum induction melting (VIM) coupled with inert gas atomization (IGA) instead of air induct melted (AIM) IGA given the high toughness of many of the tested samples.

Before proceeding to fabricate a large nozzle and RPV shell section with a chemistry and CE closely matching Heat 160116, reconfirmation testing was performed on two test coupons from Heat 160116 material. One coupon was tempered at 1,200°F for 10 h, and another for 20 h. The coupon tempered for 10 h provided similar toughness values to those produced in earlier testing, with Charpy impact testing values approaching 160 ft-lb at the upper shelf.

Results of the confirmation testing are shown in Figure 31 against earlier Charpy testing data ("Screening Data" shown as green x marks in Figure 31). Figure 31 shows the Charpy impact energy from -200 to 120°F after tempering at 1,200°F. The upper shelf toughness was ~160 ft-lb, whereas the toughness transition temperature was estimated at -85°F (-65°C). These toughness values are considerably higher than the required SA-508 minimum value of 30 ft-lb at 40°F. The screening data from the original testing of Heat 160116 (solution anneal, normalize, temper at 1200°F) do not represent a full Charpy curve; it only represents several data points. The red squares represent solution annealed heat treatment with no normalizing, followed by a 1,200°F temper for 10 h. The green triangles represent testing performed on samples subjected to the same thermal cycles as the screening data.

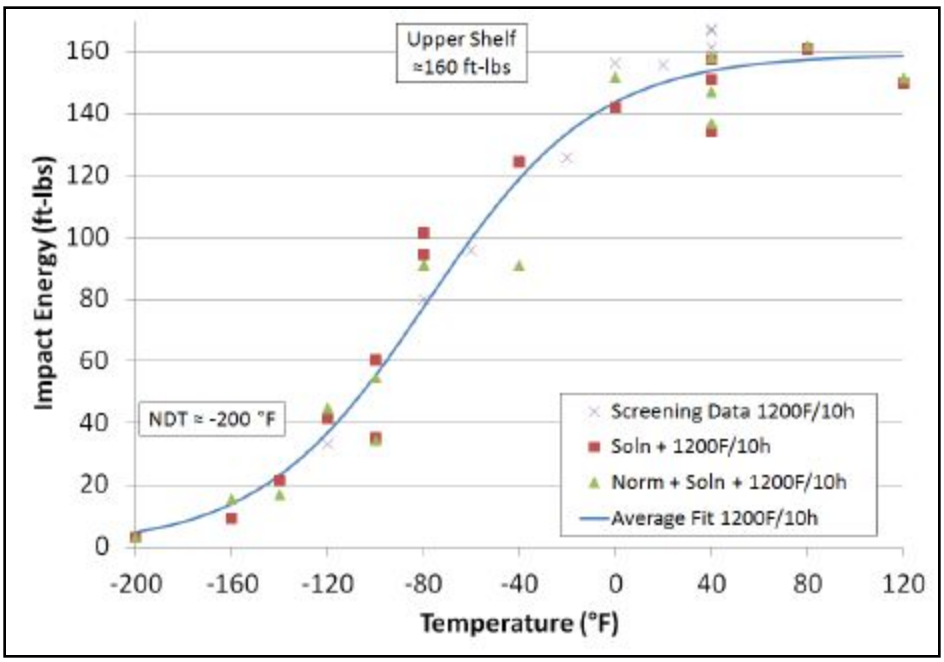

Figure 31. Charpy impact toughness results produced during the reconfirmation testing of the low hardenability (CE=0.55) heat 160116 [49].

With respect to the RPV toughness requirements, as shown in Figure 31, the 50 ft-lb requirement was met at about -100°F, which would then equate to an RT_{NDT} of approximately -160°F. Although there is no minimum RT_{NDT} requirement for RPV steels in Section III, Subsection NB, or Section XI, an unirradiated RT_{NDT} of -160°F compares favorably to the unirradiated RT_{NDT} of many RPV materials in service in the operating reactor fleet. For other ferritic components ≤2.5 in., such as piping, pumps, and valves, the minimum ASME requirements range from 20 to 40 MLE (depending on the component thickness) at a temperature lower than or equal to the lowest service temperature as established in the design specification, with no absorbed energy requirement. For ferritic piping and material for pumps, valves, and fittings with nominal thickness >2.5 in., the requirements for vessels discussed above must be met.

After this work was complete, EPRI prepared to scale up the manufacturing process and demonstrate very large components with good toughness. However, subsequent work resulted in toughness values ranging from 65 to 130 ft-lb, a range which is significantly less than the 160 ft-lb achieved previously. Therefore, EPRI investigated the cause of the lower toughness and determined that reducing oxygen and silicon levels, improving handling, storage and transportation, and performing vacuum annealing to further reduce residual gas levels would help achieve improved properties. Data supporting these conclusions is provided in Gandy and Albert [49], but in particular, the vacuum annealing data are of high relevance.

Steel cans were filled with the A508 powder that was then cold degassed. This was followed by vacuum annealing at 700 or 800ºC for 4 h, and then they were degassed to remove the back-filled Ar gas. They were welded shut and underwent HIP at 1,120°C for 4 h. The HIP components were solution annealed at 1,120°C for 2 h, normalized at 900°C for 10 h and water quenched, and finally temper annealed at 650°C for 10 h and air cooled. Following Charpy impact testing, the results showed that the samples that were vacuum annealed at 800°C exceeded the EPRI goal of 100 ft-lb, whereas the 700°C anneal was less than 100 ft-lb, as shown in Figure 32. It was suggested that a longer vacuum annealing time at the lower temperature of 700°C may allow for necessary reduction of oxides on the surface of the powder particles, thus leading to improved toughness properties.

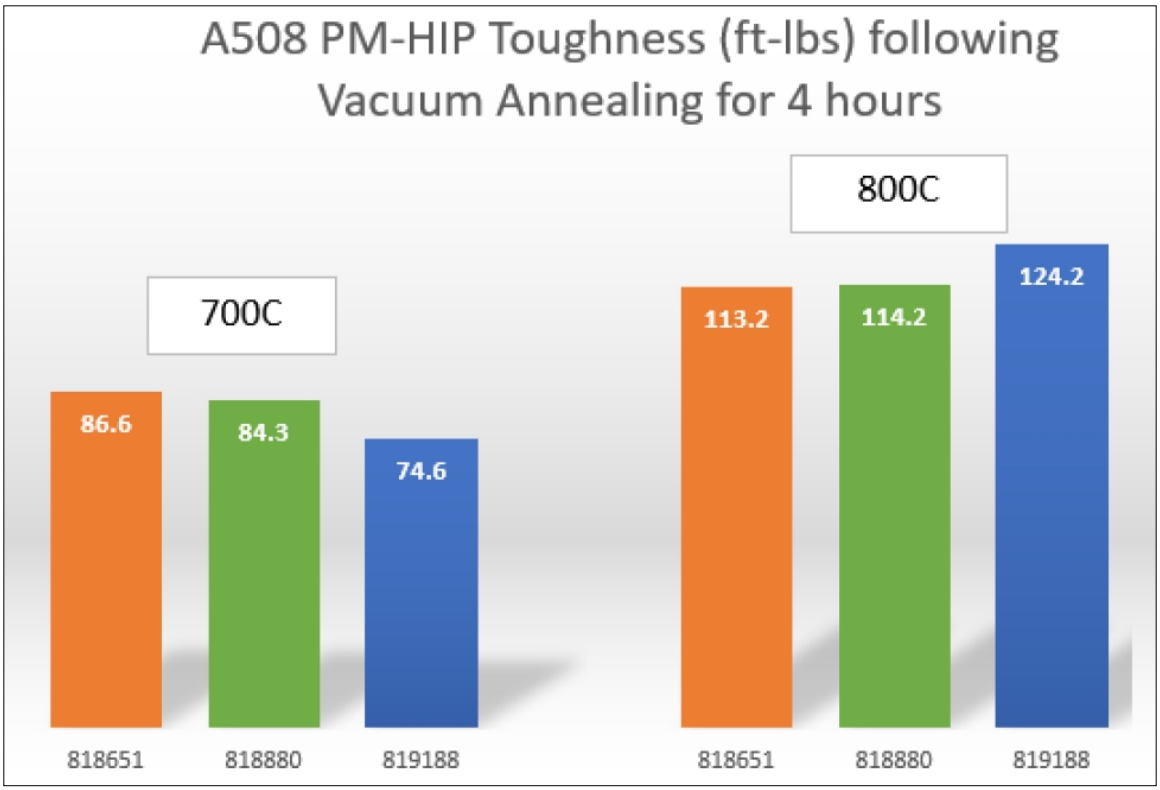

Figure 32. Charpy impact energy of A508 capsules that received 700 or 800°C vacuum annealing followed by HIP and heat treatment. C_v testing was conducted at room temperature [49]. A benchmark value (non-vacuum annealed) for these heats is 74 ft-lb.

Stainless Steels

Because of the inherently exceptional fracture toughness of austenitic SS, ASME Code, Section III, does not have requirements for impact toughness testing of austenitic SS made by conventional manufacturing methods. Therefore, analysis of impact toughness of PM-HIP SS is focused on confirming that PM-HIP also produces SS with excellent toughness.

The impact toughness of PM-HIP 316L SSs at room and higher temperatures are similar to those of conventional forged components when the oxygen levels are kept sufficiently low [95]. However, following the approval of the ASME Code Case N-834 in 2013, studies showed that a decrease in impact toughness occurred for PM-HIP 316L components at cryogenic temperatures that was not observed with forged 316L components. Austenitic SS components in NPPs do not operate at cryogenic temperature, but knowledge can be gained regarding the impact of oxygen on overall impact toughness.

The reasons for the drop in impact toughness of PM-HIP 316L at cryogenic temperatures were associated with a high concentration of oxide inclusions in the microstructure that were generally larger in size than in conventionally manufactured components. The correlation of oxygen content with the impact toughness of PM-HIP 316L was investigated by Berglund and Östlund [95]. In this study, three powders of 316L were produced by gas atomization using a nitrogen atmosphere followed by HIP consolidation. Two of the powders, P1 and P2, were produced with conventional induction melting, and the third powder, P3, was produced with vacuum induction melting. For comparison, a 5 cm diameter conventionally rolled bar of 316L was produced and referred to as *C1*. Figure 33 shows the measured

oxygen levels of the three atomized powders after sieving in four size ranges. The results show lower oxygen levels for the vacuum induction melting of P3 compared to conventional induction melting of P1 and P2. Higher oxygen levels were associated with the smallest powder size range of 32-45 µm that decreased with increasing powder size range to the lowest level in the largest 240-355 µm size range. The higher oxygen content of smaller powder sizes is commonly observed and is to the result of the higher surface area that promotes larger oxide coverage, or mass, compared to the bulk volume.

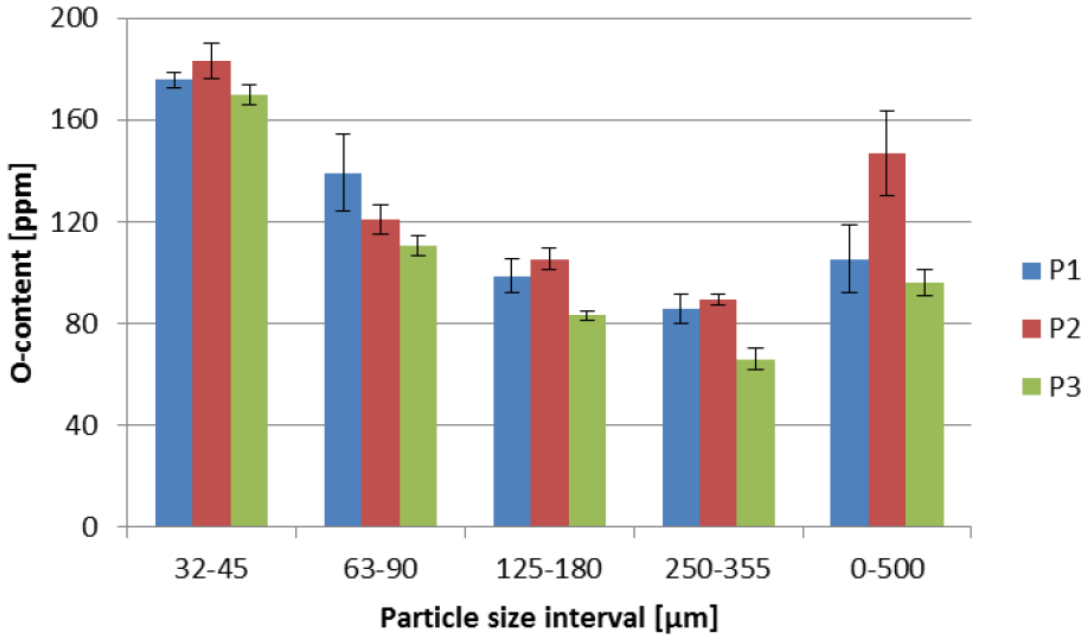

Figure 33. The measured oxygen content of the three powders of 316L sieved into four size ranges.

The temperature dependences of impact toughness for the three PM-HIP 316L (P1, P2 and P3) and the rolled bar of 316L SS (C1) are shown in Figure 34 [91]. This figure also includes the impact toughness results for a forged 316L, which was obtained from reference 7 in the study by Berglund and Östlund [95]. The impact toughness of the three PM-HIP 316L and the rolled bar of 316L varied significantly more than that of forged 316L over the temperature range from -198 to 200°C. Compared to the forged 316L, which showed little dependence of impact toughness from -198 to 200°C, both the P3 PM-HIP 316L and the C1 rolled bar of 316L possessed higher toughness values above 0°C. Although P1 and P2 PM-HIP 316L had higher impact toughness values than the forged 316L at 200°C, the impact toughness values of P1 and P2 were about 50 Joules, or ~37 ft-lb lower than the forged 316L at room temperature. However, all three PM-HIP 316L have lower impact toughness values at -198°C compared to the C1 rolled bar of 316L and the forged 316L. These results are not critical, because LWR components do not operate at cryogenic temperatures, but they do provide some guidance on PM-HIP process conditions. The vacuum induction melting used to produce the P3 316L powder led to lower oxygen levels compared to the conventional induction melting used for the production of the P1 and P2 316L powders. The microstructural characterization of the nonmetallic inclusions present in the three PM-HIP 316L materials showed that P3 possessed the largest number of nonmetallic inclusions with the smallest sizes compared to the P1 and P2 PM-HIP 316L [95]. This correlation between a higher number of smaller size inclusions with the lower oxygen level may be responsible for the improved temperature-dependent impact toughness properties of P3 PM-HIP 316L.

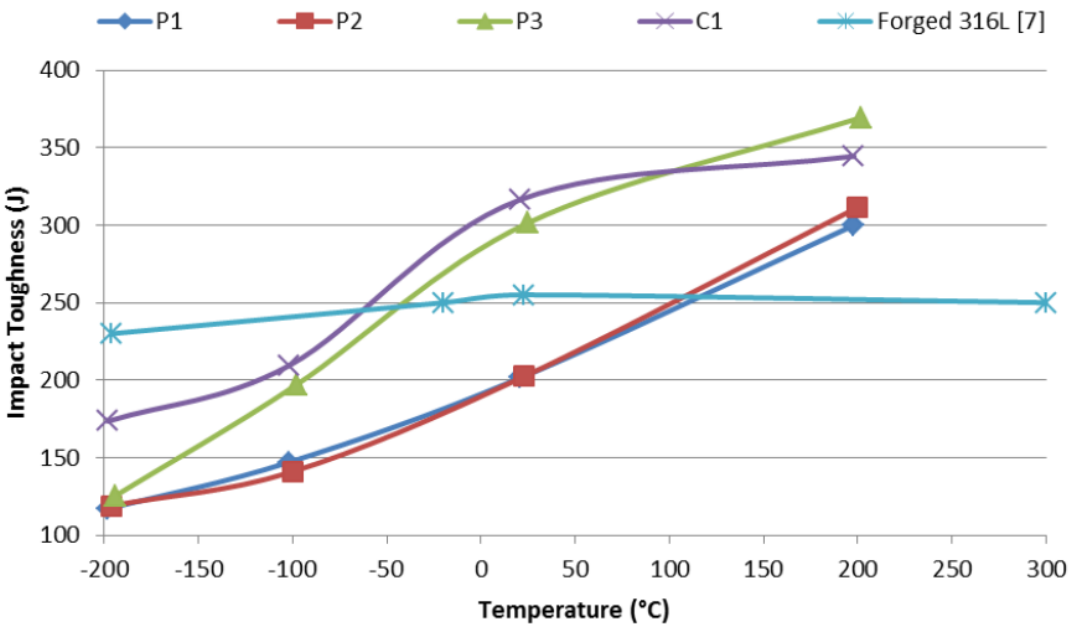

Figure 34. Comparison of impact toughness properties of the three gas-atomized powders (P1, P2 and P3) with a rolled bar of 316L (C1) and a forged 316L material from reference 7 in [95]. ***Note: Conversion from Joules to ft-lb is 0.737572.***

2.3.5 Stress Corrosion

Intergranular stress corrosion cracking (IGSCC) is known to exist for 304 and 316 SSs in BWR primary coolant systems [96]. The two main factors that contribute to IGSCC of these SSs is thermal sensitization and cold working. Welding processes can produce sensitization in the heat-affected zone of these SSs as a result of precipitation of chromium-rich carbides on GBs, accompanied by the depletion in chromium adjacent to the GBs. There are several ways to control or reduce the chances for sensitization, including post-weld heat treatment and reducing the carbon level by using 304L and 316L SSs. Cold work has also been shown to increase stress corrosion cracking (SCC) susceptibility. The mechanism by which cold work increases SCC is thought to involve formation of martensite, increase in residual stresses, and inhomogeneous formation of localized deformation [96].

SCC tests include slow strain rate and crack growth rate (CGR) tests. Early results obtained by EPRI on SCC testing of PM-HIP 316L produced using AIM, N-gas atomized powder that was solution annealed after compaction have shown similar SCC crack growth rates with wrought 316L [97]. Table 4 compares the SCC growth rate for the wrought and PM-HIP 316L in the as-received and 20% cold-worked conditions. The corrosion tests were conducted in water at 288°C with 20 ppb sulfates as H_2SO_4 at ~30 and 40 MPa$\sqrt{m}$ with low and high electrochemical potentials (ECPs). As seen in this table, the SCC growth rates are very similar for all test conditions between the wrought and PM-HIP 316L SS indicating that PM-HIP does not significantly increase SCC susceptibility compared to that of wrought materials.

Table 4. Preliminary results of EPRI corrosion tests on wrought and PM-HIP 316L and 600M [97]

			SCC Growth Rate, mm/s	
Alloy	**Specimen**	**K, MPa√m**	**High ECP**	**Low ECP**
			As-Received	
Wrought 316L	---	~40	(≈3 x 10^{-8})	(≈2 x 10^{-9})
PM 316L	C720	~40	~1 x 10^{-7}	~2 x 10^{-9}s
			20% Cold Work	
Wrought 316L	C126	~30	~2 x 10^{-7}	~2 x 10^{-8}
PM 316L	C719	~30	~2 x 10^{-7}	~1 x 10^{-8}
			As-Received	
Wrought 600	---	~35	(≈2 x 10^{-8})	(≈1 x 10^{-9})
PM 600M	C735	35	5 x 10^{-8}	2 x 10^{-9}
			20% Cold Work	
Wrought 600	C129	30	2 x 10^{-7}	3 x 10^{-8}
PM 600M	C734	30	1 x 10^{-7}	1 x 10^{-8}

2.3.6 Fatigue

Very little data exist comparing the low cycle fatigue (LCF) data of PM-HIP SSs with wrought SSs. Only one study was identified comparing LCF properties of wrought and PM-HIP 316L SS in air and PWR water conditions [98]. The 316L powder used in this study was supplied by Carpenter to fabricate a large pipe using PM-HIP by Bodycote. The pipe had outer and inner diameters of 97.8 and 74.4 cm, respectively, and a length of 150 cm. The pipe was sintered by HIP at 1,150°C for 3.5 h at a pressure of 105 MPa (heating rate of 220°C/h and a cooling rate of 240°C/h). The pipe was then heat treated at 1055°C for 3 h (heating rate of 65°C/h) and was subsequently water quenched [98]. Numerous specimens were fabricated from the PM-HIP 316L pipe with a gauge length of 1.35 cm and a diameter of 0.9 cm. The fatigue tests were carried out in air and in PWR water at 300°C according to the A03-403 AFNOR standard (or ASTM E606-04e1), using either Schenck or MTS servo-hydraulic–driven closed loop machines equipped with autoclaves. Several parameters were controlled to simulate the chemistry of the PWR water used in the LCF tests. The LCF tests were conducted using total axial strain control at various strain amplitudes and strain rates. Because there were little LCF data on 316L SS in PWR water, existing LCF data obtained for the 304L SS products were used for comparison with the data on PM-316L. The existing LCF 304L data were obtained from a pipe and several blocks fabricated by PM-HIP. The 304L pipe and blocks were sintered by HIP at 1,150°C for 3 h at a pressure of 105 MPa (heating rate of 360°C/h, cooling rate of 240°C/h). The pipe and blocks were then heat treated at 1,056°C for 4.6 h (heating rate of 360°C/h) and subsequently water quenched [98].

The results of the LCF tests on PM-HIP 316L SS at 300°C in air and PWR water are shown in Figures 36 and 37, respectively. For comparison with the data for PM-HIP 316L, both figures also include LCF data for 304L SS and the mean air fatigue curve generated by Argonne National Laboratory (ANL) for

austenitic SSs. The curves plot the theoretical fatigue life for a failure criterion of 25% load drop (N_{25}). The comparison of LCF data for LCF tests in air at 300°C shown in Figure 35 indicates that the fatigue life of PM-HIP 316L SS agrees very well with that of 304L and the ANL mean air curve. These results indicate that the fatigue strength of PM-316L is similar to the wrought product form at 300°C in air. For PWR water at 300°C, the results of the LCF tests for PM-HIP 316L shown in Figure 36 also indicate a similar fatigue life compared to the wrought materials. Furthermore, the data in PWR water showed that the fatigue life of PM-HIP 316L was conservative compared to the ASME C (2007) fatigue design curve. Therefore, the limited data suggests that PM-HIP does not adversely affect LCF properties in air or PWR water compared to conventional manufacturing.

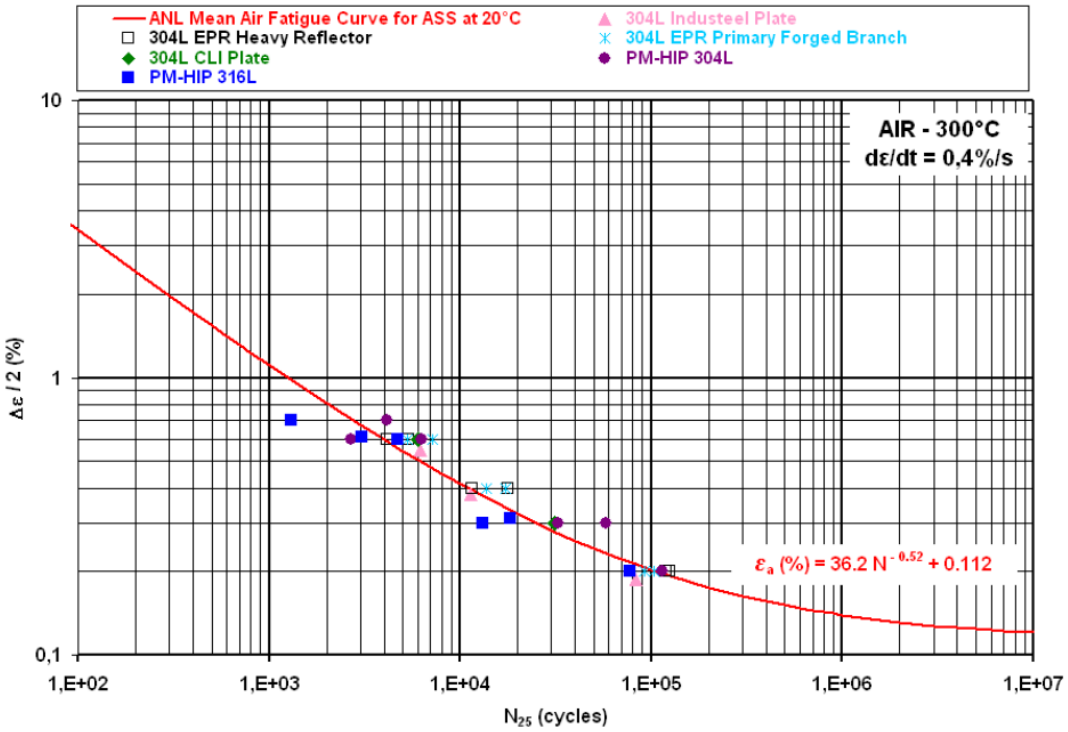

Figure 35. Comparison of the fatigue life of PM-HIP 316L in air at 300°C with data obtained for 304L and the ANL mean fatigue curve for austenitic SSs [98].

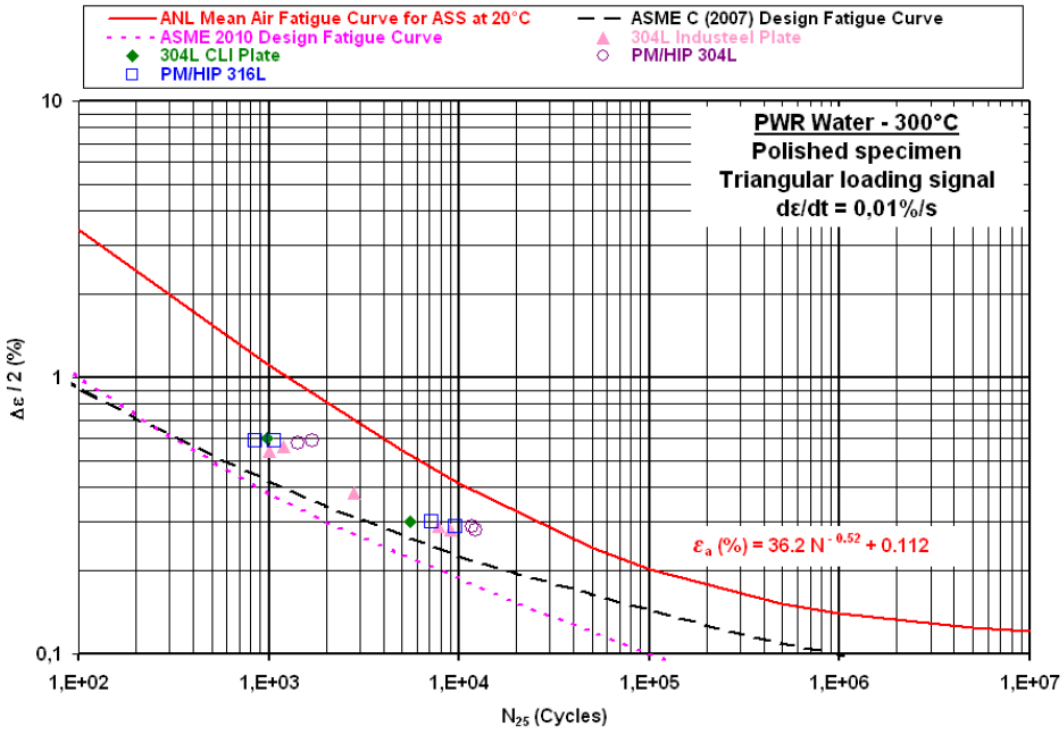

Figure 36. Comparison of the fatigue life of PM-HIP 316L in PWR water at 300°C with data obtained for 304L, the ANL mean fatigue curve for austenitic SSs, and the fatigue design curves from ASME C 2007 and ASME 2010 [98].

2.3.7 Irradiation Effects

Very few investigations have been reported in the literature regarding the effects of neutron irradiation on PM-HIP SSs or low alloy steels. Because the performance of PM-HIP components of SSs and low alloy steels of nuclear reactors are unknown, limits on the neutron irradiation fluence are established for the design life of the component. For PM-HIP SSs such as 304L and 316L, ASME Code Case N-834 (endorsed by the NRC) limits their use to components in applications in which the neutron irradiation fluence levels do not exceed 1×10^{17} n/cm^2 (E > 1 MeV) within the component's lifetime [99].

To enable the use of PM-HIP materials in components that receive significant irradiation, testing in neutron-irradiated conditions should be performed to obtain data for assessing the irradiated material performance of PM-HIP components. A review of the literature identified only two studies published in the early 2000s that covered the neutron irradiation behavior of PM-HIP 316L for high heat flux (HHF) components of ITER [100-102].

In a study by Rodchenkov et al. [100], neutron irradiations were conducted on 316LN-IG (ITER Grade) rolled plate, powder-HIP (PM-HIP), solid HIP (plate that was HIPed) and HIPed joints (SS/SS plate). Samples fabricated for tensile, fracture toughness and IGSCC testing were irradiated in the SM-3 reactor in Dimmitrovgrad, Russia, to doses of ~4 and 10 dpa (displacements per atom) at 175 and 265°C. Figure 37 shows the effect of the neutron irradiation conditions on the plate, solid HIP, and powder HIP of 316LN-IG. Compared to the stress-strain curves of the unirradiated samples (not shown in this publication), the irradiation conditions caused hardening and loss of ductility, as well as a decrease in strain hardening capacity. These are typical irradiation effects on SSs.

In general, the higher dose of 10 dpa compared to 4 dpa at 265°C resulted in the largest amount of hardening and lowest ductility. The more limited data obtained for irradiation at 175°C showed a similar trend for the solid HIP material (Figure 32). The effects of neutron dose at 265°C on the tensile properties of the plate, solid HIP, and powder HIP materials are shown in Figure 38. The tensile results shown in these figures compare the YS, UTS, uniform elongation (UEL), total elongation (TEL) and reduction in area (RA) for each of the manufactured materials in the unirradiated condition and after neutron irradiation at 265°C to doses of 4 and 10 dpa. These results show increases of ~400 to 500 MPa for YS and ~200 to 250 MPa for UTS for all 316LN-IG materials. After irradiation to 4 dpa, the UEL observed for the three 316LN-IG manufactured materials in the unirradiated condition decreases from ~20 to 4% for the rolled plate, from ~24 to 12% for the solid HIP, and from ~24 to 5% for the powder HIP conditions, whereas the TEL decreases from ~24 to 18%, from ~42 to 24%, and ~40 to 18% for the rolled plate, solid HIP, and powder HIP conditions, respectively. When the neutron dose reached 10 dpa, the UEL of the rolled plate is below 1%, whereas that of the solid HIP and powder HIP are ~7 and ~4%, respectively. The TEL remains higher than 10% for all three manufactured materials. In general, the results show that changes in tensile properties of neutron irradiated PM-HIP components of 316LN-IG (and 316L) are similar or better than components manufactured by traditional technologies such as casting, rolling, or forging.

The effects of neutron irradiation on the fracture toughness and IGSCC properties of the three manufactured materials of 316LN-IG was also investigated [100]. The fracture toughness was determined by crack-opening displacement (COD) using miniature three-point bend specimens with tests performed at the same temperature as the irradiation. The COD is a measure of the strain or displacement of the crack tip propagating through the specimen during the test. The COD of the unirradiated materials in all three conditions (rolled plate, solid HIP, and powder HIP) was more than 0.4 mm. After exposure to 4 dpa, the COD decreased to 0.06–0.1 mm, with no significant differences between the rolled plate, solid HIP, and powder HIP materials. However, the powder HIP material showed the lowest COD of 0.06, whereas the solid HIP material had the highest COD of ~0.1 mm. A further decrease in COD was observed for all three manufactured materials after neutron irradiation to 10 dpa. Therefore, the PM-HIP material had similar but slightly lower toughness than the plate material. Although no data were shown, the study reported that the resistance to IGSCC measured by electrochemical potential reactivation method showed no susceptibility to SCC. This was true for all tests conditions, including the unirradiated condition and after irradiation to 10 dpa at 265°C for the rolled plate, solid HIP, and powder HIP materials of 316LN-IG.

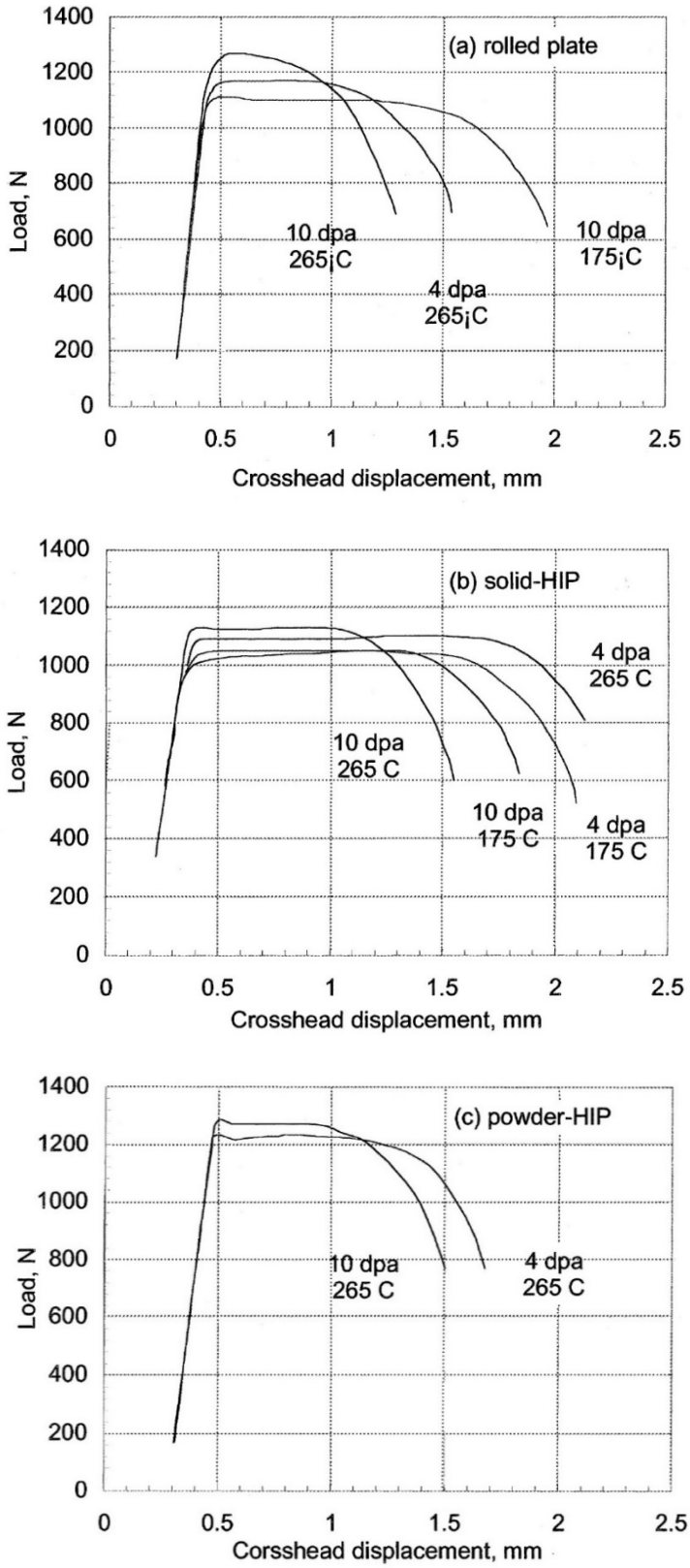

Figure 37. Stress-strain curves of neutron-irradiated 316LN-IG manufactured as (a) rolled plate, (b) solid HIP, and (c) powder HIP [100].

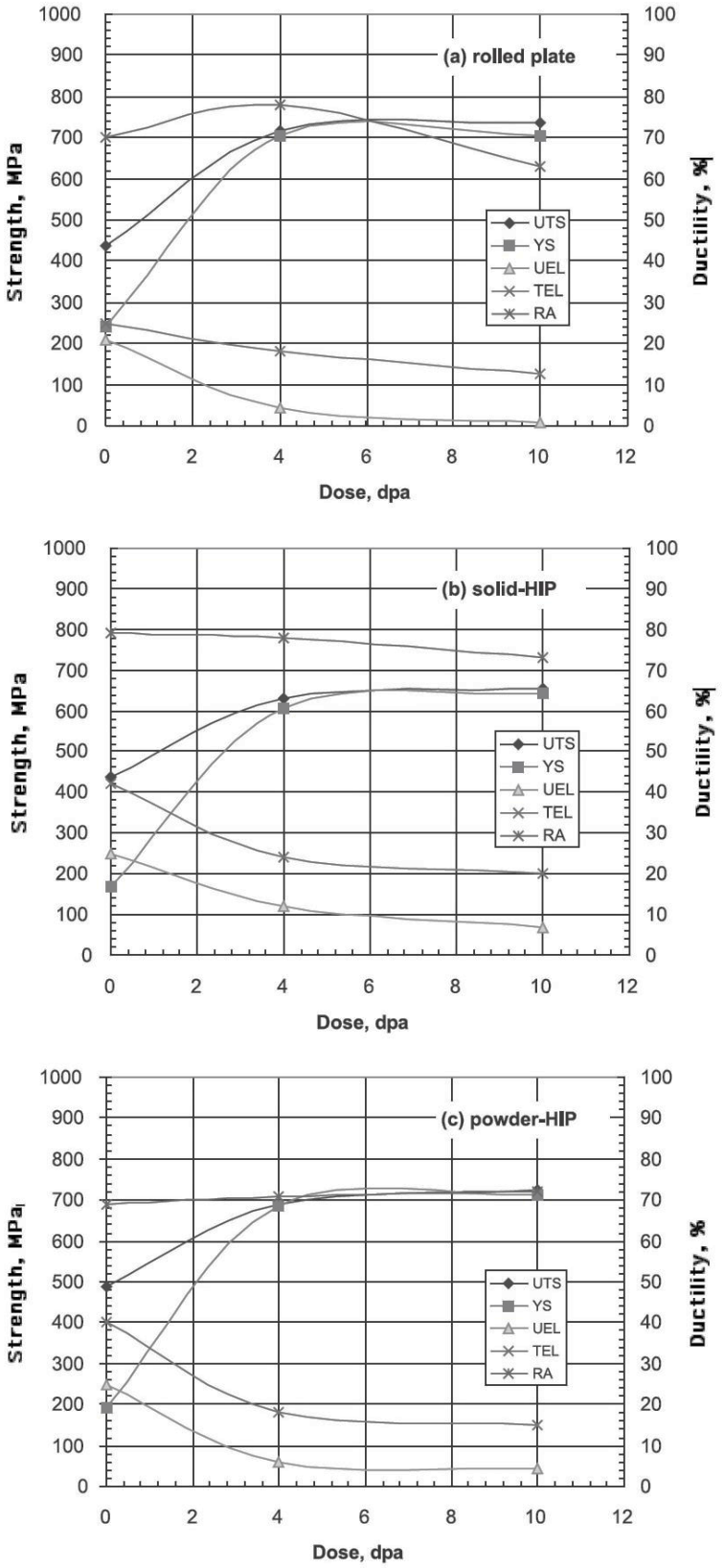

Figure 38. Effect of neutron irradiation dose at 265°C on the tensile properties of 316LN-IG manufactured as (a) rolled plate, (b) solid HIP, and (c) powder HIP [100].

In studies by Lind and Bergenlid [101, 102], neutron irradiations were also conducted on PM-HIP 316LN-IG SS for primary wall components of ITER. Samples of the European type wrought 316LN-IG SS and the PM-HIP 316LN-IG SS were fabricated for tensile, low cycle fatigue, and fracture toughness testing before and after being neutron irradiated in a pressurized water loop in the Studsvik R2 test reactor in Sweden. The samples were exposed to neutron doses of 0.7 and 2.5 dpa at 290°C. The 316LN-IG powder with an oxygen content of 195 wppm was HIPed at 140 MPa, 1,160°C, for 2 h to produce a large block from which a smaller section was cut for fabricating the specimens for testing.

The tensile tests were conducted on specimens with a circular gauge section 3 mm in diameter and 20 mm in length. Two specimens of the wrought and PM-HIP 316LN-IG materials were tested at 290°C. An hourglass shaped specimen with a minimum diameter of 3.2 mm was used for the low cycle fatigue tests using a constant diametral strain amplitude of 0.17% and a frequency of 0.125 Hz. The fracture toughness tests were conducted using compact tension (CT) specimens with a thickness of 6.25 mm and a width of 12.5 mm. The CT specimens of the wrought 316LN-IG were prepared in the L-T orientation, where L is the longitudinal direction, and T is the transverse direction. The CT specimens were pre-cracked at room temperature after irradiation and tested at 290°C using the J-integral method following the ASTM E813. The J term is a measure of the strain energy release per fracture surface area created by propagation of the fatigue pre-crack through the specimen. Because of the miniature size of the CT specimens, the critical J_{IC} value near the onset of stable crack extension could not be determined. Therefore, the J_Q (kJ/m^2) value was evaluated at the intersection of the power law regression and the 0.2 mm offset line.

The results of the tensile, low cycle fatigue, and fracture toughness tests conducted on unirradiated and irradiated specimens of the wrought and PM-HIP 316LN-IG specimens are shown in Figure 39 (tensile) and Tables 4 (tensile), 5 (low cycle fatigue) and 6 (fracture toughness). The stress-strain curves shown in Figure 39 indicate that the PM-HIP and wrought 316LN-IG specimens were very similar. After neutron irradiation to 0.7 dpa, the PM-HIP specimens showed higher YS and lower elongation compared to the wrought specimens, but there were essentially no differences in stress-strain behavior after irradiation to 2.5 dpa. Table 5 shows the measured values for YS (R_{p02}), UTS (R_m), uniform reduction (A_u) and total reduction (A) for the wrought and PM-HIP 316LN-IG in the unirradiated condition and after neutron irradiation at 290°C to 0.7 dpa and 2.5 dpa. The values for Z (%) were not described in the publication [102], but it seems to define the percent reduction in area after reaching the instability in deformation, referred to as *necking*, at A_u. The decrease in Z follows the same decreasing trends in elongation with increasing neutron dose at 290°C for the wrought and PM-HIP 316LN-IG specimens. Therefore, the PM-HIP material appears to have generally similar properties to the wrought material, with slightly higher strength and slightly lower ductility.

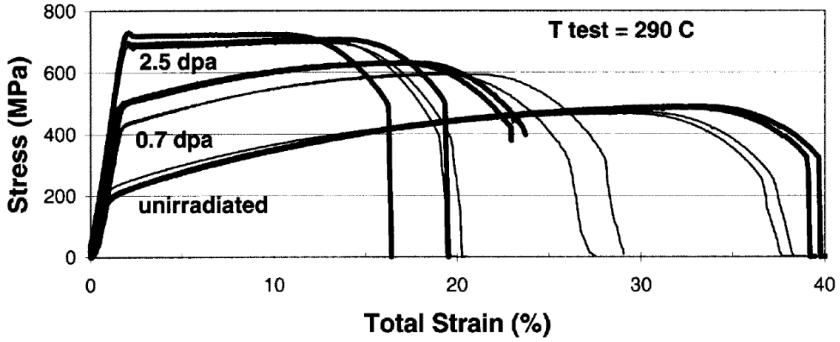

Figure 39. Stress-strain curves of the unirradiated and irradiated specimens of 316LN-IG obtained from tensile tests at 290°C, which was the irradiation temperature [102].
The bold stress-strain curves are for the PM-HIP 316LN-IG specimens.

Table 5. Compilation of tensile properties from the tensile tests at 290°C for the unirradiated and irradiated specimens of 316LN-IG. $R_{p0.2}$ is the YS, R_m is the UTS, A_u is the uniform area reduction, and A is the area reduction [102]. *Note: no definition was provided for the Z (%) value, but it is likely the percent reduction in the area after necking*

Materials	Data	Unirrad. [3]	0.7 dpa [3]	2.5 dpa
SS ref. wrought	$R_{p0.2}$ (MPa)	219	426	695
	R_m (MPa)	486	595	702
	A_u (%)	28	18	10
	A (%)			19
	Z (%)	92	94	79
SS-HIP	$R_{p0.2}$ (MPa)	213	493	710
	R_m (MPa)	494	632	715
	A_u (%)	28	16	10
	A (%)			17
	Z (%)	85	79	61

The low cycle fatigue endurance results shown in Table 6 indicate similar average cycles to failure (N_F) between the unirradiated and low-dose irradiation to 0.7 dpa for the wrought and PM-HIP 316LN-IG specimens. At the higher dose of 2.5 dpa, the N_F decreases for both the wrought and PMHIP 316LN-IG, but the average fatigue endurance of the PM-HIP 316LN-IG is more than 20% lower. The results of the J-integral fracture toughness tests for the wrought and PM-HIP 316LN-IG specimens after neutron irradiation at 290°°C to 0.7 dpa and 2.5 dpa are shown in Table 7. The J_Q values of the PM316LN-IG were significantly lower than that of the wrought 316LN-IG at both neutron doses. As was mentioned in Lind and Bergenlid [102], the oxygen content of the powder used for the PM-HIP 316LN-IG may be related to the reduced ductility properties after neutron irradiation compared to the wrought 316LN-IG. The role of oxygen may also have influenced the differences in the fracture toughness behavior between the wrought and PM-HIP 316LN-IG after neutron irradiation.

Table 6. The results of the low cycle fatigue tests conducted on unirradiated and irradiated specimens of the wrought and PM-HIP 316LN-IG [102]

Materials 316LN IG	dpa	Cycles to failure N_F		
		Test 1	Test 2	Average
Wrought	0	10 994	16 147	13 600
HIPed	0	14 808	11 133	13 000
Wrought [3]	0.7	9009	18 403	13 700
HIPed [3]	0.7	12 358	16 425	14 400
Wrought	2.5	13 381	7667	10 500
HIPed	2.5	8941	7568	8300

Table 7. The results of the fracture toughness tests conducted on the irradiated CT specimens of the wrought and PM-HIP 316LN-IG [102]

Materials	dpa	J_Q kJ/m^2
316LN IG		Average
Wrought [3]	0.7	1230
HIPed [3]	0.7	380
Wrought	2.5	903
HIPed	2.5	255

Overall, the data on irradiated PM-HIP 316LN-IG compared to wrought 316LN-IG suggests that PM-HIP has fairly similar performance after irradiation in terms of strength and SCC. However, the PM-HIP material does show significantly lower toughness after irradiation, as well as minor decreases in ductility and fatigue performance compared to wrought material. This suggests that further investigation is warranted before using PM-HIP 316L in irradiated environments.

2.4 TECHNICAL REVIEW OF PM-HIP FOR NUCLEAR APPLICATIONS

In the late 1990s to early 2000s, PM-HIP was explored by international teams in Europe, Japan, and the United States for fabricating thick-section first-wall (closest to the fusion reaction) components from 316 L(N)-IG SS for the ITER fusion experiment [103-105]. Because of the complex design and geometry of the components, the ITER team considered PM-HIP among the manufacturing options. In the course of this investigation, several PM-HIP mockups were produced ranging in size from ~500 × 250 × 250 mm up to a full size shield block prototype (~2,000 × 1,000 × 400 mm), as shown in Figure 40. This PM-HIP development worked through some challenges associated with geometric irregularities and deficiencies with respect to the required tolerances. Through subsequent larger mockups with process improvements, ITER largely overcame these issues. However, an alternative manufacturing method was ultimately chosen as a result of concerns about PM-HIP being able to meet the stringent tolerance requirements for the primary first-wall components. The lessons learned for using PM-HIP in the future included designing the component for fabrication by PM-HIP and improving the uniformity of powder consolidation to reduce distortion and improve tolerances.

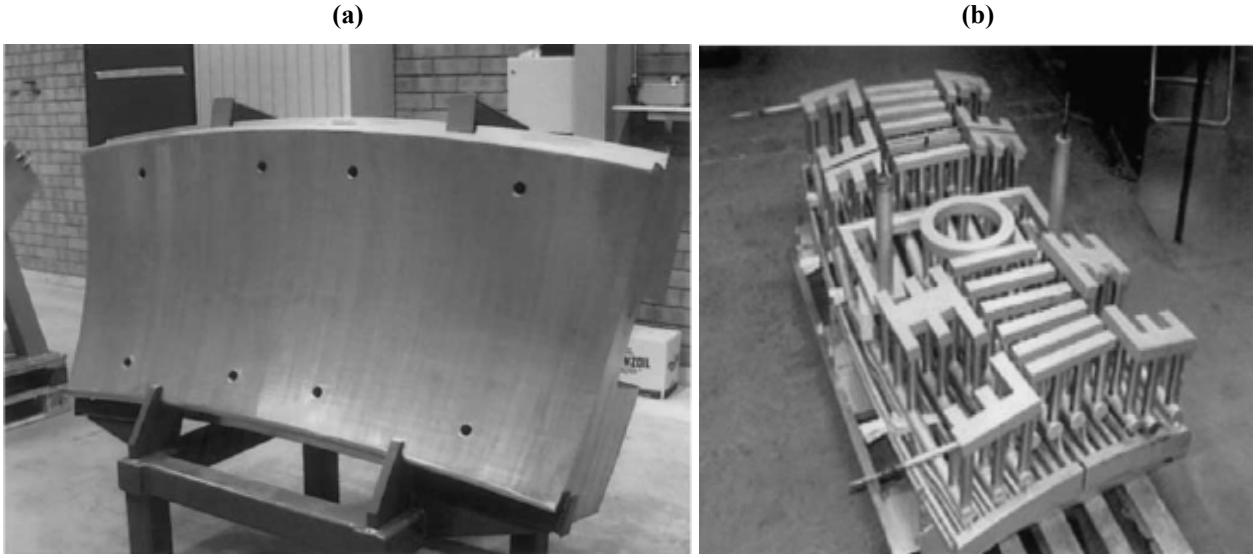

Figure 40. PM-HIP fabrication of (a) the shield block prototype and (b) coolant channel system insert in the shield block (both were made from 316L(N)-IG) [99].

Beginning in the early 2000s, R&D programs led by Rolls-Royce in the United Kingdom and the Electric Power Research Institute (EPRI) in the United States investigated the use of PM-HIP for producing large components of 304L and 316L SSs for nuclear applications and Grade 91 ferritic steel non-nuclear applications [28, 30-33, 36, 49, 50, 86, 106, 107]. PM-HIP has an advantage over current processes such as casting, forging, and rolling: PM-HIP produces near-net shaped components in different sizes and dimensions [10, 25, 27]. Other benefits of PM-HIP include precise composition control of stainless and ferritic steels throughout the microstructure of the component and reduction or elimination of welding [10]. The initial R&D efforts of these programs focused on the feasibility assessment of PM-HIP for producing components from 316L SS and Grade 91 ferritic steel powders [10, 28]. One such component produced by PM-HIP of 316L was a valve body 12 inches (30.5 cm) in diameter weighing 1,716 lb (780 kg), demonstrating that large components could be manufactured by this technology [10].

Following the demonstration of PM-HIP on large 316L components, in the 2010s, EPRI began an R&D program focused on manufacturing heavy-section low alloy steel components for nuclear applications. These applications include RPV components for SMRs. An advantage for producing large components using PM-HIP instead of forging is that the latter produces internal defects and nonuniform grain structures, whereas the former can reproducibly produce components with uniform fine grain structure throughout the microstructure and isotropic mechanical properties. Nevertheless, the transition to using PM-HIP to manufacture large components for nuclear reactors creates several practical and technical challenges associated with scaling up the technology to larger sizes.

2.4.1 Large Component Production

The recent developments in PM-HIP technologies for producing large structural components with near-net shape and full density have been led by the nuclear energy industry. However, these developments present challenges to manufacturers of HIP equipment, because large components for current generation nuclear reactors and advanced light-water reactors (ALWRs) exceed the work zone size in pressure vessels of current HIP units [106]. Producing large products by PM-HIP places large demands on the pressure vessel and the furnace to be able to uniformly heat and cool the workpiece. As the pressure vessel increases in size, the mass and weight increase too, which makes it more difficult to manufacture

the pressure vessel with sufficient strength for safe operation of the HIP unit during production of large components.

In 2010, EPRI initiated a project team with utility and industry stakeholders to assess the interest and feasibility of manufacturing the largest HIP unit in the United States. This large HIP unit is referred to as *Advanced Technology Large-Scale* (ATLAS) and is intended to produce large components for fossil and nuclear energy applications such as pressure vessel heads, valves, pumps, nozzles, headers, and flanges [106]. Leading HIP manufacturer, Quintus Technologies AB (formerly Avure Technologies of Västerås, Sweden) partnered with EPRI to develop ATLAS. In 2012, Azure announced the development plan for the Azure Tera-HIP, or TeraPi, system that would include a work zone of 3 m diameter and 5 m in height. The HIP design was modular for quicker installation, with a pressure vessel that consisted of high-strength steel wire wound around four frames and forged together. The loading frame lifts the workpiece container and places it in the pressure vessel. The pressure vessel containing the workpiece is placed in the HIP unit by the transfer rail. It was reported that the pressure vessel would weigh more than 250 tons.

HIP units based on convection furnaces are suited for larger workpieces. Natural convection furnaces heat the Ar gas in the furnace heating element area, and heat is transferred by convection as the gas flows into the pressure vessel work zone [21, 87]. Once the temperature is reached during heating, the gas circulation is stopped. Because convection heating does not produce direct heat on the workpiece as with radiation furnaces, pressure vessels with larger work zones can be heated effectively. Further improvements can be achieved with forced-convection furnaces, because the gas flow is accelerated by a fan which increases the heating and cooling rates and reduces distortions of complex shaped workpieces [21]. Referring to the very large Avure HIP (now Quintus Technologies), the furnace system of the TeraPi would incorporate Uniform Rapid Cooling (URC) that is designed for rapid heat transfer during cooling, with cooling rates of up to 100°C/minute.

2.4.2 Applied Research of PM-HIP for Nuclear Application

2.4.2.1 Development History

Early research by Rolls-Royce in England starting in the late 1980s showed that PM-HIP could be used for producing components of 304L and 316L SSs for current generation NPPs [26, 28, 30-33, 107]. The components consisted of valves, inserts, and toroids. From the success in early investigations for using PM-HIP to fabricate components for NPPs, several R&D efforts followed to demonstrate producing larger components by PM-HIP. Figure 41 shows a HIPed 316L SS (RCP) bowl blank and the final machined RCP pump bowl that Rolls-Royce produced by PM-HIP [31]. First, an RCP bowl blank was produced by PM-HIP, followed by solution annealing, pickling off the carbon steel can, and then final machining. Prior to machining, a large protrusion with a thickness of 140 mm was removed from the bowl discharge area of the HIP consolidated blank for destructive testing. The PM-HIP consolidated blank weighed 8,100 kg. Non-destructive inspection using UT showed no internal defects in the RCP bowl blank. The tensile properties of the RCP bowl showed that the strength and ductility properties exceeded material specifications.

Figure 41. (a) RCP bowl blank produced from 316L SS by PM-HIP after consolidation and can removal (a) and finished machined RCP bowl (b) [31].

Starting around 2010, EPRI has led the development of PM-HIP for producing components for pressure-retaining nuclear and non-nuclear applications [10, 26]. The early research by EPRI involved producing PM-HIP components from 316L SS for nuclear applications and Grade 91 steel for fossil energy applications. The goal was to obtain the results on processing and mechanical properties from the development of PM-HIP to be introduced into the ASME Boiler and Pressure Vessel Code. EPRI teamed with Carpenter Technologies to produce valve bodies from 316L SS and Grade 91 steel as shown in Figure 42. The mechanical properties and microstructure characterization by optical metallography were obtained from both 316L SS and Grade 91 steel valve bodies. The elevated temperature tensile and Charpy impact toughness properties were obtained for support of an ASME Code Case. For the Grade 91 steel valve body, the elevated temperature tensile properties exceeded that published in ORNL Report 6303 [92], and the thermal creep performance was comparable to that of a large database of creep values for Grade 91, which is covered in Section 2.3 of this report.

(a) (b)

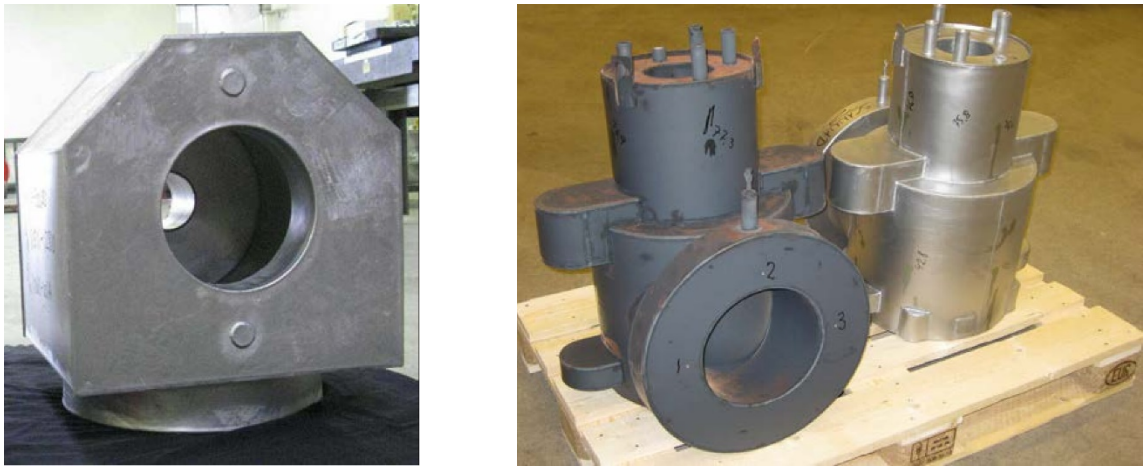

Figure 42. Valve bodies of 316L SS (a) and Grade 91 steel (b) produced by PM-HIP [26].

EPRI's more recent applications using PM-HIP include pressure retaining components from low alloy A508 steel [4, 36, 49, 86]. In an early demonstration project conducted by EPRI, PM-HIP was used to produce a mock-up RPV upper head of the NuScale SMR [36]. The goal of this project was to demonstrate that PM-HIP could be used to produce the pressure vessel upper head at 44% scale of the actual size. This scale was selected based on the size of the largest HIP pressure vessel available in the United States. The procedure involved joining inner and outer shells with 27 integral penetrations to form the can. As part of the can fabrication, numerous tube stems were installed for filling the steel can with A508 powder. After degassing, the tube stems were crimped and then welded shut. No details about the HIP conditions were provided in the progress report [50]. Figure 43 (a) shows the outer shell following the fabrication of the 27 penetrations. Figure 43(b) shows the completed can with fill stems.

(a) (b)

Figure 43. Fabrication can for the 44% scale can of the pressure vessel upper head for the NuScale SMR (a), and completed can with tube stems installed (b) [17].

The reproduced photo in Figure 44 shows the upper vessel head produced by PM-HIP at 44% scale. The diameter of the upper vessel assembly is ~50 in. (1,270 mm), and the weight is 3,650 lb (1,650 kg).

Figure 44. The 44% scale upper vessel head assembly produced by PM-HIP [36].

In 2017, an extensive research project funded by DOE consisting of EPRI and Nuclear Advanced Manufacturing Research Centre (Nuclear-AMRC) began investigating the use of PM-HIP for producing large structural ⅔ scale component assemblies of an SMR vessel [36, 108]. It is generally recognized that there are inherent problems with scale-up of nuclear components using PM-HIP, mainly because of the costs associated with building a HIP unit with a very large pressure vessel to produce the large RPV components. Therefore, the overall goal of this project was to demonstrate that PM-HIP could be effective in producing large structural components for nuclear reactors, with a potential cost savings of 40%, in a reduced time frame of less than 12 months compared to traditional manufacturing methods of products for LWRs [19, 36, 49]. Because a ⅔ scale head is too large to fit into the largest PM-HIP unit in the United States, the plan was to produce two half head sections by PM-HIP which would be welded together with electron beam welding. Producing a seamless full-scale upper head or ⅔ scale upper head requires a larger HIP pressure vessel such as ATLAS. The early phase of research by EPRI showed that powder with the composition of the low alloy A508 steel produced commercially by gas atomization, consolidated by HIP, and heat treated could meet the mechanical properties of ASME Code for SA508 Grade 3, Class 1 material.

The research plan in Phase 1 also focused on manufacturing the lower head and the transition shell of the pressure vessel at ⅔ scale for the NuScale Power RPV [36]. Figure 45 shows a schematic of the pressure vessel for the NuScale RPV. Phase 1 of the project includes fabrication and assembly of the lower reactor vessel assembly. The lower reactor vessel assembly consists of the lower head (PM-HIP), lower flange shell (forging), and upper transition shell (PM-HIP). Phase 2 of the project will focus on the fabrication and assembly of the upper reactor vessel assembly, which is more complex, consisting of the upper head with 27 penetrations (PM-HIP), the pressurizer shell (forging), the integral steam plenum (PM-HIP except divider plate) and the steam plenum access port assembly (PM-HIP).

The vessel components were consolidated using the 66 in. diameter HIP unit at Bodycote, Oregon, which was the largest HIP in the United States. In Phase 1, year 2 of the project, extensive research was conducted on smaller billets of an A508 steel that was produced by PM-HIP. The purpose was to

understand the effects of composition and contamination on the gas-atomized A508 powders and post-HIP heat treatments on the mechanical properties, including impact toughness. It also sought to apply the knowledge obtained from the research to improve the quality and reproducibility of large components such as the nuclear RPV by PM-HIP [49].

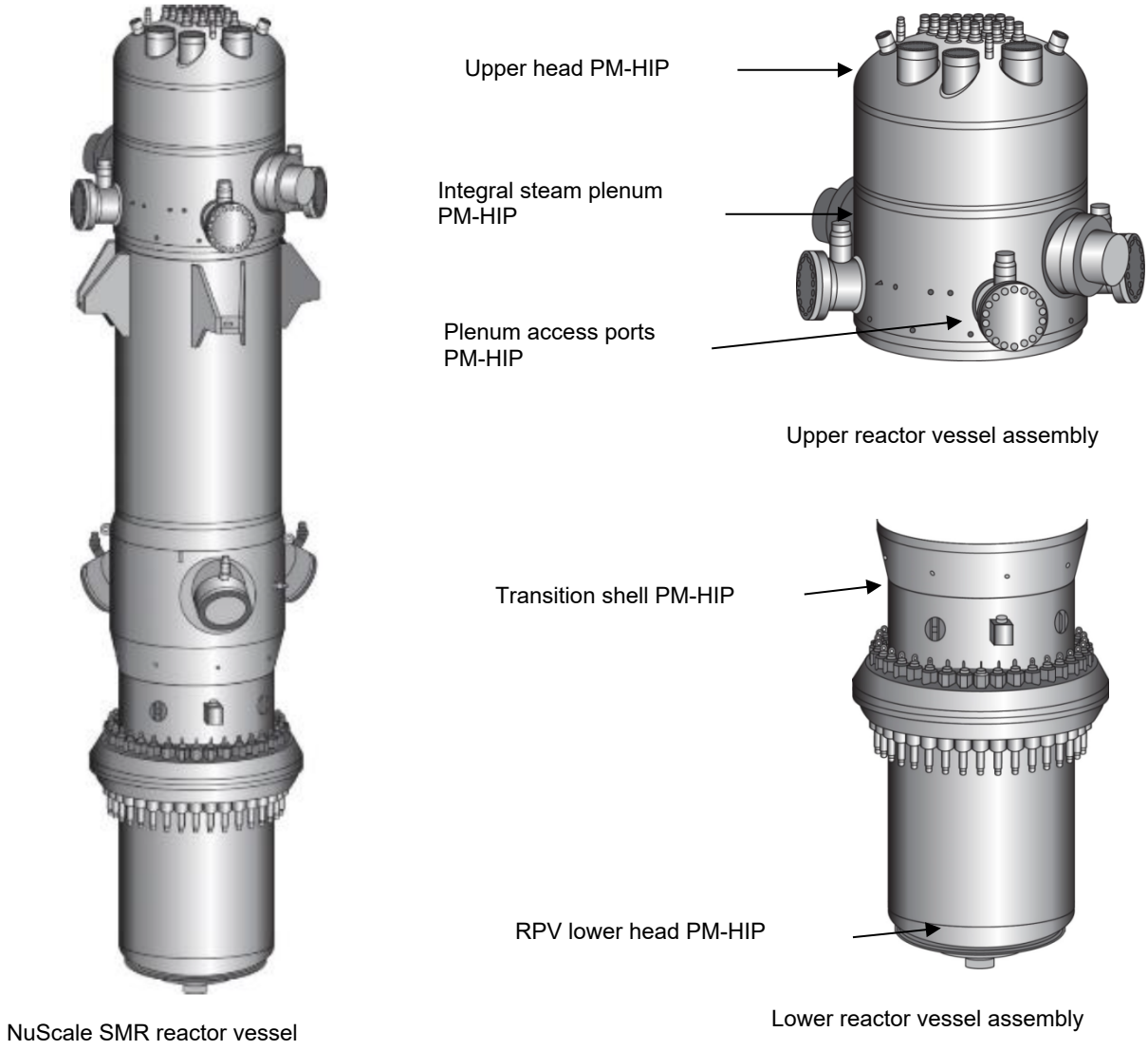

Figure 45. Schematic model representing the pressure vessel of the NuScale SMR [19].

2.4.2.2 Lower Pressure Vessel Head

The lower vessel head was produced in two sections by PM-HIP and welded together using electron beam welding (EBW). EBW of PM-HIP is addressed in a separate EBW technical letter report [86]. The can design consisted of an inner dome and outer surface sections as illustrated in Figure 46. The inner and outer sections of the can were welded together. An image showing the can after fabrication and welding is reproduced in Figure 47. The size of the half section can is ⅔ scale of the pressure vessel and is heavy; once filled with powder, it weighs ~6,910 lb (3,134 kg), which makes it difficult to manage. Ports were fabricated on the top surface of the can spaced around the outer diameter for filling with the A508 steel

powder. A shaker table was used to ensuring that the powder filled every internal section of the can. After this, the can was degassed in vacuum, hermetically sealed by crimping the filling ports, and then welded shut to remove any residual air and moisture that was adsorbed on the surface of the A508 steel powder before sealing. Three half-section cans were fabricated for consolidating the A508 powder by HIP. The first half-section can, or Article 1, was for developing the procedures for fabrication, filling with and degassing the powder, and obtaining important data on volume shrinkage and distortions that may be encountered during HIP. The second and third half-section cans, or Articles 2 and 3, were fabricated and consolidated using procedures similar to that developed for Article 1. The final dimensions of the three half-section cans were measured and used to correlate with modeling the volumetric shrinkage during HIP. However, estimating the volume shrinkage of the can during HIP was difficult to model because of the complex, nonsymmetrical design that included an external boss-support and two internal support structures. Measurements of each can were obtained in 3D using a portable coordinate measuring machine (FaroArm). Subsequently, a fourth article was produced which is discussed below.

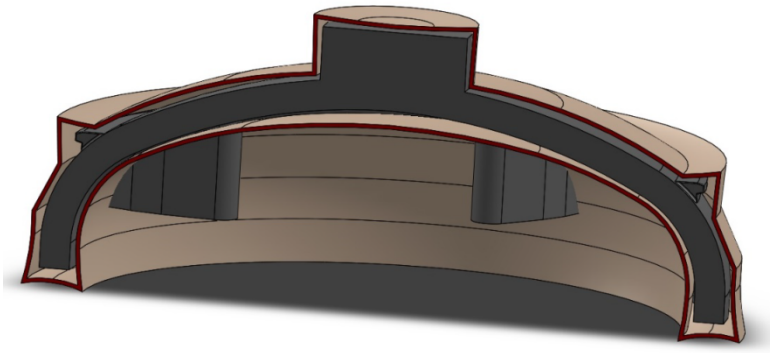

Figure 46. Illustration of the two sections of the can for the lower vessel head [36].

Article 1 was fabricated with a wall thickness of 0.375 in. (9.5 mm) for the can. The model indicated that this wall thickness could accommodate the large size of the half-section capsule that was estimated to weigh ~7,000 lb (3,175 kg), when filled with the A508 powder. This can was consolidated using the large HIP unit at Bodycote. The can was positioned upright in a rack during HIP to minimize unpredicted distortions during HIP. The HIP parameters were 4 h at 2,050°F (1,120°C), but the applied gas pressure was not specified in the progress report. The measured dimensions of Article 1 showed that considerable distortions occurred during HIP. This consisted of a decrease in the diameter of the can and deflection of the bottom support structure from the dimensions predicted by modeling the shrinkage [36]. The 0.375 in. wall thickness of Article 1 was considered the cause of the distortions.

Articles 2 and 3 are almost identical, exception that Article 3 incorporates a backing bar for welding. Articles 2 and 3 were manufactured in a manner similar to that used for Article 1, including the HIP procedure. Some adjustments were made for Articles 2 and 3 to more closely match the near-final vessel dimensions. Based on the distortions measured on the HIP Article 1, the wall thicknesses of the cans for Articles 2 and 3 were increased to 0.50 in. (12.5 mm). This increase was predicted by modeling to improve the dimensional stability of the half-section can during HIP. The dimensional measurements of Article 2 showed smaller distortions in the can during HIP, with two locations on the inner surface out of specification by less than 0.125 in. (3.2 mm) of the can and one location on the outer surface near the centrally located boss support out of specification by 0.12 in. (3.1 mm). Article 3 showed good dimensional accuracy with specifications, with only minor undersize distortions of 0.20 in. (5 mm) at sharp radius grooves on the inside surface and 0.25 in. (6 mm) on the boss support. The conclusion of this task was that large and heavy half-section cans with nonsymmetric dimensions could be produced by PM-HIP. Plug samples were removed from Articles 2 and 3 for mechanical testing and metallographic

examination. Although Articles 2 and 3 had Charpy impact values of 72 and 59 ft-lb, respectively, the objective is to ultimately achieve the goal of >100 ft-lb. Additionally, no thermally induced porosity was observed as in Article 1, but optical metallography revealed prior particle boundary decoration with what appeared to be silicates with occasional pores. Energy dispersive spectroscopy (EDS) elemental mapping showed the particles to be predominantly silicates with occasional manganese sulfides. The investigators continue to improve the fabrication process. In the event that the welding of Articles 2 and 3 failed, EPRI commissioned a fourth article which has been fabricated for further EBW developmental work. A 3D analysis was performed to compare the final geometry of Article 4. The support feature near the center was slightly undersized, but all other dimensions had a positive machining allowance. Mechanical testing results for Article 4 were not available at the time of this report.

Figure 47. The half-section of the can for the lower vessel head after fabrication and welding [36].

2.4.2.3 Transition Shell Section

Another component of the pressure vessel reported in the Phase 1 progress reports was fabrication of the transition shell sections by PM-HIP. Based on the size of the pressure vessel for the large HP unit, the transition shell was divided into five equal size sections. Each section is the full height of the transition shell, and all will be joined together by EBW to develop the full-diameter transition shell. To fit the large size of the transition shell section into the HIP unit, a frame was required to support the section in a vertical position (Figure 48). The purpose of fabricating the transition shell sections is to demonstrate that

this complex part can be produced through PM-HIP and that vertical EBW welds can be used to join them together to fabricate the complete the transition shell. However, it is anticipated that for a production NuScale RPV, the upper transition shell will be produced using conventional forging technologies.

Although five transition shell sections are needed to complete the full diameter of the transition shell, six sections will eventually be produced. As reported in the Phase 1 progress reports, four sections have been produced. The first section, referred to as Article 1, was produced primarily to understand dimensional movement during HIP and to adjust the witness can (discussed below) model/geometry. Article 1 was produced without vacuum annealing, because this process was developed later and implemented on the future shell sections. EPRI observed inconsistencies in toughness results across similar A508 powder chemistries. Therefore, additional processing steps were implemented to keep the powder in the best possible condition before consolidation. The vacuum anneal at 800°C was implemented in the manufacturing procedure based on results obtained in later studies conducted by EPRI that showed improvements in the toughness properties of the A508 steel after HIP with smaller test samples, which was documented in the progress report for the second year and discussed in Section 2.3 of this report [49].

The second section, referred to as Article 2, was fabricated and filled with the A508 steel powder, followed by cold degassing and vacuum annealing at 800°C by Solar Atmospheres [49]. Figure 48 shows Article 2 before and after the vacuum annealing. The vacuum annealing was performed on the transition shell section in the horizontal position, resulting in severe distortions occurring in the lower section of the can that damaged the frame after bulging (Figure 48b). The subsequent investigation determined that the bulging was likely caused by an increase in gas pressure inside the can during vacuum annealing [49]. This problem resulted from insufficient degassing of the can to remove residual gases associated with the A508 steel powder.

A decision was made to proceed with the HIP of the can with the bulge. Figure 49 shows the transition shell section after consolidating the A508 steel powder using the large HIP unit. Similar HIP conditions as those used for producing the three lower vessel head articles were employed for the transition shell section. The dimensional measurements showed acceptable distortions of the transition shell section after HIP, consisting of slight undersize sections in the upper left corner and the mid-section of the outer surface by 0.2 in. (5 mm). This may be due to the more symmetric design of the transition shell can section as compared to the lower vessel head can sections.

(a) (b)

Figure 48. Side views of the transition shell section before vacuum annealing (a) and after (b) [36].

Figure 49. View of the inner surface of the transition shell section after consolidation by HIP [37].

After determining that the final dimensions of Article 2 after HIP were acceptable for meeting the project goals, although additional machining will be necessary to use Article 1 in the mockup assembly, two more sections of the transition shell, Articles 3 and 4 were fabricated for HIP using similar procedures [49]. Initially, it was decided that stem ports for filling, degassing, and vacuum annealing of the A508 steel powder would only be fabricated along the upper section of the transition shell cans. However, additional ports were fabricated on the outer surface of the curved transition shell face to assist in the vacuum annealing to remove residual gases to reduce risks of bulging. This procedure was implemented for Articles 3 and 4. No distortions or bulging of Articles 3 and 4 were observed after vacuum annealing at 800°C for 19.75 and 10.67 h, respectively. The vacuum annealing time for Article 4 was reduced based upon residual gas analyses conducted for Article 2. Articles 3 and 4 were successfully consolidated by HIP. Dimensional measurements showed that the tolerances were found to be acceptable for Articles 3 and 4 after HIP.

To evaluate Charpy impact toughness, two capsules were produced for each transition shell section using the same lot of powder. For each transition shell section, one capsule was consolidated by HIP upon receipt of the powder. The second capsule was consolidated by HIP at a later date and included vacuum annealing of the powder. These capsules were used for conducting Charpy impact tests to establish the baseline toughness values without vacuum annealing and with vacuum annealing for each transition shell section. These capsules were consolidated by HIP independently of the transition shell sections. Details on the dimensions, shapes, and weights of the capsules were not provided in the EPRI progress reports.

In addition, three plugs were extracted from each HIPed transition shell section to determine the Charpy impact properties in the lower, middle, and upper regions of the HIPed transition shell section. Oxygen measurements were also taken directly from the plugs. A witness can was also generated and consolidated in the HIP unit simultaneously with the transition shell section. A single Charpy impact toughness value was reported for the witness can. Oxygen measurements were taken from each of the witness cans except for Article 1. The progress reports did not identify the reason for this exception. Details on the dimensions, shapes, and weights of the plugs and witness can were also not provided in the EPRI progress reports.

For Article 1, the baseline Charpy toughness values at room temperature for the powder were 84 ft-lb (114J) for the non-vacuum annealed powder and 114 ft-lb (155J) for the vacuum annealed powder. Table 8 is reproduced from the EPRI progress report and provides the Charpy toughness values and oxygen measurements of the three plugs and the witness can [86]. The impact toughness values of the plugs and the witness can showed values that were lower than the baseline value of 84 ft-lb and scatter in the values with location of the plug in the shell component. From this table, the oxygen levels vary with location of the plug but do not correlate with the impact toughness values. Again, Article 1 was produced without vacuum annealing.

Table 8. Room temperature Charpy impact toughness values obtained from the three plugs removed from Article 1 that was produced by PM-HIP with no vacuum annealing

ID	Location in Shell	Toughness, ft-lbs (ave)	Toughness, J (ave)	Oxygen (ppm)
1ID1	upper	64	86	200
2ID1	middle	70	95	80
3ID1	lower	55	75	90
0ID1	Witness	68	92	NA

For Article 2, the baseline Charpy toughness values for the powder were 72 ft-lb (98J) for the non-vacuum annealed powder and 79 ft-lb (107J) for the vacuum annealed powder. Table 9 is reproduced from the EPRI progress report and provides the Charpy toughness values and oxygen measurements of the three plugs and the witness can [86]. The vacuum annealing conducted for Article 2 reduced the scatter in the oxygen levels for the three plugs removed from the upper, middle, and lower sections of the shell component. Although the impact toughness values for the middle and lower sections were acceptable, the low value for the upper section is of concern for producing heavy-section large components of the RPV by PM-HIP using the low alloy A508 steel.

Table 9. Room temperature Charpy impact toughness values obtained from the three plugs removed from Article 2 that was produced by PM-HIP with vacuum annealing

ID	Location in Shell	Toughness, ft-lbs (ave)	Toughness, J (ave)	Oxygen (ppm)
1A	upper	54	73	140
2A	middle	81	110	110
3A	lower	78	106	100
0A	Witness	78*	106	80

* corresponds well with capsule toughness value

For Article 3, the baseline Charpy toughness values for the powder were 68 ft-lb (92J) for the non-vacuum annealed powder and 78 ft-lb (106J) for the vacuum annealed powder. Table 10 is reproduced from the EPRI progress report and provides the Charpy toughness values and oxygen measurements of the three plugs and the witness can [86]. The impact toughness values of the plugs showed that none of the three locations on Article 3 achieved toughness similar to the vacuum annealed capsule. Similar to Article 2, a significant drop in toughness was observed from the bottom to the top of the transition shell section. From this table, the oxygen levels do not correlate with the impact toughness values.

Table 10. Room temperature Charpy impact toughness values obtained from the three plugs removed from Article 3 that was produced by PM-HIP with vacuum annealing

ID	Location in Shell	Toughness, ft-lbs (ave)	Toughness, J (ave)	Oxygen (ppm)
1B	upper	38	52	130
2B	middle	54	73	120
3B	lower	67	91	120
0B	Witness	79*	107	100

* corresponds well with capsule toughness value

For Article 4, the baseline Charpy toughness values for the powder were 87 ft-lb (118J) for the non-vacuum annealed powder and 104 ft-lb (141J) for the vacuum annealed powder. Table 11 is reproduced from the EPRI progress report and provides the Charpy toughness values and oxygen measurements of the three plugs and the witness can [86]. As seen in the witness can, a toughness value greater than 100 ft-lb can be achieved with proper handling and processing. However, the plugs did not achieve optimum results. As in Articles 2 and 3, toughness values were reduced from the lower part of the transition shell section to the top. From this table, the oxygen levels vary with location of the plug but do not correlate with the impact toughness values.

Table 11. Charpy impact toughness values obtained from the three plugs removed from Article 4 that was produced by PM-HIP with vacuum annealing

ID	Location in Shell	Toughness, ft-lbs (ave)	Toughness, J (ave)	Oxygen (ppm)
S4A	upper	68	92	110
S4B	middle	70	95	90
S4C	lower	85	115	100
S4W	Witness	102	138	80

3. GAP ANALYSIS

The nuclear industry is interested in PM-HIP as an advanced processing method for producing components of current generation of LWRs and RPV components of small modular nuclear reactors using SSs and low alloy steels. The primary goal of a recent and ongoing R&D project led by EPRI, Nuclear-AMRC in the United Kingdom, and NuScale Power is to demonstrate that PM-HIP can be used for manufacturing large structural components of a SMR vessel from low alloy A508 steel economically and with properties that meet or exceed those of wrought A508 steel. Section 3 builds on the information presented in Section 2 regarding PM-HIP and its development for nuclear applications by analyzing the important challenges and technical gaps that must be addressed to effectively develop and demonstrate PM-HIP for the fabrication of heavy-section low alloy steel components for nuclear applications.

Section 3.1 discusses key challenges in applying the PM-HIP fabrication process to nuclear components, with a focus on applications using heavy-section low alloy steel components. Section 3.2 provides an

analysis that identifies and prioritizes technical gaps in a series of tables. Finally, Section 3.3 overviews the codes and standards landscape relevant to PM-HIP manufacturing for nuclear applications and assesses the gaps that must be filled for PM-HIP for heavy-section low alloy steel components for nuclear applications.

3.1 PM-HIP PROCESSING

Any manufacturing process, including PM-HIP, has a number of steps that must be completed successfully to reliably produce components with sufficient performance for the application. In this section, key challenges in applying the PM-HIP fabrication process to heavy-section low alloy steel components for nuclear applications are divided into three general areas of powder production, PM-HIP process, and properties and performance.

3.1.1 Powder Production

The primary prefabrication step in the PM-HIP process is powder production. The powder production process is very important to the success of the overall PM-HIP manufacturing process in producing quality components because it provides the starting materials for PM-HIP. The initial powders can introduce unacceptable deficiencies, such as contamination, that significantly degrade final component performance and cannot be recovered later in the PM-HIP process. Therefore, the powder production processing conditions must include careful control of the chemical composition, particularly key contamination elements such as oxygen and nitrogen.

Some variation with metal powders produced by different gas atomization companies is expected because each will use proprietary processing conditions that influence the composition, size, size distribution, morphology, and internal microstructure (including porosity) of the metal powders. Because small metal particles have a higher surface area–to–bulk volume ratio compared to that of larger metal particles, they will have a higher tendency for contamination by adsorption of oxygen, nitrogen, and water moisture from exposure to air. The inclusion of the small particles with the larger particles could introduce inhomogeneities in and degrade the mechanical properties of the final component processed by PM-HIP. A sieving operation is important for removing the small particle sizes of powder that may be more likely to be contaminated. Therefore, to effectively manage composition and contamination, a variety of powder quality characteristics should be considered and carefully managed.

This understanding of composition and contamination, as the key factors for powder quality, are consistent with the information presented in Section 2.1.1.2. Tables 1 and 2 demonstrate through heat-to-heat and producer-to-producer comparisons that the most significant variation in elements tends to be contamination by oxygen and nitrogen. Furthermore, oxygen and nitrogen contamination, along with other interstitial elements such as carbon, have been shown to degrade the impact toughness of low alloy A508 steel investigated by EPRI for heavy-section RPV components. The observation that RPV steels are sensitive to carbon, oxygen, and nitrogen levels is consistent with the generally accepted knowledge in metallurgy that mechanical properties of body-centered cubic (bcc) crystal structures of low alloy ferritic steels are more susceptible to changes than face-centered cubic (fcc) crystal structures of SSs because of the more complicated dislocation slip systems and lower atomic packing of bcc metals compared to fcc metal.

The quality assurance for powder production is primarily the responsibility of the companies that specialize in powder production by gas atomization. Important powder quality characteristics to consider are powder composition (particularly contamination elements), particle size, size distribution, and morphology, which can impact powder flow. Certification of the metal powder composition should be obtained from accredited laboratories that specialize in chemical analysis of powders. Depending on the

elements contained in the SS and low alloy steels, these laboratories will use a variety of techniques such as x-ray fluorescence, inductively coupled plasma mass spectroscopy, and combustive analysis to quantify the amount in terms of weight percent of each element present in the composition. A report documenting the chemical analysis should be provided by the powder production company to its customer to confirm conformance with the relevant material specification.

A variety of ASTM standards for analyzing metal powder characteristics (e.g. particle size, size distribution, and flow characteristics), are described in greater detail in Section 3.3 below, as well as in a recent NIST report [58]. The NIST report assesses testing methods for determining properties of metal powders that enable industry to choose the optimum metal powder based on the production method that will provide the desired microstructure and properties for the intended application. Key properties addressed in the report include to the processes for sampling metal powders and for measuring the size, morphology, density and composition of metal powders, as well as measurement of other properties such as flow behavior and thermal properties. In addition, existing ASTM specifications specify the composition levels and ranges of the elements for several SSs (ASTM A988/A988M), nickel-based alloys (ASTM B834), and Cr-Mo steels (ASTM A989/989M) that must be met by each powder manufacturer. As described in Section 3.3 below, a similar ASTM specification must be developed for PM-HIP low alloy A508 steel. The standard methods for analyzing powder characteristics can then be used to confirm acceptability under the ASTM specification for the specific material.

3.1.2 HIP Process

Applying the HIP process to heavy-section low alloy steel components presents several unique challenges, including powder handling and storage, can design and fabrication, degassing, scaling up the HIP furnace and vessel, and optimizing HIP process parameters. Some of these challenges have been effectively addressed through prior experience and R&D activities to date, whereas others continue to be active areas of work. In general, powder handling and storage practices are well established, but they must be followed carefully to minimize and manage contamination that can degrade final component properties. To minimize contamination, it is important that the gas-atomized metal powders are stored in a container filled with inert argon or nitrogen gas for shipment and storage prior to HIP.

Scaling up HIP can designs to larger sizes with complicated geometries (including curved surfaces and protrusions such as ports for control rod drives) creates a number of potential technical issues. However, this challenge has been a key area of work for the EPRI program and has generally been addressed in terms of dimensional tolerances. EPRI demonstrated the ability to design and fabricate large steel cans to enable successful component fabrication via HIP. In addition, EPRI has demonstrated the effective use of modeling and simulation of the steel can design to predict the volumetric shrinkage of the large component during HIP [76]. Therefore, this key challenge to scaling up the HIP process appears to be largely addressed. The broader challenge of scaling up the HIP process and demonstrating sufficient mechanical properties, including toughness, remains to be addressed.

The most significant gap in the HIP process development is the need to determine proper degassing treatment of the metal powder enclosed in the steel can to prevent and reduce contamination in the final component. This topic is discussed extensively in Section 2.2.3. It is crucial to remove all gas (whether inert or contaminant air) from the can before HIP begins. Scaling up the HIP process to larger components makes degassing more challenging because there is a greater volume of gas to remove. The design plan for fabricating the feedthrough pipes on the steel can is a key consideration when degassing a larger component. A significant number of feedthrough pipes is required for very large steel can designs, and their location and size must be carefully considered to ensure uniform gas pumping. The type and size of the vacuum pump must also be considered carefully. A high-vacuum pump maximizes the obtainable vacuum pressure, which improves the molecular flow mechanism of the gas molecules that must pass

through available spaces between the metal particles inside the steel can. The size of the vacuum pump will also determine the pumping speed, which will influence the time required for sufficient degassing. The temperature during degassing must also be considered to prevent contaminant gases from forming stronger bonds (e.g., oxides and nitrides) with the metal powder particles.

Once degassing is complete, the HIP cycle must be monitored to confirm that the proper heating rate and the specified temperature, pressure, and holding times are maintained for consolidation of the metal powder. These optimized HIP parameters are important to ensure full densification, to manage distortion, and to achieve the desired microstructure. Following HIP, visual inspections and dimensional measurements of the consolidated component must be made. Dimensional measurements are particularly important to ensure that dimensional tolerance requirements are met. These measurements also provide important validation data regarding distortion during densification that can be used to improve simulations and models [36, 49]. An accurate method for obtaining precise 3D measurements relies on no-contact scanning laser projections on the surface of the HIP component and a camera detection system that records the position of the laser probe.

In addition to visual and dimensional measurements, witness specimens and protrusions are used to validate component quality. ASME Code Case N-834 for PM-HIP 316L SS requires that a protrusion be added to the steel can with a length equal to or larger than the thickest section of the large PM-HIP component to conduct density measurements, microstructural analysis, chemical analysis, and mechanical properties testing. Witness specimens and protrusions should be carefully designed for larger components due to the potential for greater inhomogeneities across a large component. Section 2.2.7 provides further detail on the use of witness specimens and protrusions to validate component quality.

Finally, post-processing to improve the surface finish is an important step for any application involving fatigue or corrosion as potential aging effects. A rough surface can have significant adverse effects on fatigue and corrosion performance.

3.1.3 Properties and Performance

Ultimately, the powder production, prefabrication, fabrication, and post-fabrication steps are designed to produce a component with sufficient properties and capabilities to perform its necessary functions. For nuclear components, key properties and performance characteristics generally include tensile properties, impact toughness, SCC resistance, irradiation effects, and aging (e.g., corrosion, wear, thermal aging). The component's operating environment (temperature, stress, chemistry, irradiation) and safety function will determine the relevance of these properties and performance characteristics.

Fracture toughness is particularly important for low alloy steels used in RPVs, particularly after irradiation. For existing LWRs, extensive programs are in place using surveillance capsules to monitor irradiation embrittlement as fluence increases. The safety significance of the RPV makes it critical to ensure sufficient pre- and post-irradiation toughness of the PM-HIP low alloy steel materials. EPRI has led the development efforts to produce heavy-section large components by PM-HIP using low alloy A508 steel powder [19, 36, 49, 86]. Early demonstrations by EPRI successfully produced PM-HIP billets with tensile and Charpy impact toughness properties that were superior to the minimum ASTM values established for wrought conditions of ASME SA-508 Class 3 steel. However, it should be noted that the ASME Code Section III Charpy impact toughness requirements are more stringent than those in the ASME SA-508 Specification.

Upon scaling up to larger PM-HIP components, problems were encountered that reduced the impact properties of the A508 steel. After investigating the issue, EPRI determined that handling, storage, and transportation of the A508 steel powder should be improved to minimize the powder contamination that

degrades toughness properties. Also, EPRI added a step for vacuum annealing of the A508 steel powder after it is loaded in the steel can to help reduce the oxygen level prior to HIP. Implementing the improved practices to manage the oxygen level in the powder, EPRI then produced several heavy-section large components based on ⅔-scale for the NuScale RPV. As seen in greater detail in Section 2.4, the results from the articles built with the modified procedure show some improvements in impact toughness, but they significant variability across the component remains. Some areas show sufficient impact toughness, whereas others indicate more marginal properties. This variability in properties may be tied to oxygen content, but the issue is still under investigation by EPRI and requires resolution.

Therefore, EPRI is focused on identifying an effective approach to manage oxygen content and produce components with sufficient impact toughness. This issue should be assessed closely to ensure that PM-HIP can reliably produce large components with sufficient impact toughness for their intended applications.

3.2 TECHNICAL GAP ANALYSIS

This technical gap analysis presented below focuses primarily on the issues and concerns with using PM-HIP for producing heavy-section large components of RPVs with low alloy A508 steel. The components produced by PM-HIP in the past using 316L SS are generally smaller in size and weight and have undergone an extensive development effort that led to the ASME Code Case N-834 for Class 1 components. There are more technical issues with using the low alloy A508 steel and producing heavy-section large components by PM-HIP.

3.2.1 Powder Production

Importance	Topic	
Low	Composition assurance of the gas-atomized metal powders	
	Related in-document sections	2.1.1.1, 2.1.1.2
	Ranking rationale	Commercial production of gas-atomized metal powders is very mature by numerous capable manufacturers, so assurance of an appropriate composition is high, resulting in a low importance ranking for this gap.
	Discussion	The composition of gas-atomized metal powders must be carefully controlled within specifications to ensure adequate properties and performance of the final product. Each company uses feedstock to correctly obtain the specified composition of the metal powder such as SSs and low alloy steels and gas atomization conditions that produce spherical or nearly spherical powders with controlled levels of contamination. These production processes are well-established and mature, which provides strong assurance of an acceptable composition.
Medium	Metal powder production by gas atomization	
	Related in-document sections	2.1.1.1
	Ranking rationale	The method of melting the elemental constituents of SSs and low alloy steels and the atomization environment can significantly affect the quality of the powder and the resulting component properties and performance. However, these powder production methods have been carefully studied.
	Discussion	EPRI has predominantly used air induction melt with IGA to produce powder, which may contribute to an increase in scatter of Charpy impact properties in low alloy steels [84]. The use of cleaner melting

Importance	Topic	
		methods such as VIM may result in lower oxygen contamination levels in SS and low alloy steel powders prior to gas atomization as the molten stream of metal passes through the tundish [84]. It should be noted that in the work performed so far by EPRI and others, air induction melt with IGA (nitrogen) for SS powders has been shown to be an acceptable method to produce the powder used to fabricate pressure boundary components by PM-HIP. However, low alloy steel PM-HIP components may benefit significantly from the use of VIM powders. VIM IGA powder is two to three times more expensive than air induction–melted IGA powders, adding significant cost to the fabrication of large components.
Medium	Powder particle size distribution	
	Related in-document sections	2.1.1.4, 2.1.2.3, 2.2.3
	Ranking rationale	Particle size has tradeoffs in terms of densification and the likelihood of contamination. Sieving practices are well-established and adequately mature to control particle size and size distribution.
	Discussion	Particle size and size distribution can significantly impact densification during HIP, as well as the amount of contamination introduced through the powder. Generally, smaller particle sizes help achieve higher packing density and greater densification after HIP, but they can also increase the likelihood of contamination of smaller particles. Sieving is an essential activity to effectively control the particle size and size distribution. The most important aspect of sieving is to remove the lower size range (e.g., -325 mesh, or less than 45 μm for low alloy steel) particles, which are more prone to higher surface contamination than larger powder sizes because of the higher surface area–to–volume ratio. Sieving also ensures a proper size range for filling and packing the inside of the steel can, which improves the densification and microstructure of consolidated component after HIP.

3.2.2 HIP Process

Importance	Topic	
Low	Fabrication of heavy-section large steel cans	
	Related in-document sections	2.2.2, 2.2.8
	Ranking rationale	EPRI demonstrated that steel cans can be fabricated from design specifications for producing heavy-section large components by PM-HIP.
	Discussion	The steel used to construct heavy-section large cans may have imperfections in wall sections and weld seams that can result in abnormal distortions during HIP. It is important that the mechanical properties of the steel used to fabricate the large cans include sufficient strength and ductility so that the wall thickness can deform properly and as predicted by models during HIP based on time, temperature, and pressure conditions. The steel can must also be weldable to ensure the mechanical integrity of the can during volumetric shrinkage associated with HIP. In addition, the can material must be selected to ensure that it

Importance	Topic	
		has no deleterious effect on the final product. For ferritic PM-HIP components, cans are removed by machining.
Medium	Filling the large steel can with the metal powders	
	Related in-document sections	2.1.2.3, 2.2.2
	Ranking rationale	Improper filling of large cans may result in nonuniform densification. There is limited industry experience with properly filling large cans for PM-HIP, particularly for components with more complex shapes.
	Discussion	There is limited industry experience with filling heavy-section large cans with metal powder to produce components by PM-HIP. Improper filling may result in nonuniform packing of the SS and low alloy steel powders, particularly in large, complex-shaped steel cans. This may result in different local tap densities of the powder inside and cause nonuniform consolidation and local density variations of the HIP component, which may impact component properties and performance. Depending on the complexity of the design and size of the can, a shaker table may be used to help ensure that powder fills all sections of the can. Physical rotation of the can may also improve the uniform flow of powder to all sections of the can.
High	Degassing and vacuum annealing of metal powders	
	Related In-document sections	2.2.3
	Ranking rationale	Improper degassing conditions may cause contamination of the metal powder, and there are no standard methods for degassing
	Discussion	In the EPRI report [37], several degassing and annealing heat treatments were performed on the low alloy A508 steel powder loaded into heavy-section large steel cans (see Section 2.2.3 for more details). The order and conditions of degassing and annealing can significantly impact the amount of contamination retained in the powders. Because of its inert nature, cold degassing can remove Ar gas. However, if the powder is exposed to partial pressures of air (O and N molecules) or oxygen (due to limited purity of Ar gas), then these contaminant molecules will adsorb onto the surface of the particles to form either physisorbed or chemisorbed bonds that will likely prevent them from being pumped out by vacuum at room temperature. At 700°C, bonding of the adsorbed O/N molecules may strengthen to form oxides/nitrides before the vacuum can pump them out of the can. Therefore, selection of the annealing temperature is important. This is a potential concern that may lead to degradation of the mechanical properties of the HIPed component.
High	Scale-up of the vacuum system for degassing powders in heavy-section large steel can	
	Related in-document sections	2.4
	Ranking rationale	Vacuum degassing has not been effectively demonstrated on the large cans needed for heavy-section PM-HIP components and may pose unique challenges with scaling up to larger sizes.
	Discussion	Vacuum degassing is important to reduce contaminant gas molecules of residual Ar gas used in handling storage and transportation of the atomized metal powder. Multiple feed-through ports and a manifold for pumping lines to the vacuum system may degrade the degassing of metal powders in the heavy-section large steel can. Effective degassing

Importance	Topic	
		methods and procedures must be demonstrated for these larger scale applications.
Low	Predicting the volume shrinkage of heavy-section large components during HIP	
	Related in-document sections	2.1.2.3, 2.1.2.4, 2.4
	Ranking rationale	EPRI demonstrated that design models for predicting the volume shrinkage of heavy-section large steel cans containing low alloy A508 steel powder HIP densification were accurate with low or no distortions [17, 37, 109].
	Discussion	Accurate prediction of the volume shrinkage is important for producing heavy-section large components by PM-HIP with minimal distortion. The accuracy of modeling to predict the volume shrinkage of the large can will influence the design aspect of the can, including selection of material, complexity, and HIP parameters. The combination of accurate models and successful fabrication procedures are important to ensure consistent production of quality components within specific dimensional tolerances given the limited number of heavy-section large components that can be produced by PM-HIP. Large complex-shaped components may require a demonstration run to verify the HIP procedure, including shrinkage prediction and achievement of dimensional tolerances.
Medium	HIP conditions for heavy-section large components	
	Related in-document sections	2.2.4, 2.2.5, 2.4
	Ranking rationale	Improper HIP parameters may affect the densification, microstructure, and mechanical properties of the large component. However, optimized HIP parameters have been developed for various other applications. If post-HIP heat treatment is needed to obtain the optimal microstructure and properties, then it should also be demonstrated and performed consistently.
	Discussion	HIP process parameters (e.g., time, temperature, pressure) must be understood and optimized to reduce and eliminate pores to achieve high theoretical density of the metal. Proper HIP parameters—combined with rapid cooling rates through the use of Ar cooling systems may eliminate the need for post-process heat treatment. Nonuniform densification can occur, depending on the HIP parameters for applied pressure, temperature, heating rate, and component size. When large component sizes undergo rapid heating rates, preferential densification of the metal powder can occur near the can's surface [105], which can result in distortions.
High	Witness specimens and protrusions	
	Related in-document sections	3.1.2, 3.1.3
	Ranking rationale	The use of protrusions and witness specimens must be implemented carefully to effectively correlate with the actual density and properties of the heavy-section large component.
	Discussion	Although the use of protrusions and witness specimens are generally accepted for measuring the density and mechanical properties of heavy-section large components, any inhomogeneities in the microstructure of the heavy-section large component from variations with tap density of the metal powder, local densification rate, and

Importance	Topic	
		cooling rates between the surface and interior may result in witness specimen measurements that do not correlate with the actual values of the heavy-section large component. It is not clear whether current research has sufficiently demonstrated the representativeness of witness specimens and protrusions to verify component quality and densification.
Low	Can removal / surface finish / processing	
	Related in-document sections	2.2.8
	Ranking rationale	Post-HIP surface finish is a potential concern, but the steps for can removal, final machining, and surface post-processing are generally performed in a manner that makes surface finish similar to that of conventionally manufactured components.
	Discussion	A series of secondary and finishing operations is generally used to remove the can after HIP and to produce the final component with the specified dimensions. Furthermore, surface finish is generally specified by the ASME Code or relevant specification. However, if a component were proposed to be used without post-HIP machining or surface processing (such as peening or grinding), then there would be a greater susceptibility to SCC, corrosion, and fatigue that should be addressed to ensure that design requirements would be met. If can removal is implemented by acid pickling, then the effects of the acid on the component surface should be carefully considered. For low alloy steel materials, can removal should be accomplished by machining rather than acid pickling because of low alloy steel's susceptibility to acid.

3.2.3 Properties and Performance

Importance	Topic	
High	Impact toughness variability of heavy-section large components	
	Related in-document sections	2.4, 2.4.2.3
	Ranking rationale	Low alloy steels produced by PM-HIP must have acceptable impact toughness for use in RPV components. Nonuniform oxygen levels and other microstructural or compositional variations in these components may lead to variations in fracture toughness of the low alloy steel component that can be challenging to manage.
	Discussion	To date, large components produced by PM-HIP have not had sufficient impact toughness that is consistent across the component. A variety of microstructural or composition variations may contribute to this toughness variability, including oxygen contamination. Varying oxygen levels may contribute to reduced impact toughness in PM-HIP low alloy steel components. EPRI has demonstrated some correlation between oxygen levels and fracture toughness within a component (Section 2.4.2.3). Control of the oxygen and other contamination in PM-HIP–produced large components must be managed effectively through the powder production, handling, storage, and degassing stages.

Importance	Topic	
Low	Stress corrosion cracking (SCC)	
	Related in-document sections	2.3.5
	Ranking rationale	SCC of low alloy steel materials in operating LWRs has been fairly minimal because of the use of cladding to separate the low alloy steel from the water environment. PM-HIP is not expected to significantly change the SCC performance in these materials, but test data would be helpful to confirm this expectation.
	Discussion	SCC is one of the most common failure modes in NPP applications, but it has generally not been a significant issue in low alloy steel components because SS cladding is used to separate the low alloy steel from the coolant. In addition, water chemistry is tightly controlled to reduce the corrosion potential of the system.
Low	Fatigue	
	Related in-document sections	2.3.6
	Ranking rationale	The fatigue properties of PM-HIP low alloy steels are important considerations when determining the safety factors of nuclear power reactors.
	Discussion	Low cycle fatigue is important to consider for lifetime extensions of NPPs. Very few publications discuss fatigue of PM-HIP SSs or low alloy steels. In a study by Baglion [98], the microstructures, mechanical properties, and low cycle fatigue of type 304L and 316L were similar or better than that of the wrought SSs.
High	Irradiation effects	
	Related in-document sections	2.3, 3.1.3
	Ranking rationale	Irradiation effects, including embrittlement, are a significant consideration, particularly for RPV applications. While there are approaches to manage irradiation effects such as surveillance capsules, the data on irradiation effects, particularly on embrittlement, are needed to confidently confirm that PM-HIP materials perform in a manner similar to that of traditionally manufactured materials.
	Discussion	Low alloy steels in the wrought condition are susceptible to irradiation effects, including embrittlement, at LWR-relevant temperatures and neutron doses. PM-HIP-produced SSs and low alloy steels are expected to exhibit similar responses to irradiation, but test data are needed to confirm this expectation.
Medium	Other material aging (corrosion, wear, thermal aging)	
	Related in-document sections	2.3
	Ranking rationale	There are limited data on other material aging effects such as corrosion, wear, and thermal aging on PM-HIP materials in LWR conditions.
	Discussion	Additional data on other material aging mechanisms would be helpful to confirm the expectation that the PM-HIP production process does not significantly impact the performance of these materials. For example, thermal aging can be highly sensitive to microstructure that may be different in a PM-HIP material.

Importance	Topic	
Low	Tensile properties	
	Related in-document sections	2.3.2
	Ranking rationale	The tensile properties of PM-HIP components produced using current best practices are typically comparable to or better than those of components produced by traditional casting, forging, drawing, and rolling methods.
	Discussion	The amount of data on PM-HIP materials is sufficient to provide confidence that tensile properties will be comparable or better than those associated with traditional manufacturing methods as long as standardized and current best practices are followed during production.

3.3 CODES AND STANDARDS GAP ANALYSIS

A variety of ASTM and ASME codes and standards are applicable to the use of PM-HIP for fabricating components for industrial applications. This section outlines the process for adoption of a new material into nuclear codes and standards, describes the current state of nuclear and non-nuclear codes and standards for PM-HIP, and discusses the gaps in codes and standards that must be addressed to enable the fabrication of heavy-section low alloy steel components by PM-HIP.

ASTM Standards for Powder Characterization

A variety of fundamental ASTM standards support the front end of the PM-HIP process related to powder characterization. These include standards for sampling metal powders (ASTM B215-10) and for particle size and size distribution using the sieve analysis (ASTM B214-07), precision electroformed sieves (ASTM E161-00), light scattering (ASTM B822-20), and x-ray monitoring of gravity sedimentation (ASTM B761-06). The flow characteristics of metal powders are important when filling the steel can to ensure complete distribution of the metal powder into every part of the can. The ASTM standard test methods for measuring the flow rate of metal powders consist of using the Hall Flowmeter Funnel (ASTM B213-11), the Carney Funnel (ASTM B964-09) and the combined Arnold Meter and Hall Flowmeter Funnel (ASTM B855-11). In general, these standards are well-established and sufficient to support the use of PM_HIP for heavy-section low alloy steel nuclear components. Standards related to powder handling and storage should be developed further to minimize contamination and to consequently improve final component performance. This topic could also be addressed in any future ASME Code specification for PM-HIP to fabricate low alloy steel components.

Adoption of a New Material into ASME Code for NRC Acceptance

With limited exceptions (See NB/NC/NC-2121), according to ASME Code Section III, Division 1 of the Boiler and Pressure Vessel Code (BPVC), pressure retaining materials must conform to the requirements of one of the specifications for material referenced in Section II, Part D. Part D is used as a reference by the BPVC construction sections, including Sections I, III, and VIII. Part D provides ready identification of materials to specific sections of the BPVC and provides tables of material properties on allowable stress, design, tensile and YS values, physical properties, and external pressure charts and tables. The material specifications referenced in Section II, Part D are given in Section II, Part A (ferrous material specifications) and Section II, Part B (non-ferrous specifications).

A materials specification may include more than one type of material (e.g., low-alloy steel and SS) and several grades within each material type. Part D may identify one or several grades of materials—in an

ASME material specification listed in Part A or Part B—as being acceptable for use with a specific book section. For a material specification to be adopted into Part A or Part B, ASME Code requires that requests for approval typically be limited to materials for which there is a recognized national or international specification. Section II, Part D, Mandatory Appendix 5, *Guidelines on the Approval of New Materials Under the ASME Boiler and Pressure Vessel Code,* provides guidelines on approval of new materials under ASME BPVC. In the 2019 Edition of ASME Code, Section II, Part D, Mandatory Appendix 5 added Table 5-100, *Hot Isostatically Pressed Component Requirements for Austenitic Stainless Steels, Austenitic–Ferritic (Duplex) Stainless Steels, Martensitic Stainless Steels, Ferritic Steels, and Nickel Alloys*. Table 5-100 provides requirements for PM-HIP material approval.

Once a materials specification is adopted into Part A or B, a material specification and grade to Part D for Section III can be added by an ASME Code committee action.

A few different options are available to provide for use of a material specification not listed in Section II, Part D for Section III. The most commonly used option is an ASME code case. An ASME code case that references the use of a material specification not listed in Part D for a particular book section uses an ASTM specification or a specification issued by another national or international organization as its basis. The code case may also list requirements beyond those included in the ASTM or other specification. ASME code cases may not be used for nuclear applications unless they are endorsed by the NRC via their inclusion in RG 1.84, or on a case-by-case basis by the NRC for those code cases that have not yet been listed in RG 1.84. The use of a material specification not listed in Part D could also be approved by the NRC as part of its review and approval of a design certification of a new reactor design.

Current Status of PM-HIP Materials in Nuclear and Non-Nuclear Codes and Standards

Many ASTM standard specifications exist for products manufactured by PM-HIP. For example, ASTM A1080 standard specification defines the basic quality control requirements for using HIP to densify castings of steels, SSs, and related alloys. The three ASTM PM-HIP specifications of interest to manufacture components for NPPs are listed in Table 12 below. There is currently no ASTM PM-HIP specification that covers low alloy pressure vessel steels such as A508 or SA-508.

Table 12. List of ASTM specifications for PM-HIP materials

Applicable materials	Specification
SSs	ASTM A988 *Standard Speciation for Hot Isostatically-Pressed Stainless-Steel Flanges, Fittings, Valves, and Parts for High Temperature Service*
Cr-Mo steels	ASTM A989 *Standard Specification for Hot Isostatically-Pressed Alloy Steel Flanges, Fittings, Valves, and Parts for High Temperature Service*
Nickel-based alloys	ASTM B834 *Standard Specification for Pressure Consolidated Powder Metallurgy Iron-Nickel-Chromium-Molybdenum (UNS N08367), Nickel-Chromium-Molybdenum-Columbium (Nb) (UNS N06625), Nickel-Chromium-Iron Alloys (UNS N06600 and N06690), and Nickel-Chromium-Iron-Columbium-Molybdenum (UNS N07718) Alloy Pipe Flanges, Fittings, Valves, and Parts*
Low alloy steel	None

Stainless Steels

ASTM A988-17 covers PM-HIP for flanges, fittings, valves, and other parts for high-temperature service. The materials covered include several grades of martensitic, austenitic, age hardening, and austenitic-

ferritic (duplex) SSs. This specification was first published in 1998 and did not include age hardening grades which were added in a subsequent version. After a substantial amount of R&D to support the use of SS PM-HIP components for nuclear applications, ASME Code Case N-834 was developed, which permits the use of A988, UNS S31603 (316L SS), with additional requirements specified in the code case for Class 1 nuclear components. Although this code case was published by ASME in 2013 and it is currently approved for use by the NRC in Regulatory Guide 1.84, the code case has never been used to fabricate a pressure-retaining component installed in an NPP in the United States. Currently, the ASME Code committee is developing an appendix to ASME Code Section III to incorporate Code Case N-834. In the 2021 Edition of ASME Code, A988 was adopted, with additional requirements, and is listed as SA-988 in ASME Code Section II, Part A. Although this specification is now listed in Section II, Part A, it has not been endorsed for use by any of the ASME Code book sections other than via Code Case N-834 for nuclear applications and Code Case 2840 for non-nuclear applications.

To date, only 316L SS is permitted as described above for nuclear applications. However, several grades of SS listed in SA-988 could be approved in the future for use in LWRs, in Section III, Division 1 or in Section III, Division 5, for high-temperature advanced reactors. Non-nuclear ASME Code Case 2840 permits the use of A988, UNS S32906 (duplex SS), with additional requirements specified in the code case to manufacture flanges, fittings, valves, and parts in welded construction under the rules of ASME Code Section VIII, Division 1, *Rules For Construction Of Pressure Vessels, and* Division 2 *Alternate Rules*.

Cr-Mo Steels

ASTM A989-18 covers PM-HIP for flanges, fittings, valves, and other parts for high-temperature service. The materials covered include 9Cr, 9Cr-1Mo-V (Grade 91), 3Cr 1 Mo, annealed 2.25Cr 1 Mo (Grade 22) and normalized and tempered 2.25Cr 1Mo (Grade 22). This specification was first published in 1998.

In the 2021 Edition of ASME Code, A989 was adopted, with additional requirements, and is listed as SA-989 in ASME Code Section II, Part A. Although this specification is now listed in Section II, Part A, it is not listed in Section II, Part D and has not been endorsed for use in any of the ASME Code book sections, including nuclear (Section III, Divisions 1 and 5). However, non-nuclear Code Case 2770 permits the use of PM-HIP 9Cr-1Mo-V (Grade 91) for high-temperature service in ASME Code Section I, *Rules For Construction Of Power Boilers,* for components for welded construction. The types of materials listed in ASTM A989 have limited use in LWRs with the exception of Grade 22, which could be used in systems susceptible to flow-accelerated corrosion (FAC). Grades 91 and 22 are permitted to be used in reactors designed to Division 5. However, no PM-HIP specifications are listed for elevated temperature service.

High-Temperature Materials

For ASME Code Section III, Division 5, *Subpart A, Low Temperature Service*, pressure-retaining materials are required to meet the specifications permitted under ASME Section III, NB-2121. For *Subpart B, Elevated Temperature Service*, several specifications for 304 SS, 316 SS, Grade 22, 800H and Grade 91 are listed in Division 5 as permitted materials. However, none of the permitted material specifications include PM-HIP–fabricated components. Part D does not cover materials used under Division 5, Subpart B. The addition of PM-HIP to Division 5 would mostly likely be accomplished via an ASME code case. Division 5 code cases endorsed by the NRC are listed in RG 1.87 Revision 2 *Acceptability of ASME Code, Section III, Division 5, "High Temperature Reactors."*

Nonferrous Alloys

ASTM B834 was first published in 1995 and originally covered alloys UNS N08367(AL-6XN) and UNS N06625 (Alloy 625). The 2015 version added alloys UNS N06600 (Alloy 600), N06690 (Alloy 690) and N07718 (Alloy 718). The specification covers pressure-consolidated powder metallurgy (PM-HIP) for pipe flanges, fittings, valves, and parts intended for general corrosion or heat-resisting service. Under other specifications, standard product forms of Alloys 600 and or 690 are used in pressure-retaining components in all operating PWRs in the United States.

In the 2021 Edition of ASME Code, ASTM B834 was adopted, with additional requirements, and is listed as SB-834 in ASME Code Section II, Part A. Although this specification is now listed in Section II, Part A, it is not listed in Section II, Part D, and it has not been endorsed for use in any of the ASME Code book sections, including nuclear (Section III, Divisions 1 and 5). Table 13 lists the PM-HIP specifications that were adopted into ASME B&PVC.

Table 13. Adoption of PM-HIP specifications into ASME B&PVC

Applicable materials	ASTM specification	ASME code case or section	Nuclear use
316L SS	ASTM A988	Code Case N-834	Approved for use by the NRC in Regulatory Guide 1.84 for Class 1 components
Duplex SS	ASTM A988	Code Case N-2840	No nuclear approval; N-2840 endorses for use under ASME Code Section VIII, Division 1
Cr-Mo steels (Grade 91 and Grade 22)	ASTM A989	Code Case N-2770	No nuclear approval.;N-2770 endorses for use under ASME Code Section I
Nonferrous alloys (AL-6XN, Alloy 625, Alloy 718)	ASTM B834	Section II, Part A	Not endorsed by any ASME Code book sections, including nuclear
Low Alloy Steels (A508)	None	None	

Gaps and Path Forward for Heavy-Section Low Alloy Steel Components

The only PM-HIP material currently permitted by ASME Code Section III for nuclear is Code Case N-834 (316L SS). Additional work will be required to permit other PM-HIP materials for Section III, Division 1 or Division 5 use. The developmental work currently being performed by EPRI and others for PM-HIP A508 RPVs will most likely be used as a basis to develop an ASTM specification. Once an ASTM specification is developed, it is expected to be used as a basis for an ASME code case.

CONCLUSIONS

R&D efforts over the past 20–30 years by Rolls Royce and EPRI have demonstrated that the PM-HIP technology can be used to produce components such as valves, flanges, and fittings for applications in nuclear reactors. The PM-HIP manufacturing process begins with the production of metal powders, generally by atomization, and they can either be blended together or used separately, with or without alloying additions. The metal powder is compacted into a dense solid by compaction at high temperatures and pressure, through HIP, for direct densification of the metal powder. Secondary and finishing operations are generally used to produce the final part or structural component.

Components produced by PM-HIP from 316L SSs are fully dense and possess mechanical properties exceeding the minimum values listed in ASTM standard specification A988/A988M. NRC has approved ASME Code Case N-834 for use in Regulatory Guide 1.84. ASME Code Case N-834 permits the use of A988, UNS S31603 (316L SS), with additional requirements specified in the code case, for Class 1 nuclear components. This represents an important accomplishment for the use of PM-HIP technology in the nuclear power industry.

An EPRI-led team is investigating the use of PM-HIP for producing heavy-section large components of the RPV for the NuScale SMR design. Developing PM-HIP for this application involves addressing a number of challenges, including scaling up to the size and weight of RPV components and producing the low alloy steel components economically and with sufficient mechanical properties, particularly impact toughness to meet or exceed that of wrought A508 as well as meeting ASME Code Section III Division 1 impact toughness requirements. Results obtained to date shown that large heats of A508 steel powder can be commercially produced by inert gas atomization, and large steel cans for holding the A508 steel powder during HIP can be fabricated. The models developed to predict volume shrinkage of the A508 steel powder during PM-HIP are accurate based on detailed inspections of the final component shape.

A significant technical gap associated with upscaling PM-HIP technology for use with low alloy A508 steel powder is the inability to produce a component with sufficient impact toughness. Based on research to date, it is believed that identifying appropriate degassing and vacuum annealing practices to effectively manage oxygen levels in the final component will help improve toughness. There is some evidence that the oxygen level in the final component influences the impact toughness properties of the low alloy A508 steel component, but other factors in the PM-HIP fabrication process may also play important roles. In addition, there is a general need to increase the knowledge and experience with using PM-HIP to produce heavy-section large low alloy A508 steel components. As this knowledge and experience develops, the necessary data can be generated to support development of the ASTM Standards and ASME Code Cases needed to enable production of PM-HIP components for nuclear reactor applications.

REFERENCES

1. Goldberg, S. and R. Rosner. *Nuclear reactors: Generation to generation*. 2011. American academy of arts and sciences Cambridge.
2. *Nuclear Power*. Available from: https://www.nuclear-power.com/.
3. COMISSION, U.N.R., *Requirements for Renewal of Operating Licenses for Nuclear Power Plants–10 CFR PART 54*. 2019.
4. Sulley, J., et al. *Nuclear Pressure Vessel Manufacture Using the Hot Isostatic Pressing (HIP) Process*. 2020. American Society of Mechanical Engineers.
5. *World Nuclear*. Available from: https://www.world-nuclear.org.
6. "Powder Metallurgy—1962". *JOM*, 1963. 15(5): p. 338-339.
7. Hirschhorn, J.S., "Powder metallurgy research—Contemporary trends". *JOM*, 1967. 19(9): p. 25-30.
8. Lawley, A., "Modern Powder 15 Metallurgy Science and Technology". *JOM*, 1986. 38(8): p. 15-25.
9. Lenel, F.V. and G.S. Ansell, "The State of the Science and Art of Powder Metallurgy". *JOM*, 1982. 34(2): p. 17-29.
10. Gandy, D., et al. *PM-HIP Research for pressure retaining applications within the electric power industry*. in *Small Modular Reactors Symposium*. 2014. American Society of Mechanical Engineers.
11. Adams, J.P., *History of Powder Metallurgy*, in *Powder Metallurgy*. 2015, ASM International. p. 0.
12. Yadav, T.P., R.M. Yadav, and D.P. Singh, "Mechanical milling: a top down approach for the synthesis of nanomaterials and nanocomposites". *Nanoscience and Nanotechnology*, 2012. 2(3): p. 22-48.
13. Suryanarayana, C. and N. Al-Aqeeli, "Mechanically alloyed nanocomposites". *Progress in Materials Science*, 2013. 58(4): p. 383-502.
14. Bourell, D., et al., "Materials for additive manufacturing". *CIRP Annals*, 2017. 66(2): p. 659-681.
15. DebRoy, T., et al., "Additive manufacturing of metallic components–process, structure and properties". *Progress in Materials Science*, 2018. 92: p. 112-224.
16. Zhang, Y., et al., "Additive manufacturing of metallic materials: a review". *Journal of Materials Engineering and Performance*, 2018. 27(1): p. 1-13.
17. Dunkley, J.J., "Metal powder atomisation methods for modern manufacturing". *Johnson Matthey Technology Review*, 2019. 63(3): p. 226-232.
18. Torssell, K., *HIP Steel Components for the Manufacturing Industry*. 1992, Springer Netherlands. p. 195-208.
19. Gandy, D.W., et al., "Small Modular Reactor Vessel Manufacture/Fabrication Using PM-HIP and Electron Beam Welding Technologies". *Hot Isostatic Pressing: HIP'17*, 2019. 10: p. 224.
20. Koizumi, M. and SpringerLink, *Hot Isostatic Pressing- Theory and Applications Proceedings of the Third International Conference Osaka, Japan 10-14 June 1991*. 1st ed.. ed. 1992: Dordrecht : Springer Netherlands.
21. Loh, N.L. and K.Y. Sia, "An overview of hot isostatic pressing". *Journal of Materials Processing Technology*, 1992. 30(1): p. 45-65.
22. Boyer, C.B., *Historical Review of Hip Equipment*. 1992, Springer Netherlands. p. 465-510.
23. Mashl, S.J., *Powder Metallurgy Processing by Hot Isostatic Pressing*, in *Powder Metallurgy*, P. Samal and J. Newkirk, Editors. 2015, ASM International. p. 0.
24. Gilp, B.F., et al., *Bibliography on Hot Isostatic Pressing (HIP) Technology*. 1992.
25. Gandy, D.W., J. Shingledecker, and J. Siefert, "Overcoming barriers for using PM/HIP technology to manufacture large power generation components: PM/HIP opens up a new method

of manufacturing high pressure-retaining components for use in the power-generation industry". *Advanced Materials & Processes*, 2012. 170: p. 19+.
26. Gandy, D.W., *PM-HIP research for structural and pressuring retaining applications within the electric power industry*. 2015.
27. Lou, X. and D. Gandy, "Advanced Manufacturing for Nuclear Energy". *JOM*, 2019. 71(8): p. 2834-2836.
28. Burdett, W.B. and I.D. Hookham. *The Implementation of Hot Isostatically Pressed Powder Type 316L/304L Pressure Boundary Components in a PWR Plant*. ASMEDC.
29. Burdett, W.B. *Type 304L and 316L HIP Powder Processing for PWR Components: Design and Manufacturing Benefits and Safety Case Progress*. ASMEDC.
30. Burdett, W.B. *Hot Isostatic Pressing of Hardfacing and Stainless Steel Powders for PWR Components: Materials and Manufacturing Benefits*. American Society of Mechanical Engineers.
31. Sulley, J., P. Mitchell, and D. Mills. *Hot Isostatic Pressing of a Varying Thickness, Thick-Walled Vessel (Reactor Circulating Pump Bowl) for a Pressurised Water Reactor (PWR) Application*. in *Pressure Vessels and Piping Conference*. 2014. American Society of Mechanical Engineers.
32. Kyffin, W., D. Gandy, and B. Burdett. *A Systematic Study of the Material Performance of Hot Isostatically Pressed Type 316L Stainless Steel Powder for the Civil Nuclear Sector*. in *International Conference on Nuclear Engineering*. 2018. American Society of Mechanical Engineers.
33. Kyffin, W., D. Gandy, and B. Burdett. *A Study of the Material Properties and Performance of Hot Isostatically Pressed (HIP) Type 316L Stainless Steel Powders and HIP Processing Available From Today's International Supply Chain*. in *Pressure Vessels and Piping Conference*. 2018. American Society of Mechanical Engineers.
34. International, A., *Standard Specification for Hot Isostatically-Pressed Stainless Steel Flanges, Fittings, Valves, and Parts for High Temperature Service*. 2017, ASTM International.
35. International, A., *Standard Specification for Hot Isostatically-Pressed Alloy Steel Flanges, Fittings, Valves, and Parts for High Temperature Service*. 2018.
36. Gandy, D., *Small Modular Reactor Vessel Manufacture and Fabrication - Phase 1 - Progress*. 2019, Electric Power Research Institute. p. 122.
37. Ioki, K., et al., "ITER-FEAT vacuum vessel and blanket design features and implications for the R&D programme". *Nuclear Fusion*, 2001. 41(3): p. 265-275.
38. Gandy, D. *Advanced Technology*. in *National Institute of Standards and Technology*. 2016. Electric Power Research Institute.
39. *Airgas*. 2022; [Last Accessed 3/29/2022]; Available from: http://www.airgas.com.
40. Engineersedge. 2022; [Last Accessed: 3/29/2022]; Available from: https://www.engineersedge.com/heat_transfer/thermal-conductivity-gases.htm.
41. Dietrich, S., et al., "A new approach for a flexible powder production for additive manufacturing". *Procedia Manufacturing*, 2016. 6: p. 88-95.
42. Traff, A., "New developments in Hot Isostatic Press (HIP) Units". *Metal Powder Report*, 1990. 45(4): p. 279-282.
43. Sustarsic, B., et al., "Bulk and surface characterisation of metal powders for direct laser sintering". *Vacuum*, 2005. 80(1-3): p. 29-34.
44. Achelis, L. and V. Uhlenwinkel, "Characterisation of metal powders generated by a pressure-gas-atomiser". *Materials Science and Engineering: A*, 2008. 477(1-2): p. 15-20.
45. Li, X.-g. and U. Fritsching, "Process modeling pressure-swirl-gas-atomization for metal powder production". *Journal of Materials Processing Technology*, 2017. 239: p. 1-17.
46. Lagutkin, S., et al., "Atomization process for metal powder". *Materials Science and Engineering: A*, 2004. 383(1): p. 1-6.
47. Fedina, T., et al., "A comparative study of water and gas atomized low alloy steel powders for additive manufacturing". *Additive Manufacturing*, 2020. 36: p. 101675.

48. Zwiren, A., et al., "Economic Additive Manufacturing using Water Atomized Stainless Steel Powder".
49. Gandy, D. and M. Albert, *Small Modular Reactor Vessel Manufacture and Fabrication - Phase 1 - Progress (Year 2)*. 2020, Electric Power Research Institute: www.epri.com. p. 146.
50. Gandy, D., *A Study of the Material Properties and Performance of Hot Isostatic Pressed (HIP) Type 316L Stainless Steel Powders and HIP Processing Available from Today's International Supply Chain*. 2018, Electric Power Research Institute: www.epri.com. p. 104.
51. Rahaman, M.N., *Sintering Theory and Fundamentals*, in *Powder Metallurgy*, P. Samal and J. Newkirk, Editors. 2015, ASM International. p. 0.
52. Okamoto, S., T. Sawayama, and Y. Seki, "Robe Steel advances water atomized powders". *Metal Powder Report*, 1996. 3(51): p. 28-33.
53. Neikov, O.D., *Chapter 4 - Atomization and Granulation*, in *Handbook of Non-Ferrous Metal Powders (Second Edition)*, O.D. Neikov, S.S. Naboychenko, and N.A. Yefimov, Editors. 2019, Elsevier: Oxford. p. 125-185.
54. Entezarian, M., et al., "Plasma atomization: A new process for the production of fine, spherical powders". *JOM*, 1996. 48(6): p. 53-55.
55. Hoelzer, D.T., et al., "Influence of particle dispersions on the high-temperature strength of ferritic alloys". *Journal of Nuclear Materials*, 2007. 367: p. 166-172.
56. Cooper, A.J., et al. *On the Microstructural Evolution and Porosity Consolidation in 316L Stainless Steel During Hot Isostatic Pressing*. in *Pressure Vessels and Piping Conference*. 2019. American Society of Mechanical Engineers.
57. Chappell, J.S., T.A. Ring, and J.D. Birchall, "Particle size distribution effects on sintering rates". *Journal of Applied Physics*, 1986. 60(1): p. 383-391.
58. Cooke, A. and J. Slotwinski, *Properties of metal powders for additive manufacturing: a review of the state of the art of metal powder property testing*. 2012: US Department of Commerce, National Institute of Standards and Technology.
59. Mashl, S., "Powder metallurgy processing by hot isostatic pressing". *ASM Handbook*, 2015. 7: p. 260-270.
60. Gregorski, S.J., *High green density metal parts by vibrational compaction of dry powder in three dimensional printing process*. 1996, Massachusetts Institute of Technology.
61. Suresh, K., et al., "Influence of powder composition & morphology on Green density for powder metallurgy processes". *International Journal of Innovative Research in Science, Engineering and Technology*, 2015. 4(1): p. 18629-18634.
62. *Introduction to Powder Metallurgy The Process and its Products*, E.P.M. Association, Editor. 2008: epma.com. p. 36.
63. Bocanegra-Bernal, M.H., "Hot Isostatic Pressing (HIP) technology and its applications to metals and ceramics". *Journal of Materials Science*, 2004. 39(21): p. 6399-6420.
64. "Award winning PM in the USA and Europe". *Metal Powder Report*, 1991. 46(7-8): p. 20-21.
65. Widmer, R., *Future Prospects for Hot Isostatic Pressing*. 1992, Springer Netherlands. p. 3-8.
66. EPMA, *Introduction to Hot Isostatic Pressing Technology (Brochure)*, E.P.M. Association, Editor. 2018: https://www.epma.com/epma-free-publications/product/introduction-to-hot-isostatic-pressing-brochure.
67. Neikov, O.D., *Chapter 3 - Mechanical Alloying*, in *Handbook of Non-Ferrous Metal Powders (Second Edition)*, O.D. Neikov, S.S. Naboychenko, and N.A. Yefimov, Editors. 2019, Elsevier: Oxford. p. 91-124.
68. Neikov, O.D., *Chapter 2 - Mechanical Crushing and Grinding*, in *Handbook of Non-Ferrous Metal Powders (Second Edition)*, O.D. Neikov, S.S. Naboychenko, and N.A. Yefimov, Editors. 2019, Elsevier: Oxford. p. 65-90.
69. Benjamin, J.S., "Mechanical alloying — A perspective". *Metal Powder Report*, 1990. 45(2): p. 122-127.

70. Whittaker, D., “Hot Isostatic Pressing at World PM2016: Developments in production and processing”. *Powder Metallurgy Review*, 2017. 6 No. 1 Spring 2017: p. 65-73.
71. Whittaker, D., “Euro PM2018: Powder Metallurgy processing by hot pressing technologies”. *Powder Metallurgy Review*, 2019. 8 No. 1: p. 69-78.
72. German, R.M., “Powder Metallurgy fundamentals: An introduction to the principles of sintering metal powders”. *Powder Metallurgy Review*, 2016. 5 No. 3(Autumn/Fall): p. 112.
73. Swinkels, F.B., et al., “Mechanisms of hot-isostatic pressing”. *Acta Metallurgica*, 1983. 31(11): p. 1829-1840.
74. Akhtar, S., et al., “Recent advancements in powder metallurgy: A review”. *Materials Today: Proceedings*, 2018. 5(9): p. 18649-18655.
75. Reactor, S.M. *Small Modular Reactor Vessel Manufacture/Fabrication Using PM-HIP and Electron Beam Welding Technologies*. in *Potential Nuclear Components - Enabling the Next Generation of Nuclear Plants*. 2017.
76. Shima, S., *Constitutive Equation for Compressible Materials and its Application to Simulation of Powder Forming Processes*. 1992, Springer Netherlands. p. 11-16.
77. Chung, S.H., et al., *Modeling and Simulation of Press and Sinter Powder Metallurgy*, in *Powder Metallurgy*, P. Samal and J. Newkirk, Editors. 2015, ASM International. p. 0.
78. Lin, D., et al., “Experimental and simulation analysis of hot isostatic pressing of gas atomized stainless steel 316L powder compacts”. *Korean Journal of Metals and Materials*, 2016. 54(10): p. 732-742.
79. Bhattacharya, S., K. Jakus, and I. Grosse, “Modelling pressure-assisted densificationby power-law creep”. *Journal of Materials Science*, 1997. 32(23): p. 6183-6189.
80. Chung, S.H., et al., “An Optimal Container Design for Metal Powder Under Hot Isostatic Pressing”. *Journal of Engineering Materials and Technology*, 2001. 123(2): p. 234-239.
81. Arzt, E., M.F. Ashby, and K.E. Easterling, “Practical applications of hotisostatic Pressing diagrams: Four case studies”. *Metallurgical Transactions A*, 1983. 14(1): p. 211-221.
82. Jinka, A.G.K. and R.W. Lewis, “Finite element simulation of hot isostatic pressing of metal powders”. *Computer Methods in Applied Mechanics and Engineering*, 1994. 114(3-4): p. 249-272.
83. Olevsky, E., et al., “Container influence on shrinkage under hot isostatic pressing—I. Shrinkage anisotropy of a cylindrical specimen”. *International Journal of Solids and Structures*, 1998. 35(18): p. 2283-2303.
84. Olevsky, E. and A. Maximenko, “Container influence on shrinkage under hot isostatic pressing—II. Shape distortion of cylindrical specimens”. *International Journal of Solids and Structures*, 1998. 35(18): p. 2305-2314.
85. Gandy, D., “Program on Technology Innovation: Manufacture of Large Nuclear and Fossil Components Using Powder Metallurgy and Hot Isostatic Processing Technologies”. *EPRI Report*, 2012. 1025491.
86. Gandy, D. and M. Albert, *Program on Technology Innovation: Small Modular Reactor Vessel Manufacture and Fabrication - Phase 1 - Progress (Year 3)*. 2021, Electric Power Research Institute. p. 284.
87. VADOLIA, G., et al., *Survey on Hot Isostatic Pressing Technique for Development of Tokamak Components*. 2018.
88. *EPSI Pilot Production HIP Unit*. Available from: https://epsi-highpressure.com.
89. Hoffman, D., B. Singh, and J.H. Thomas III, *Handbook of vacuum science and technology*. 1997: Elsevier.
90. O'Hanlon, J.F., *A user's guide to vacuum technology*. 2003: John Wiley & Sons.
91. Kowalski, L., B. Korevaar, and J. Duszczyk, “Some new aspects of the theory of oxidation and degassing of aluminium-based alloy powders”. *Journal of Materials Science*, 1992. 27(10): p. 2770-2780.

92. Distefano, J.R., et al., *Summary of Modified 9Cr-1Mo Steel Development Program: 1975 - 1985(ORNL-6303)*. 1986.
93. WRC, P., "Ad Hoc Group on Toughness Requirements, PVRC recommendations on toughness requirements for ferritic materials". *WRC bulletin*, 1972. 175.
94. Gandy, D., *Innovative Manufacturing Process for Nuclear Power Plant Components via Powder Metallurgy-HIP*. 2016, Electric Power Research Institute. p. 204.
95. Berglund, T. and M. Östlund. *Impact toughness for PM HIP 316L at cryogenic temperatures*. in *Pressure Vessels and Piping Conference*. 2016. American Society of Mechanical Engineers.
96. International Atomic Energy, A., *Stress Corrosion Cracking in Light Water Reactors - Good Practices and Lessons Learned*. 2011, Internationsl Atomic Energy Agency (IAEA).
97. Gandy, D. *Innovative Manufacturing Process for Nuclear Power Plant Components via Powder Metallurgy & Hot Isostatic Pressing Methods*. in *DOE Advanced Methods of Manufacturing Workshop*. 2015.
98. De Baglion, L., et al. *Low Cycle Fatigue Behavior in Air and in PWR Water of Type 304L and 316L Austenitic Stainless Steels Manufactured by Hot Isostatic Pressing Process*. in *Pressure Vessels and Piping Conference*. 2015. American Society of Mechanical Engineers.
99. Institute, E.P.R., *Nuclear Sector Roadmaps - January 2015*. 2015. p. 4.
100. Rodchenkov, B., et al., "Effect of ITER components manufacturing cycle on the irradiation behaviour of 316L (N)-IG steel". *Journal of Nuclear Materials*, 2000. 283: p. 1166-1170.
101. Lind, A. and U. Bergenlid, "Mechanical properties of hot isostatic pressed type 316LN steel after irradiation". *Journal of Nuclear Materials*, 2000. 283: p. 451-454.
102. Lind, A. and U. Bergenlid, "Mechanical properties of hot isostatic pressed type 316LN steel after irradiation to 2.5 dpa". *Fusion Engineering and Design*, 2001. 58: p. 713-717.
103. Dänner, W., et al., "ITER R&D: Vacuum Vessel and In-Vessel Components: Shield Blanket Module". *Fusion Engineering and Design*, 2001. 55(2-3): p. 205-217.
104. Lind, A. and J. Collen, *Shield fabrication development of ITER primary wall modules by powder Hip*. 1998, France: Association Euratom-CEA Cadarache.
105. Hatano, T., *Fabrication and testing of small scale mock-ups of ITER shielding blanket(JAERI-Tech-98-058)*, S. Sato and S. Suzuki, Editors. 1998.
106. Gandy, D., *Advanced Technology for Large-Scale (ATLAS) Powder Metallurgy-Hot Isostatic Pressing Technology Assessment*. 2016, Electric Power Research Institute: epri.com. p. 62.
107. Kyffin, W., D. Gandy, and B. Burdett, "A Study of the Reproducibility and Diversity of the Supply Chain in Manufacturing Hot Isostatically Pressed Type 316L Stainless Steel Components for the Civil Nuclear Sector". *Journal of Nuclear Engineering and Radiation Science*, 2020. 6(2).
108. David, G., et al., "Assessment Of Powder Processing Methods For Production Of A Small Modular Reactor Vessel Component Assemblies Via Powder Metallurgy-HIP". 2019.
109. Park, J.-Y., et al., "Spheroidization behavior of water-atomized 316 stainless steel powder by inductively-coupled thermal plasma". *Materials Today Communications*, 2020. 25: p. 101488.

Impending Publication - The Use of PM-HIP for Fabricating Components of NPPs DATE June 17, 2022

DISTRIBUTION:
MYoo, RES/DE/CIB
MHiser, RES/DE/CMB
JMcKirgan, RES/DE
LLund, RES/DE
RTregoning, RES/DE
RIyengar, RES/DE/CIB
IAnchondo-Lopez, R-IV/DRS/EB2
CFairbanks, NRR/DNRL/NVIB
RDavis, NRR/DNRL/NPHP
ABuford, NRR/DNRL/NVIB
MMitchell, NRR/DNRL/NPHP
AHiser, NRR/DNRL
DRudland, NRR/DNRL
BThomson, NRR/DNRL
BSmith, NRR/DNRL

ADAMS Accession No.: ML22164A37; ML22164A438

OFFICE	RES/DE/CIB	RES/DE/CMB	RES/DE	
NAME	MYoo *MY*	MHiser *MH*	LLund JMcKirgan for *JM*	
DATE	Jun 14, 2022	Jun 16, 2022	Jun 17, 2022	

OFFICIAL RECORD COPY